

INVESTIGATING RED BLOOD CELLS IN AUTOIMMUNE DISEASES

By

Tiffany Janes

A DISSERTATION

Submitted to
Michigan State University
in partial fulfillment of the requirements
for the degree of

Chemistry – Doctor of Philosophy

2018

ProQuest Number:10809821

All rights reserved

INFORMATION TO ALL USERS

The quality of this reproduction is dependent upon the quality of the copy submitted.

In the unlikely event that the author did not send a complete manuscript and there are missing pages, these will be noted. Also, if material had to be removed, a note will indicate the deletion.



ProQuest 10809821

Published by ProQuest LLC (2018). Copyright of the Dissertation is held by the Author.

All rights reserved.

This work is protected against unauthorized copying under Title 17, United States Code
Microform Edition © ProQuest LLC.

ProQuest LLC.
789 East Eisenhower Parkway
P.O. Box 1346
Ann Arbor, MI 48106 – 1346

ABSTRACT

INVESTIGATING RED BLOOD CELLS IN AUTOIMMUNE DISEASES

By

Tiffany Janes

Work presented in this dissertation demonstrates that red blood cells (RBCs) from patients with multiple sclerosis (MS) or type 1 diabetes (T1D) have an altered cell metabolism compared to healthy RBCs. An overview of each disease, along with implications of increased or decreased RBC metabolism and downstream events are presented here. Additional experiments investigated methods to increase or decrease the RBC metabolism in an effort to alleviate complications of each disease.

Glucose transporter 1 (GLUT1) is the main glucose transporter on RBCs, and all metabolism within the RBC involves glucose. RBC GLUT1 content was used as a measure of RBC metabolism, and elevated RBC GLUT1 content is proposed to be associated with increased cell metabolism. RBCs obtained from MS patients contained $23.3 \pm 4.8\%$ more GLUT1 than control RBCs, while T1D RBCs contained $23.6 \pm 4.2\%$ less GLUT1 than control RBCs. Further studies evaluated the effects of various therapies on RBCs with respect to MS and T1D.

Steroids are commonly prescribed to MS patients to manage exacerbations of the disease; however, hyperglycemic conditions often result. Evidence presented here using measurements of RBC adenosine triphosphate (ATP) release, suggests that the steroids estriol and prednisolone decrease RBC metabolism. ATP is a product of glycolysis, which utilizes the glucose transported into the cell to produce energy. While MS RBCs released 104 ± 18 nM more ATP than control RBCs, treatment with estriol or prednisolone

significantly decreased the RBC ATP release, thought to correlate to RBC metabolism. RBC ATP release stimulates endothelial nitric oxide (NO) production *in vivo*, which is detrimental at the high levels seen in MS due to its toxicity to the blood brain barrier. Results presented here also suggest that RBCs treated with physiological levels of estriol or prednisolone significantly decrease the downstream endothelial NO production up to 30%, thought to correlate to decreased blood brain barrier damage in MS patients.

Shear stress is a main mechanism of RBC ATP release; however, chemical stimulus also leads to RBC ATP release. Further studies investigated the effect steroids had on C-peptide and Zn²⁺ binding to RBCs, a proven chemical stimulus of RBC ATP release. Results suggest that RBC treatment with prednisolone decreased the Zn²⁺ binding from 1.99 ± 0.12 nM to 0.18 ± 0.30 nM, and decreased the C-peptide binding from 2.02 ± 0.22 nM to -0.47 ± 0.27 nM. It follows that any effect that C-peptide and Zn²⁺ have on RBCs is attenuated as their binding to RBCs is attenuated, such as ATP release.

Further studies investigated T1D RBCs and a proposed therapy involving a complex of C-peptide, Zn²⁺, and albumin. T1D patients suffer from insufficient blood flow, and this work suggests that the complex of C-peptide, Zn²⁺, and albumin may enhance blood flow and alleviate T1D complications. Evidence is presented here showing that an increase in RBC ATP release (34 ± 1.5 nM increase), RBC GLUT1 content ($25.5 \pm 1.3\%$ increase), RBC C-peptide binding (1.95 ± 0.14 nM increase), and RBC Zn²⁺ binding (2.26 ± 0.20 nM increase) is only measured when the full complex of C-peptide, Zn²⁺ and albumin is present. While T1D RBCs have a lower RBC metabolism at basal level, treatment with this complex is suggested to enhance RBC metabolism and ATP release leading to enhanced blood flow, which will greatly help with the treatment of T1D.

ACKNOWLEDGMENTS

I would first like to thank Michigan State University and the National Institutes of Health for the funding that made all of this work possible, and the College of Natural Science for funding allowing me to travel to and attend many conferences throughout my time in graduate school. The Neurology and Ophthalmology Clinic at Michigan State University collaborated with our group, and I would like to thank Dr. Eric Eggenberger for his guidance and help obtaining blood samples from MS patients early on in my graduate school career.

I would also like to thank my guidance committee, Dr. Merlin Bruening, Dr. Heedeok Hong, Dr. Kurt Zinn, and Dr. Liangliang Sun. Their unceasing willingness to help with my research throughout the years has been appreciated and very beneficial.

My advisor, Dr. Dana Spence, has also been instrumental in furthering my research throughout graduate school. Creating an environment to obtain proper work-life balance, Spence treats all group members as family, which allows all to remain motivated and feel comfortable talking through research struggles. My accomplishments in graduate school would not have been possible without the positive environment present in the Spence Lab.

Much of this work would not have been possible without the help and teamwork of the Spence group, past and present. I would especially like to thank Dr. Suzanne Summers,

who collected much of the C-peptide data presented in this work. She also began most of the work involving MS and is the reason I was drawn to this project from the beginning. In addition to her lab work, Suzanne and I have become good friends throughout the years. I would also like to thank Dr. Sarah Lockwood, who is not only a good friend, but who also collected many blood samples from MS patients for analysis in this work. Hamideh Keshavarz performed many of the ATP measurements presented here, and in addition to sitting next to each other for four years, we have become great friends and she is my number one puppy-sitter. I would also like to thank all other current Spence lab members for their encouragement, positive attitudes, and advice: Cody Pinger, Andrew Heller, Andre Castiaux, Morgan Geiger, Marcus Bunn, Lisa Meints, and Brit Eggly.

Finally I would like to thank all of my friends and family for their continued love and support. My parents, Maurice and Mary have always encouraged me to perform at my best, regardless of the environment. Without them, I would not have made it this far. I would also especially like to thank my husband Steve, who has been my rock throughout graduate school. His calming presence kept me grounded while his attitude kept me always smiling. Lastly, I would like to thank my puppy, Nash. Her unconditional love turns my worst days around, and she always brings so much joy to everyone she meets.

TABLE OF CONTENTS

LIST OF TABLES.....	viii
LIST OF FIGURES.....	ix
Chapter 1 – Introduction.....	1
1.1 Introduction to the Red Blood Cell.....	1
1.1.1 Red Blood Cell Glucose Metabolism.....	2
1.1.2 Red Blood Cell Membrane GLUT1.....	4
1.1.3 Red Blood Cell ATP Release and NO Stimulation.....	5
1.1.4 The Production of C-peptide and its Ability to Bind to Human Cells.....	8
1.1.5 Red Blood Cell Zn ²⁺ Binding.....	12
REFERENCES.....	15
Chapter 2 – Red Blood Cell GLUT1 Levels in Autoimmune Diseases.....	21
2.1 Introduction to Autoimmune Diseases.....	21
2.1.1 Overview of Diabetes Mellitus.....	21
2.1.1.1 Classifications and Diagnoses of Diabetes.....	23
2.1.1.2 Diabetic Complications.....	27
2.1.2 Overview of Multiple Sclerosis.....	29
2.1.2.1 Diagnosis of Multiple Sclerosis.....	32
2.1.2.2 Remyelination in Multiple Sclerosis.....	35
2.2 Glucose Metabolism in Autoimmune Diseases.....	36
2.2.1 Glucose Metabolism in Diabetes.....	37
2.2.2 Glucose Metabolism in Multiple Sclerosis.....	38
2.3 Experimental.....	39
2.3.1 Isolation and Purification of Red Blood Cells.....	39
2.3.2 Preparation of Reagents.....	39
2.3.3 Preparing RBC Ghost Samples.....	40
2.3.4 SDS-PAGE and Coomassie Blue Staining.....	41
2.3.5 Western Blot Analysis.....	42
2.4 Results.....	43
2.5 Discussion.....	45
REFERENCES.....	48
Chapter 3 – Effects of Multiple Sclerosis Therapies.....	56
3.1 Multiple Sclerosis Therapies.....	56
3.2 Multiple Sclerosis Traits.....	61
3.2.1 ATP and NO in Multiple Sclerosis.....	61
3.2.2 Zinc and Multiple Sclerosis.....	63
3.2.3 Pregnancy and Multiple Sclerosis.....	64
3.3 3D Printed Device and Design for Experimental Analysis.....	69

3.4 Experimental.....	70
3.4.1 Isolation and Purification of Red Blood Cells.....	70
3.4.2 Preparation of Reagents.....	71
3.4.3 Red Blood Cell Prednisolone and Estriol Treatment.....	74
3.4.4 3D Printed Device Preparation.....	75
3.4.5 ATP Detection Procedure.....	77
3.4.6 Bovine Pulmonary Arterial Cell Culture.....	79
3.4.7 NO Detection Procedure.....	81
3.4.8 Deformability Procedure.....	82
3.4.9 Red Blood Cell Radioactive $^{65}\text{Zn}^{2+}$ Binding.....	84
3.4.10 Red Blood Cell C-peptide Binding.....	84
3.4.11 Preparing Red Blood Cell Ghost Samples.....	85
3.4.12 SDS-PAGE and Western Blot Analysis.....	86
3.5 Results.....	87
3.6 Discussion.....	107
REFERENCES.....	114
Chapter 4 – The Role of Albumin in Delivering C-peptide and Zinc to the RBC.....	122
4.1 Insulin and C-peptide.....	122
4.1.1 Diabetes and Insulin.....	122
4.1.2 Biological Effects of C-peptide.....	124
4.2 Albumin.....	127
4.3 Experimental.....	129
4.3.1 Isolation and Purification of Red Blood Cells.....	129
4.3.2 Preparation of Reagents.....	130
4.3.3 Radioactive $^{65}\text{Zn}^{2+}$ Binding Determination.....	131
4.3.4 C-peptide Binding to Red Blood Cells.....	132
4.3.5 Detection of Red Blood Cell Released ATP.....	133
4.3.6 Preparing Red Blood Cell Ghost Samples.....	134
4.3.7 GLUT1 SDS-PAGE and Western Blot Analysis.....	135
4.4 Results.....	135
4.5 Discussion.....	145
REFERENCES.....	149
Chapter 5 – Overall Conclusions and Future Directions.....	153
5.1 Overall Conclusions.....	153
5.1.1 Steroids and Multiple Sclerosis.....	154
5.1.2 Type 1 Diabetes Therapy to Improve Blood Flow.....	159
5.2 Future Directions.....	162
5.2.1 Red Blood Cell Interferon Beta Treatment.....	162
5.2.2 Red Blood Cell Glucose Utilization Measurements.....	166
REFERENCES.....	170

LIST OF TABLES

Table 2.1 - Overview of the four main classifications of diabetes.....	26
Table 2.2 – Overview of common diabetic complications.....	28
Table 3.1 – HPLC gradient method for C-peptide purification.....	73
Table 3.2 – The Effect of Estriol and Prednisolone on Luminescence Detection.....	87

LIST OF FIGURES

Figure 1.1 – Glucose Metabolism within the RBC. About 90% of the glucose metabolism within the RBC is through glycolysis (left), and the remaining 10% of the metabolism is through the pentose phosphate pathway (PPP) (right). Glycolysis consists of 10 steps broken down into two phases, the preparatory phase and the payoff phase. The preparatory phase requires 2 ATP molecules, while the payoff phase produces 4 ATP molecules, leading to a net gain of 2 ATP molecules overall. The PPP oxidizes the first carbon of glucose to carbon dioxide, and the energy extracted reduces NADP to NADPH, which protects the cell against oxidative stress. The oxygen saturation of the RBC dictates which glucose utilization pathway is used. High oxygen saturation levels are associated with PPP utilization, while deoxygenated RBCs utilize glycolysis.....3

Figure 1.2 – Mechanism of RBC ATP Release and Subsequent Endothelial NO Production. A potential mechanism of action of RBC ATP release and sequential endothelial cell NO production. This mechanism involves the activation of heterotrimeric G protein (G_i), adenylyl cyclase (AC), phosphokinase A (PKA), and cystic fibrosis transmembrane conductance regulator (CFTR), which causes the release of ATP from the RBC through Pannexin 1. ATP then binds to P2Y receptors on endothelial cells to stimulate NO production through eNOS, converting L-arginine to L-citrulline.....7

Figure 1.3 – Proinsulin Structure and RBC C-peptide Binding. A. The structure of proinsulin. C-peptide is shown in yellow, and the A and B chains of insulin are shown in orange. B. RBC C-peptide uptake with (black circles) and without (open circles) Zn^{2+} . As more C-peptide was added to the RBCs, the cells become saturated when about 10 pmoles was added, correlating to about 2 pmoles on the cells. The presence of Zn^{2+} does not affect the amount of C-peptide binding to RBCs. $n = 4$, error bars = SEM.....10

Figure 1.4 – RBC C-peptide Binding. When 20 nM C-peptide was added to control and MS RBCs, a statistically significant increase in C-peptide binding was measured from MS RBCs compared to control RBCs. This increase in C-peptide binding may suggest properties of MS RBCs that cause experienced complications downstream. $n = 12$ MS patients and 6 healthy controls, * $p < 0.001$ to Control, error bars = SEM.....11

Figure 1.5 – RBC $^{65}Zn^{2+}$ Binding. When 20 nM C-peptide and $^{65}Zn^{2+}$ were added to RBCs and the $^{65}Zn^{2+}$ binding measured, a statistically significant increase in $^{65}Zn^{2+}$ binding was measured by MS RBCs compared to control RBCs. The measured increase correlates to the increased C-peptide binding (Figure 1.4), which together may be the cause of certain experienced complications. $n = 22$ MS patients and 11 healthy controls, * $p < 0.001$ to Control, error bars = SEM.....13

Figure 2.1 – Myelinated Nerve Cell. Axons of nerve cells are coated in myelin to increase the speed of nerve signal propagation from cell bodies to the axon terminals. This is done by inhibiting the electric current from leaving the axon while it propagates. When axons become demyelinated, lesions form and nerve signals are compromised, which is seen in MS.....31

Figure 2.2 – Depiction of the Four Types of MS. Relapsing-remitting MS (RRMS) consists of relapses followed by periods of disease remission. Secondary-progressive MS (SPMS) originally presents as RRMS and suddenly begins to decline without periods of remission. Primary-progressive MS (PPMS) consists of a steady increase in disability without attacks, and progressive-relapsing MS (PRMS) consists of a steady decline of health along with relapses.....33

Figure 2.3 – Overview of Glucose Metabolism in the Body. Glucose can be metabolized in the body to glucose-6-phosphate which has three distinct fates: glycogen synthesis, glycolysis, or the pentose phosphate pathway. Glycogen is a form of glucose that is stored until required for energy. Glycolysis produces pyruvate which is involved in the synthesis of certain amino acids, is a precursor for the citric acid cycle, and is also involved in fermentation processes. The pentose phosphate pathway produces ribose-5-phosphate, and also protects cells against oxidative stress. Machinery of the cell dictates which method of glucose metabolism is required for cells at a given time for survival.....37

Figure 2.4 – RBC Membranes Separated by SDS-PAGE and Stained with Coomassie Blue. After the cytosolic contents was removed from the RBCs using lysis buffer, the resulting ghosts were subject to SDS-PAGE to separate the remaining proteins. Coomassie Blue staining was used to visualize all proteins present, and a molecular weight ladder was used to evaluate the mass of each protein band. Bands that are thought to be GLUT1 and Beta Spectrin are labeled above.....43

Figure 2.5 – Resulting Western Blots. Western Blot analysis was utilized to probe for Beta Spectrin and GLUT1. To confirm that the antibodies for Beta Spectrin and GLUT1 did not interfere with each other, they were initially probed on a membrane alone, and then probed simultaneously on the same membrane for comparison. A. Membrane probed for Beta Spectrin only. B. Membrane probed for GLUT1 only. C. Membrane probed for both Beta Spectrin and GLUT1 simultaneously. The resulting bands are labeled.....44

Figure 2.6 – Normalized RBC Membrane GLUT1 Content of MS, Control, and T1D RBCs. When the GLUT1 content of control and MS RBS were probed, a significant 23.3% increase in the RBC membrane GLUT1 content was measured by Western Blot analysis. Contrary to the MS RBCs, a significant 23.6% decrease in RBC GLUT1 content was measured in T1D RBCs compared to control RBCs. n = 12 MS donors, 7 control donors, and 8 T1D donors, error bars = SEM, * p < 0.05 to Control.....45

Figure 3.1 – Steroid Mechanism of Action. Steroids act on cells by binding to a cytoplasmic receptor within the cell, and the steroid-receptor complex is subsequently translocated to the nucleus of the cell. Once in the nucleus, the steroid-receptor complex binds to the promoter region of the target genes, resulting in regulation of gene expression. At low concentrations steroids decrease the expression of pro-inflammatory genes, and at high concentrations, steroids active the expression of anti-inflammatory genes.....59

Figure 3.2 – 3D Printed Device Design and Dimensions. The device used for all ATP and NO measurements is shown above. Six channels allow for high throughput, and each channel can hold two membrane inserts. The dimensions of the device are 127.00 mm x 66.24 mm x 13.40 mm. Each channel is 2.00 mm in diameter, and a membrane insert with a diameter of 9.30 mm is compatible. The ends of each channel contain threads compatible with commercial finger tight fittings. When each channel contains two finger tight fittings, the device is the same size as a 96-well plate and can be integrated into a plate reader for detection.....76

Figure 3.3 – Experimental Setup and Detection. A. The device used for all experiments. Each channel contains two transwell inserts with a 0.4 μm membrane. A schematic drawing shows that the device is diffusion based, and as RBCs release ATP, the ATP will diffuse into the detection wells. bPAECs can be cultured on one of the transwell insert to measure NO production. B. View of a flow experiment. The experimental set up utilizes a peristaltic pump and Tygon tubing to create a closed loop system mimicking *in vivo* vasculature. C. Luminescence or fluorescence is measured using a plate reader. The device is the size of a 96-well plate and fits into the detection compartment of the instrument.....78

Figure 3.4 – Chemiluminescent Luciferin/Luciferase Reaction. As D-Luciferin mixes with Firefly Luciferase, Mg²⁺, and ATP in the presence of oxygen, oxyluciferin is generated along with inorganic phosphate (P_i), AMP, and carbon dioxide. The generated products produce a chemiluminescence intensity that can be measured by a photomultiplier tube (PMT), and standards are used to quantify the amount of ATP released.....79

Figure 3.5 – Optical Microscopy bPAEC Picture and DAF-FM Reaction. A. Optical microscopy picture of confluent bPAECs grown in a tissue culture flask. B. As NO is produced and reacts with DAF-FM in the presence of oxygen, a benzotriazole derivative is produced. This product can be measured by fluorescence with an excitation wavelength of 495 nm and an emission wavelength of 515 nm.....80

Figure 3.6 – 3D Printed Deformability Device Design and Experimental Setup. A. O-rings on each slab sandwich a 5 μm polycarbonate membrane which acts as a filter for this device. B. The assembled device with binder clips to hold the membrane and two slabs in place. C. View of a deformability experiment. As RBCs are forced through the device and membrane, the cells that pass through are collected and later counted. Comparing the number of RBCs that pass through the membrane in a given time is used as the measure of deformability. D. A schematic view of the filtration process. RBCs are forced through the device using a peristaltic pump, and the cells are required to deform to fit through the membrane. Cells that are deformable enough to fit through the membrane pass through and are collected, while cells that are not deformable enough will not pass through the membrane. The device was created by a former Spence lab member.....83

Figure 3.7 – RBC ATP Release from Control and MS RBCs Treated with Estriol. When both control and MS RBCs were treated with estriol, the measured ATP release significantly decreased. Control RBCs are depicted in the black circles, and MS RBCs are depicted in the white circles. At basal level, control RBCs release 216 ± 11 nM ATP, and MS RBCs release 321 ± 18 nM ATP. As higher estriol concentrations were incubated with RBCs, the ATP release continued to decrease until reaching a plateau level. Noteworthy, when MS RBCs are treated with 7 nM estriol, the RBC ATP release decreased to statistically the same level as the untreated control RBC ATP release. $n \geq 4$ donors, * $p < 0.05$ to control RBCs, ** $p < 0.05$ to MS RBCs, # $p > 0.4$ to control RBCs, E3 = estriol, error bars = SEM.....89

Figure 3.8 – RBC ATP Release from Control and MS RBCs Treated with Prednisolone. When both control and MS RBCs were treated with prednisolone, the measured ATP release significantly decreased. Control RBCs are depicted in the black circles, and MS RBCs are depicted in the white circles. As higher prednisolone concentrations were incubated with RBCs, the ATP release continued to decrease. Noteworthy: when MS RBCs were treated with 5 or 50 μM prednisolone, the RBC ATP release decreased to statistically the same level as the untreated control RBC ATP release. $n \geq 4$ donors, * $p < 0.05$ to control RBCs, ** $p < 0.05$ to MS RBCs, # $p > 0.4$ to control RBCs, P2 = prednisolone, error bars = SEM.....90

Figure 3.9 – RBC ATP Release from Control Cells Treated with Diamide. As a control, diamide was used to verify that the measured ATP was not due to cell lysis. Diamide stiffens cells, which has a direct correlation to ATP release from RBCs. When RBCs were treated with diamide, the measured ATP release decreases from 189 ± 25 nM, to 57 ± 17 nM. This result confirms that the RBCs are not lysing during the time of the experiment, as diamide would not decrease the ATP release from lysed RBCs. $n = 4$ donors, * $p < 0.05$ to control, error bars = SEM.....92

Figure 3.10 – Normalized Cell Fluorescence from bPAECs in Contact with RBCs Treated with Estriol. When the bPAEC NO production was measured as RBCs treated with estriol were flowed beneath, the NO production significantly decreased compared to bPAECs in contact with control RBCs. Shown above, the normalized bPAEC fluorescence when RBCs were treated with 3 nM, 7 nM, 30 nM, or 1 μ M estriol resulted in a decrease in fluorescence intensity up to $31 \pm 4\%$ compared to the control sample. All fluorescence intensities are normalized to the number of cells in each well, and also to the untreated control RBCs. $n \geq 5$ donors, $*p < 0.05$ to control, E3 = estriol, error bars = SEM.....94

Figure 3.11 – Normalized Cell Fluorescence from bPAECs in Contact with RBCs Treated with Prednisolone. When the bPAEC NO production was measured as RBCs treated with prednisolone were flowed beneath, the NO production significantly decreased compared to bPAECs in contact with control RBCs. Shown above, the normalized bPAEC fluorescence when RBCs were treated with various prednisolone concentrations resulted in a decrease in fluorescence intensity up to $31 \pm 5\%$ compared to the control sample. All fluorescence intensities were normalized to the number of cells in each well, and also the untreated control RBCs. $n \geq 4$ donors, $*p < 0.05$ to control, P2 = prednisolone, error bars = SEM.....95

Figure 3.12 – Normalized Cell Fluorescence from PPADS Treated bPAECs in Contact with Control RBCs. PPADS inhibit P2Y receptors on bPAECs, and was used as a control to verify that the measured NO was due to bPAEC production. A 30% decrease in the normalized cell fluorescence was measured from PPADS treated bPAECs when control RBCs were flowed beneath the cells. This decrease suggests the NO measured by fluorescence through DAF-FM is the product of NO synthesis activated by the P2Y receptor on the bPAECs. $n = 3$ donors, $*p < 0.05$ to control, error bars = SEM.....96

Figure 3.13 – The Deformability of RBCs Treated with Estriol. Deformability is reported to be directly correlated with ATP release, and a significant decrease of 5% and 13% in RBC deformability was measured when RBCs were treated with 21.4 nM or 0.74 μ M estriol, respectively. This decrease in RBC deformability is thought to correlate to a decrease in RBC ATP release (Figure 3.7). $n \geq 4$ donors, $*p < 0.05$ to 5% RBC, E3 = estriol, error bars = SEM.....98

Figure 3.14 – The Deformability of RBCs Treated with Prednisolone. Deformability is reported to be directly correlated with ATP release, and a significant decrease in RBC deformability of 15% and 25% was measured when RBCs were treated with 35.7 and 71.4 μ M prednisolone, respectively. This decrease in RBC deformability is thought to correlate to a decrease in RBC ATP release (Figure 3.8). $n \geq 4$ donors, $*p < 0.05$ to 5% RBC, P2 = prednisolone, error bars = SEM.....99

Figure 3.15 – The Deformability of Control and MS RBCs. Reported above, MS RBCs are $21 \pm 5\%$ less deformable than control RBCs. A possible explanation for this result could involve the size of MS RBCs compared to control RBCs. Reports suggest MS RBCs may be larger than control RBCs, and due to the membrane used in the device to measure deformability, different RBC sizes may skew results obtained. $n \geq 6$ donors, $*p < 0.05$ to 5% control RBCs, error bars = SEM.....100

Figure 3.16 – RBC $^{65}\text{Zn}^{2+}$ Binding in the Presence of Prednisolone. When the RBC $^{65}\text{Zn}^{2+}$ binding was measured after treatment with prednisolone, a significant decrease in RBC $^{65}\text{Zn}^{2+}$ binding was measured at all concentrations of prednisolone tested. The evaluated concentrations of prednisolone were 0.1, 0.5, 1, 5, 50, and 100 μM , and all samples contained 20 nM C-peptide and $^{65}\text{Zn}^{2+}$. P2 = prednisolone, C+Z = C-peptide and $^{65}\text{Zn}^{2+}$, $n \geq 4$ donors, error bars = SEM, $*p < 0.05$ to Control.....101

Figure 3.17 – RBC C-peptide Binding in the Presence of Prednisolone. When the RBC C-peptide binding was measured after treatment with prednisolone, a significant decrease in RBC C-peptide binding was measured at all concentrations of prednisolone tested. The evaluated concentrations of prednisolone were 5, 50, and 100 μM , and all samples contained 20 nM C-peptide and Zn^{2+} . P2 = prednisolone, C+Z = C-peptide and Zn^{2+} , $n \geq 7$ donors, error bars = SEM, $*p < 0.05$ to Control.....102

Figure 3.18 – Normalized RBC Membrane GLUT1 Content of RBCs treated with 20 nM C-peptide and Zn^{2+} . When samples of 7% RBCs were treated with 20 nM C-peptide and Zn^{2+} , a significant 25% increase in the RBC membrane GLUT1 content was measured by Western Blot analysis. This increase correlates with previous work suggesting that C-peptide and Zn^{2+} alter the cell metabolism of the RBC. C+Z = C-peptide and Zn^{2+} , $n \geq 8$ donors, error bars = SEM, $*p < 0.05$ to Control.....104

Figure 3.19 – Normalized RBC Membrane GLUT1 Content of RBCs Treated with Prednisolone. When control RBCs were treated with varying concentrations of prednisolone and the resulting RBC GLUT1 content evaluated, a significant increase in GLUT1 content was measured at prednisolone concentrations of 0.1, 0.5, 1, 5, 50, and 100 μM . P2 = prednisolone, $n \geq 6$ donors, error bars = SEM, $*p < 0.05$ to Control.....105

Figure 3.20 – Normalized RBC Membrane GLUT1 Content of RBCs Treated with Prednisolone, with and without Albumin. A significant increase in RBC GLUT1 content was measured after treatment with 50 μM prednisolone in the presence of albumin. When albumin was absent, there was no measureable change in RBC GLUT1 content due to prednisolone treatment, or due to C-peptide only, Zn^{2+} only, or the combination of the two. The prednisolone concentrations evaluated were 5, 50, and 100 μM . This results suggests that prednisolone requires albumin to specifically bind to RBCs and elicit an effect. P2 = prednisolone, Alb = albumin, CP = C-peptide, C+Z = C-peptide and Zn^{2+} , $n \geq 6$ donors, error bars = SEM, $*p < 0.05$ to RBC Control.....106

Figure 4.1 - Proinsulin. The full structure of proinsulin with the C-peptide amino acid sequence shown in yellow, and the A and B chains of insulin in orange. Before C-peptide and insulin are secreted into the bloodstream they are cleaved apart by enzymes at the locations depicted in blue. Once in the bloodstream, C-peptide has a half-life of about 30 minutes, while insulin has a half-life of about 4-6 minutes.....124

Figure 4.2 – RBC ATP Release With and Without Albumin. RBC ATP release with and without C-peptide, Zn^{2+} , and albumin. Albumin containing samples are depicted in the black bars and albumin free samples are depicted in the gray bars. An increase in ATP release is only measured in the presence of the complex of C-peptide, Zn^{2+} , and albumin. * $p < 0.005$ to RBCs with albumin, $n = 5$126

Figure 4.3 - Human Serum Albumin. The tertiary structure of human serum albumin, the most abundant blood protein. The three domains of the protein are depicted in blue, green, and red. In the bloodstream, human serum albumin is responsible for maintaining pressure and transporting drugs, hormones, metal ions, and fatty acids throughout the body.....128

Figure 4.4 – Control and T1D RBC $^{65}Zn^{2+}$ Binding. A. RBC $^{65}Zn^{2+}$ binding in the presence and absence of C-peptide and albumin as increasing concentrations of $^{65}Zn^{2+}$ and C-peptide are added to the RBCs (along the x-axis). B. RBC $^{65}Zn^{2+}$ binding with C-peptide in the presence of albumin shown on a smaller scale to more clearly highlight the specific binding curve measured. $n \geq 8$ donors, error bars = SEM. C. Control and T1D RBC $^{65}Zn^{2+}$ binding with and without C-peptide and insulin, in the presence of albumin. Control RBC = black bars, T1D RBC = gray bars. * $p < 0.05$ to Control 20 nM Zn, ** $p < 0.05$ to T1D 20 nM Zn, $n \geq 5$ donors, error bars = SEM. D. Control and T1D RBC $^{65}Zn^{2+}$ binding with and without C-peptide and insulin, all without albumin. Control RBC = black bars, T1D RBC = gray bars. $n \geq 6$ donors, error bars = SEM.....136

Figure 4.5 – Control and T1D RBC ATP Release. A. RBC ATP release in the presence and absence of C-peptide, Zn^{2+} , and albumin, with increasing concentrations of Zn^{2+} and C-peptide are added to the RBCs (along the x-axis). $n \geq 6$ donors, error bars = SEM. B. Control and T1D RBC ATP release with and without C-peptide, Zn^{2+} , and insulin, in the presence of albumin. Control RBC = black bars, T1D RBC = gray bars. * $p < 0.05$ to Control RBC, ** $p < 0.05$ to T1D RBC, # $p > 0.4$ to Control RBC, $n \geq 7$ donors, error bars = SEM. C. Control and T1D RBC ATP release with and without C-peptide, Zn^{2+} , and insulin, all without albumin. Control RBC = black bars, T1D RBC = gray bars. $n \geq 7$ donors, error bars = SEM.....138

Figure 4.6 – Control and T1D RBC GLUT1 Content. A. RBC membrane GLUT1 content in the presence and absence of C-peptide, Zn²⁺, and albumin as increasing concentrations of Zn²⁺ and C-peptide are added to the RBCs (along the x-axis). n ≥ 5 donors, error bars = SEM. B. Control and T1D RBC GLUT1 content with and without C-peptide, Zn²⁺, and insulin, in the presence of albumin. Control RBC = black bars, T1D RBC = gray bars. * p < 0.05 to T1D RBC, ** p < 0.05 to Control RBC, # p > 0.1 to Control RBC, n ≥ 7 donors, error bars = SEM. C. Control and T1D RBC GLUT1 content with and without C-peptide, Zn²⁺, and insulin, all without albumin. Control RBC = black bars, T1D RBC = gray bars. n ≥ 6 donors, error bars = SEM.....140

Figure 4.7 – RBC GLUT1 Content in Control and T1D Plasma. A. Normalized membrane GLUT1 content of control and T1D RBCs in control plasma with and without C-peptide, Zn²⁺, and insulin added to the RBCs. Control RBC = black bars, T1D RBC = gray bars. * p ≤ 0.05 to T1D RBC, ** p ≤ 0.05 to Control RBC, n ≥ 7 donors, error bars = SEM. B. Normalized membrane GLUT1 content of control and T1D RBCs in T1D plasma with and without C-peptide, Zn²⁺, and insulin. Control RBC = black bars, T1D RBC = gray bars. * p ≤ 0.05 to T1D RBC, ** p ≤ 0.05 to Control RBC, n ≥ 7 donors, error bars = SEM.....142

Figure 4.8 – Control and T1D C-peptide Binding. A. C-peptide binding to RBCs with (open circles) and without (filled circles) Zn²⁺, as increasing amounts of C-peptide and Zn²⁺ are added to RBCs (along x-axis). The C-peptide binding is not significantly different without Zn²⁺, and saturates around 2.0 pmoles C-peptide on RBCs. n = 4, error bars = SEM.¹³ B. Control and T1D RBC C-peptide binding when 20 nM C-peptide was added to RBCs with and without albumin. C-peptide binding was measured using a commercial ELISA kit and quantified using standards. Control RBC = black bars, T1D RBC = gray bars. * p < 0.05 to Control RBC no Albumin ** p < 0.05 to T1D RBC no Albumin, n ≥ 7 donors, error bars = SEM.....143

Figure 4.9 – RBC C-peptide Binding in Control and T1D Plasma. Control and T1D RBC C-peptide binding in control and T1D plasma. The addition of Zn²⁺ did not change the amount of C-peptide binding under any of the tested conditions. Control RBCs are depicted in the black bars, T1D RBCs are depicted in the gray bars. * p ≤ 0.05 to Control RBC in T1D plasma, ** p ≤ 0.05 to T1D RBC in T1D plasma, n ≥ 7 donors, error bars = SEM.....144

Figure 5.1 – RBC GLUT1 Content with C-peptide and Zn²⁺. As a 7% RBC sample is treated with 20 nM C-peptide and Zn²⁺, a 25 ± 2% increase in the GLUT1 content is measured. Interestingly, no significant increase was measured due to C-peptide only or Zn²⁺ only. n = 5 donors, *p < 0.05 to control, error bars = SEM.....164

Figure 5.2 – Control RBC GLUT1 Content with IFN- β . As samples of 7% RBCs are treated with 20 nM C-peptide and Zn²⁺ along with IFN- β , the initial increase in GLUT1 content measured due to C-peptide and Zn²⁺, decreases 26-28%. This decrease leads to a GLUT1 content statistically the same as the basal level of control RBCs and is thought to be caused by IFN- β binding the Zn²⁺ in solution, hindering any effect on the RBCs caused by Zn²⁺ binding, shown here as RBC GLUT1 content. n = 3 donors, *p < 0.05 to Control + C+Z, #p > 0.2 to Control, error bars = SEM.....165

Figure 5.3 – RBC GLUT1 Content with IFN- β . When control and MS RBCs are treated with C-peptide and Zn²⁺, MS RBCs contain more GLUT1 than control RBCs. Interestingly, as MS RBCs are treated with IFN- β after treatment with C-peptide and Zn²⁺, the GLUT1 content decreased to significantly the same levels as control RBCs treated with C-peptide and Zn²⁺. n = 3 donors, *p < 0.05 to control + C+Z, **p < 0.05 to MS + C+Z, #p > 0.05 to control + C+Z, error bars = SEM.....166

Chapter 1 – Introduction

1.1 Introduction to the Red Blood Cell

An average healthy adult has 4.5 to 5 liters of whole blood in their body, which is composed of red blood cells (RBCs, 45%), plasma (55%), and white blood cells and platelets (<1%). The RBCs, also referred to as erythrocytes, are the most common type of blood cells, have an average life span of 120 days, and are created through erythropoiesis in the bone marrow.¹⁻² The main job of RBCs is the delivery of oxygen, which is gained through binding of oxygen in the lungs, followed by release of that oxygen to various tissues throughout the body.³ Hemoglobin is the iron-containing protein that allows RBCs to bind oxygen, and is responsible for the red color of the cells. With a size of 6-8 μm in diameter and a volume of approximately 90 fL, RBCs take on a biconcave shape and have been referred to as a 'sack containing hemoglobin', as they do not contain a nucleus or any membrane-bound organelles, such as mitochondria.

Although the primary function of RBCs is to deliver oxygen throughout the body, RBCs also contain a large pool of adenosine triphosphate (ATP).⁴ RBCs can release ATP when exposed to various conditions, such as hypoxia, chemical stimuli, shear stress, or mechanical deformation.⁵⁻⁹ ATP released in the blood stream stimulates nitric oxide (NO) production by endothelial cells lining the vessels, which is a precursor for vasodilation and increased blood flow.¹⁰⁻¹²

Due to a lack of mitochondria, RBCs must produce ATP through anaerobic glycolysis, which accounts for about 90% of the glucose utilization within the RBC. The pentose phosphate pathway (PPP) makes up the remaining 10%.¹³⁻¹⁴

1.1.1 Red Blood Cell Glucose Metabolism

Glycolysis consists of glucose metabolized into lactic acid, and the transfer of energy from glucose to the high-energy bonds of ATP. Consisting of 10 different steps and two distinct phases, glycolysis achieves a net gain of two ATP molecules for the breakdown of one glucose molecule. The two phases, known as the preparatory phase and the payoff phase, and are shown in Figure 1.1. Two ATP molecules are required during the preparatory phase, and four ADP molecules are converted to four ATP molecules during the payoff phase, resulting in the net gain of two ATP molecules.

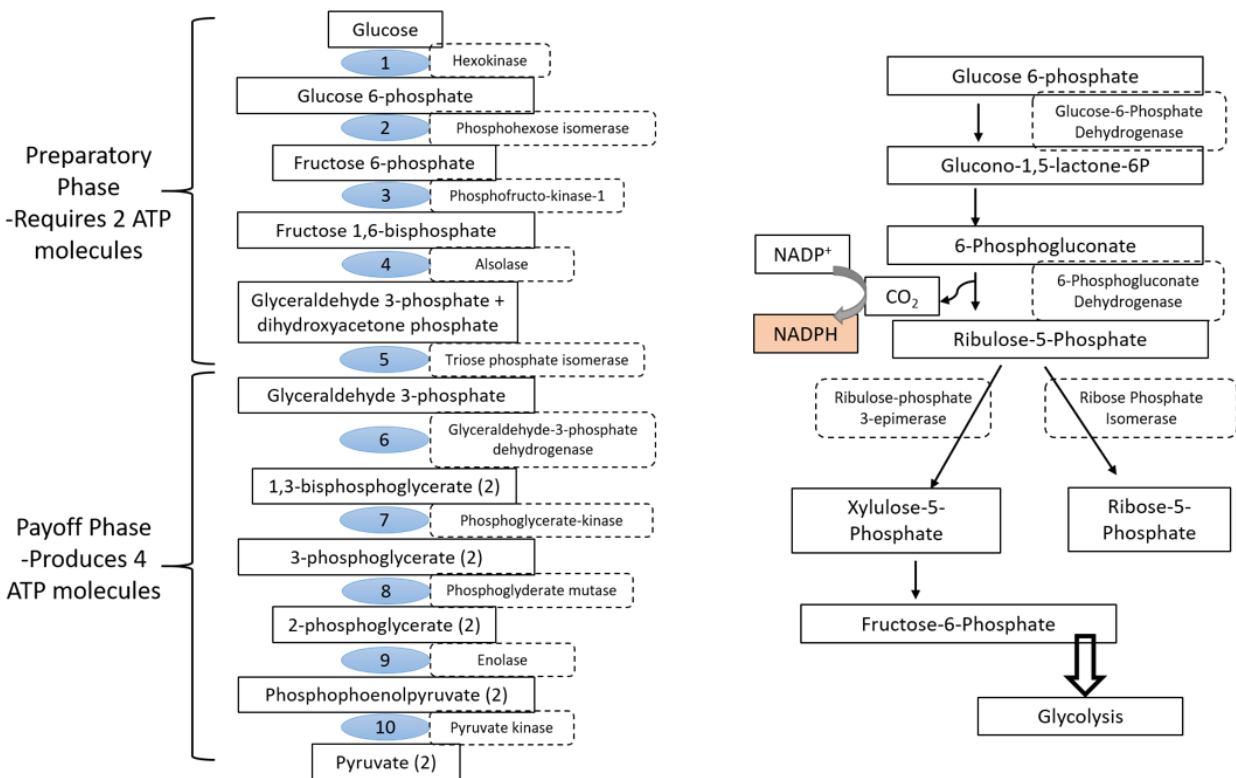


Figure 1.1 – Glucose Metabolism within the RBC. About 90% of the glucose metabolism within the RBC is through glycolysis (left), and the remaining 10% of the metabolism is through the pentose phosphate pathway (PPP) (right). Glycolysis consists of 10 steps broken down into two phases, the preparatory phase and the payoff phase. The preparatory phase requires 2 ATP molecules, while the payoff phase produces 4 ATP molecules, leading to a net gain of 2 ATP molecules overall. The PPP oxidizes the first carbon of glucose to carbon dioxide, and the energy extracted reduces NADP to NADPH, which protects the cell against oxidative stress. The oxygen saturation of the RBC dictates which glucose utilization pathway is used. High oxygen saturation levels are associated with PPP utilization, while deoxygenated RBCs utilize glycolysis.

The PPP oxidizes the first carbon of glucose to carbon dioxide (CO₂), and the energy extracted reduces NADP to NADPH, which protects the cell against oxidative stress (Figure 1.1). The resulting five-carbon sugar is then recycled through glycolysis to produce energy. Oxygen saturation of the RBC dictates the glucose utilization pathway.

At high oxygen saturation levels, more glucose is directed towards the PPP to protect

against oxidative stress, while deoxygenated RBCs allow the activation of certain enzymes to achieve greater ATP production within the cell. By varying flux between glycolysis and the PPP, the cells balance glucose utilization between energy needed and protective effects.¹³⁻¹⁴

1.1.2 Red Blood Cell Membrane GLUT1

Glycolysis begins with glucose uptake into the cell, and glucose transporter proteins (GLUTs) facilitate glucose diffusion across the cell membrane down the concentration gradient. To date, 14 GLUTs have been discovered and named chronologically.¹⁵⁻¹⁷ GLUT1 is the primary GLUT on RBCs, and is also expressed in high concentrations in cardiac muscle and astrocytes.¹⁶ As a membrane protein, GLUT1 is comprised of 12 membrane-spanning helical domains, and has a catalytic turnover of about 1,200/s.¹⁶ GLUT1 is encoded by the SLC2A1 gene in humans, and in the RBC GLUT1 comprises 10-20% of the total RBC membrane protein.^{16, 18-20} Although glucose is the most common molecule transported by GLUT1, dehydroascorbic acid is similar in structure to glucose, and is also transported by GLUT1, along with galactose, glucosamine, and mannose.²¹

Glucose transport is known to be an ATP-independent process, however, GLUT1 contains three ATP binding domains and the process is sensitive to the ATP content in the cell.¹⁹ It is unclear how the binding of ATP affects glucose transport without hydrolysis, but a possible reason could be that ATP exerts its activity through indirect methods such as activation through extrinsic proteins.¹⁹

Working as a uniporter, GLUT1 transports glucose into and out of the cell, and is defined as a constitutive transport protein that is expressed widely in both fetal and adult tissues and cells.^{16, 19} When stimulated, RBCs translocate GLUT1 from internal vesicles within the cell to the outer membrane of the cell to effectively transport glucose.^{16, 22-23}

With mutations in the SLC2A1 gene, GLUT1 deficiency syndrome may arise, with epilepsy being a common symptom. There is currently no cure for GLUT1 deficiency syndrome, however a ketogenic diet is often prescribed to help with symptoms.²⁴ The ketogenic diet consists of food high in fat and low in carbohydrates, causing the body to burn fat for energy, as instead of carbohydrates. Carbohydrates are very easily converted to glucose in the body, and it is thought that the ketogenic diet is essentially a fast for the body, and provides an alternative fuel source.²⁴

1.1.3 Red Blood Cell ATP Release and NO Stimulation

RBC ATP release is stimulated by mechanical deformation, shear stress, and hypoxia.^{5-9, 25-26} A proposed mechanism of ATP release from the RBC is shown in Figure 1.2, and involves mechanical deformation igniting heterotrimeric G protein leading to the activation of adenylyl cyclase and an increase in cyclic adenosine monophosphate (cAMP) production. Elevated cAMP activates phosphokinase A, and subsequently the cystic fibrosis transmembrane conductance regulator (CFTR), which initiates the release of ATP from the RBC through pannexin 1.²⁷ It is thought that sheer stress imposed on the RBC

causes mechanical deformation of the cell, and also that hypoxia may lead to mechanical deformation through stress on the deoxygenated hemoglobin.²⁷ Each method described here involves initial mechanical deformation, which implies the heterotrimeric G protein activation is essential to begin the process of ATP release within the RBC.

Deficient RBC ATP release has been reported in multiple diseases such as diabetes,²⁸⁻²⁹ cystic fibrosis,³⁰ and primary pulmonary hypertension.³¹ Reduced ATP release occurs from a decrease in deformability of the RBC.³⁰ Contrary to diabetes and cystic fibrosis, RBCs obtained from people with multiple sclerosis (MS) release elevated ATP, which may be a determinant of the disease.³² Diabetes and multiple sclerosis are both autoimmune diseases; however, their RBCs do not act in the same manner with respect to ATP release. The goal of this research is to better understand the cause and effect of RBC ATP release with regard to type 1 diabetes (T1D) and MS.

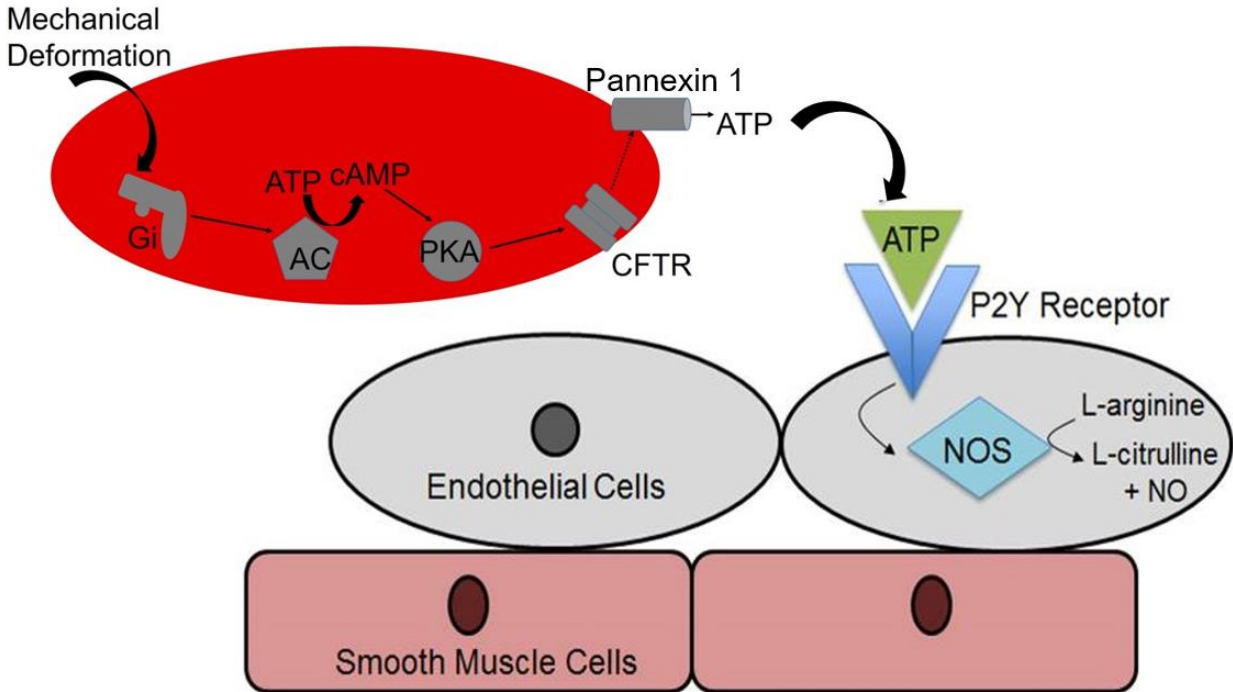


Figure 1.2 – Mechanism of RBC ATP Release and Subsequent Endothelial NO Production. A potential mechanism of action of RBC ATP release and sequential endothelial cell NO production. This mechanism involves the activation of heterotrimeric G protein (G_i), adenylyl cyclase (AC), phosphokinase A (PKA), and cystic fibrosis transmembrane conductance regulator (CFTR), which causes the release of ATP from the RBC through Pannexin 1. ATP then binds to P2Y receptors on endothelial cells to stimulate NO production through eNOS, converting L-arginine to L-citrulline.^{27, 30}

In the bloodstream, once ATP is released from RBCs, it can diffuse to the endothelium and bind to P2Y purinergic receptors.³³⁻³⁴ Binding to this receptor stimulates endothelial nitric oxide synthase (eNOS), which converts L-arginine to L-citrulline while producing NO as a by-product (Figure 1.2).¹¹⁻¹² NO is a known vasodilator, and its production in the bloodstream is crucial for the regulation of blood flow. Although endothelial cells are thought to be the main determinant of NO production leading to smooth muscle relaxation, additional theories implicate RBCs in determining vascular tone.

An alternate theory proposes that RBC hemoglobin is capable of both inactivating NO to nitrate, and converting nitrite to NO, when hemoglobin is oxygenated and deoxygenated, respectively.³⁵ It is also suggested that RBCs have the ability to bind and carry NO through the bloodstream and release it when exposed to hypoxia, although it is unlikely for RBC-released NO to diffuse from the bloodstream to smooth muscle cells and elicit relaxation without being scavenged.³⁶⁻³⁸ Previous work, along with work presented in this dissertation, suggest RBC-released ATP is capable of stimulating NO production in endothelial cells.¹⁰ In the following sections, the ability of specific pancreatic secretions to affect GLUT1 and subsequent ATP release from RBCs is described.

1.1.4 The Production of C-peptide and its Ability to Bind to Human Cells

In the pancreas, the islets of Langerhans are made up of four different cell types: α -cells, β -cells, δ -cells, and pancreatic polypeptide (PP) cells. The majority of the islet cells are made up of β -cells, which primarily secrete insulin, C-peptide, Zn^{2+} , and amylin. C-peptide is a 31-amino acid peptide synthesized in β -cell granules, initially as proinsulin prior to secretion. Proinsulin consists of a signaling peptide, the A and B chains of insulin, and C-peptide. In the rough endoplasmic reticulum, the signaling peptide is removed almost immediately after production, and the remaining peptide is termed proinsulin, shown in Figure 1.3A. After production, proinsulin is transported to the Golgi apparatus where it is packaged into vesicles prior to final maturation and release to the bloodstream. Acidic conditions arise within the granule which supports proinsulin hexamer formation consisting of two Zn^{2+} ions and six proinsulin molecules. The A and B chains of insulin

are cleaved apart from C-peptide by two endopeptidases and carboxypeptidase H, which are activated by the drop in pH. While C-peptide is cleaved apart from insulin, the Zn^{2+} content of the vesicle approaches millimolar levels facilitated through the ZnT8 protein, and the final release of the secretory vesicle is initiated by glucose levels above 5.5 mM in the bloodstream.

Originally, it was thought that the main function of C-peptide was only to help insulin fold properly, however recent work continues to provide evidence that C-peptide specifically binds and affects human cells.³⁹⁻⁴⁴ Previous work has investigated the binding of C-peptide to human fibroblasts and the measured specific binding correlated to 1,000 - 1,500 C-peptide receptors per cell.⁴⁵⁻⁴⁶ A similar result was also attained with human RBCs (Figure 1.3B). A 7% RBC solution was saturated with about 2 pmoles of C-peptide, which correlates to about 1,500 C-peptide molecules binding per cell.⁴⁷

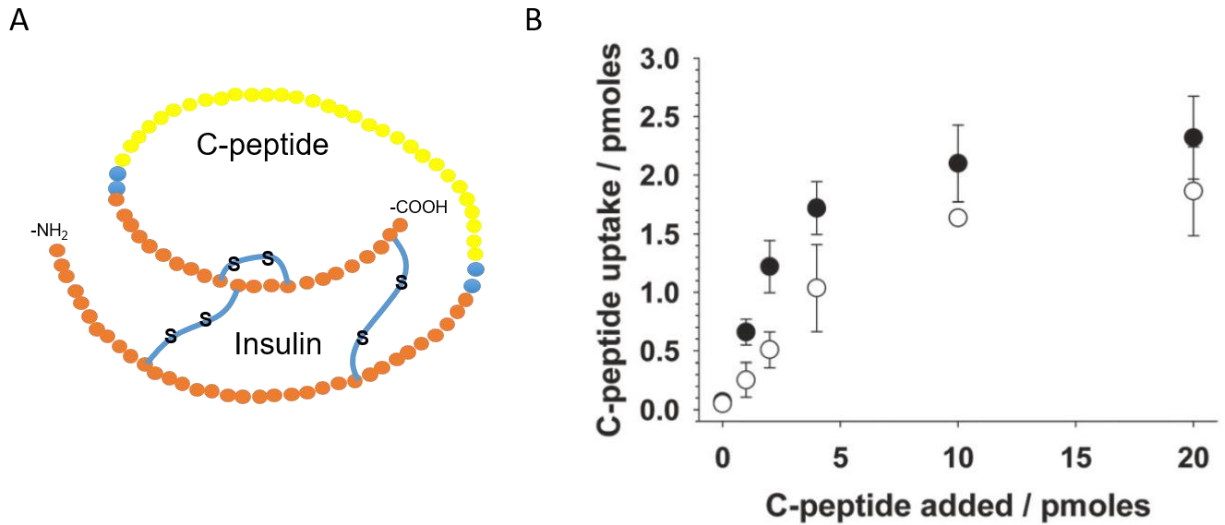


Figure 1.3 – Proinsulin Structure and RBC C-peptide Binding. A. The structure of proinsulin. C-peptide is shown in yellow, and the A and B chains of insulin are shown in orange. B. RBC C-peptide uptake with (black circles) and without (open circles) Zn²⁺. As more C-peptide was added to the RBCs, the cells become saturated when about 10 pmoles was added, correlating to about 2 pmoles on the cells. The presence of Zn²⁺ does not affect the amount of C-peptide binding to RBCs. n = 4, error bars = SEM.⁴⁷

An increase in the ATP release from RBCs treated with C-peptide and a metal was reported in 2008.⁴⁸ The original metals used were Fe²⁺ and Cr³⁺, but future realization of the high Zn²⁺ concentration in the β -cells lead to Zn²⁺ being the predicted metal to activate C-peptide *in vivo*. Further investigation in the Spence lab discovered that in order for C-peptide to elicit a biological effect it must be combined with not only Zn²⁺, but also the blood protein albumin.⁴⁷ Activated C-peptide has been shown to have positive effects on RBCs, including increased ATP release and deformability.^{10, 47-50} It is thought that the amount of C-peptide and Zn²⁺ binding to RBCs directly correlates to the downstream effects of ATP release and deformability. RBCs from MS patients release significantly more ATP compared to control RBCs, and results also suggest an increase in C-peptide

binding to MS RBCs compared to control RBCs, as shown in Figure 1.4.⁵¹ To further investigate the mechanism of action in question, previous work evaluated the RBC Zn²⁺ binding to MS RBCs to determine its correlation with C-peptide binding and ATP release.⁵¹

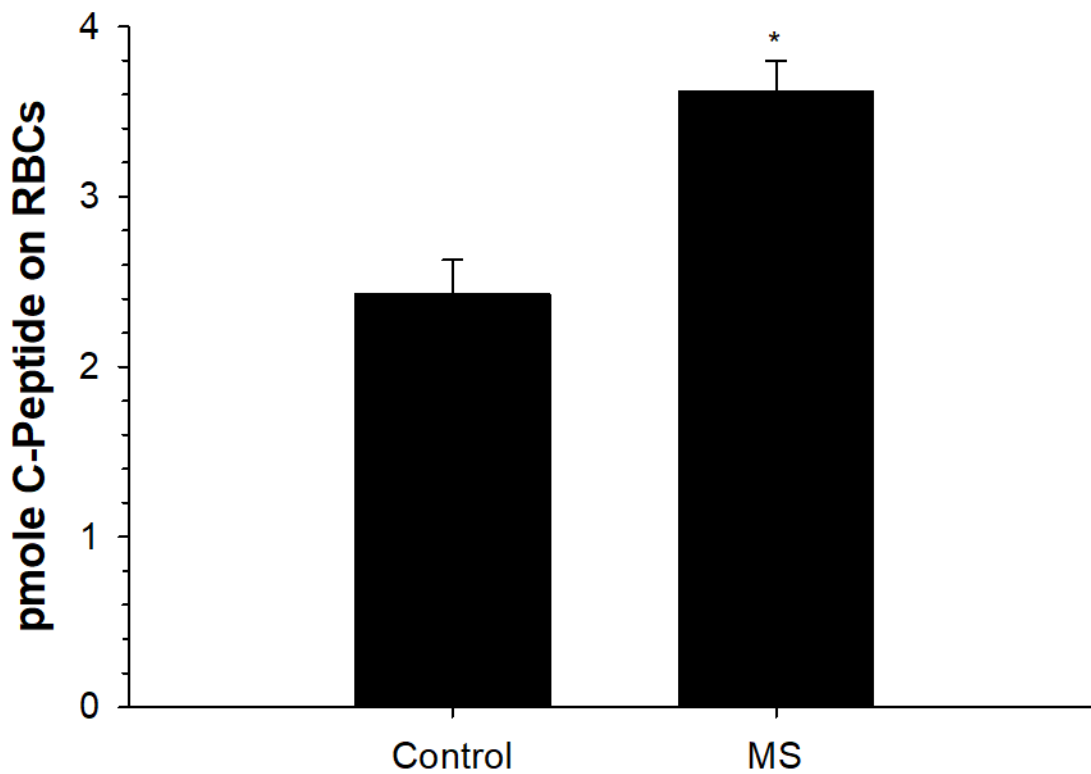


Figure 1.4 – RBC C-peptide Binding. When 20 nM C-peptide was added to control and MS RBCs, a statistically significant increase in C-peptide binding was measured from MS RBCs compared to control RBCs. This increase in C-peptide binding may suggest properties of MS RBCs that cause experienced complications downstream. n = 12 MS patients and 6 healthy controls, * p < 0.001 to Control, error bars = SEM.⁵¹

1.1.5 Red Blood Cell Zn²⁺ Binding

Zn²⁺ is secreted into the blood stream along with C-peptide and insulin. It makes sense that if a metal helps elicit the effect that C-peptide has on cells, that the metal is most likely Zn²⁺ due to its high concentration in β -cells. In order to further investigate that statement, binding of radiolabeled ⁶⁵Zn²⁺ to RBCs was previously studied.⁵¹ A significant increase in ⁶⁵Zn²⁺ binding to MS RBCs was measured compared to control RBCs (Figure 1.5).⁵¹ This result is thought to correlate with both the increase in RBC C-peptide binding, as well as the increase in RBC ATP release previously mentioned. Research suggests that although C-peptide is able to bind to RBCs in the absence of Zn²⁺, Zn²⁺ is unable to bind to RBCs without the presence of C-peptide.^{32, 47} As C-peptide and Zn²⁺ bind to RBCs, a potential hypothesis involves an increase in cell metabolism, leading to the altered RBC ATP release measured.

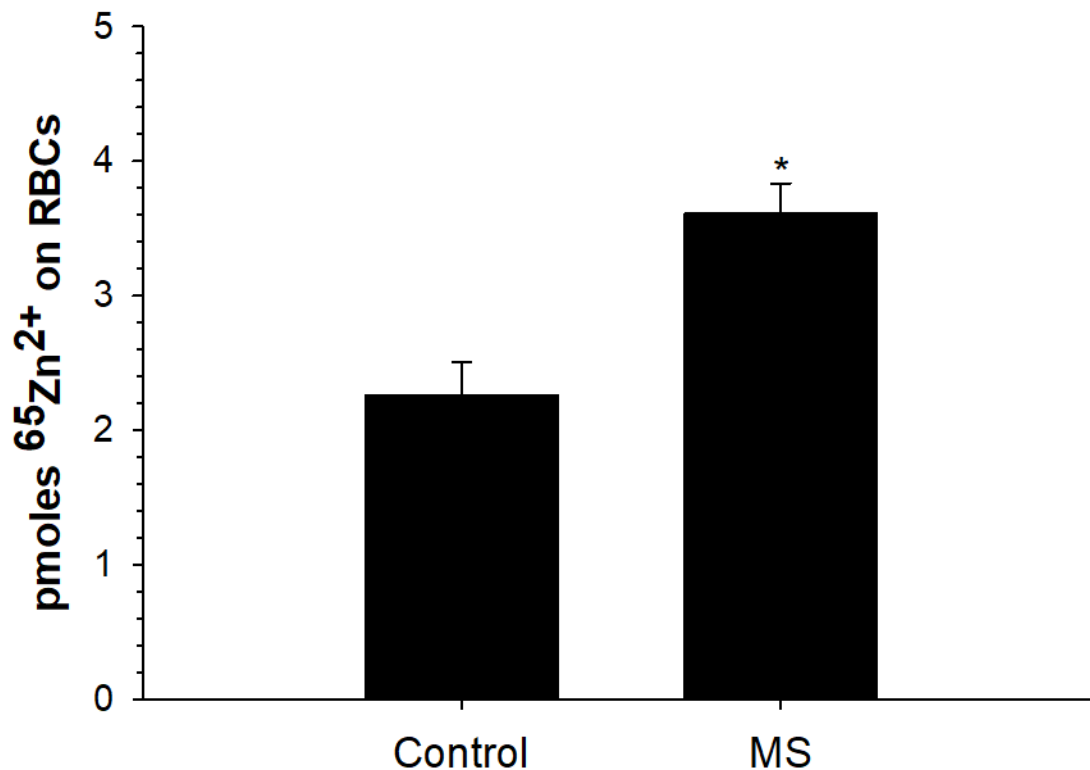


Figure 1.5 – RBC $^{65}\text{Zn}^{2+}$ Binding. When 20 nM C-peptide and $^{65}\text{Zn}^{2+}$ were added to RBCs and the $^{65}\text{Zn}^{2+}$ binding measured, a statistically significant increase in $^{65}\text{Zn}^{2+}$ binding was measured by MS RBCs compared to control RBCs. The measured increase correlates to the increased C-peptide binding (Figure 1.4), which together may be the cause of certain experienced complications. n = 22 MS patients and 11 healthy controls, * p < 0.001 to Control, error bars = SEM.⁵¹

The work presented in this dissertation aims to investigate the RBC metabolism of autoimmune patients and more fully understand the mechanisms of action within the RBC. ATP is known to be important with regard the RBC due to its ability to regulate blood flow, and certain autoimmune diseases have been characterized with RBCs that release elevated (MS) or decreased (diabetes) ATP. Evaluating the cause of the altered ATP

release may prove successful at more fully understanding the diseases as a whole, and also evaluating potential therapies.

REFERENCES

REFERENCES

1. Zucker, S.; Friedman, S.; Lysik, R. M., Bone marrow erythropoiesis in the anemia of infection, inflammation, and malignancy. *J Clin Invest* **1974**, *53* (4), 1132-1138.
2. Shemin, D.; Rittenberg, D., The life span of the human red blood cell. *J Biol Chem* **1946**, *166* (2), 627-636.
3. Winslow, R. M., The role of hemoglobin oxygen affinity in oxygen transport at high altitude. *Respir Physiol Neurobiol* **2007**, *158* (2-3), 121-127.
4. Dean, B. M.; Perrett, D., Studies on adenine and adenosine metabolism by intact human erythrocytes using high performance liquid chromatography. *Biochim Biophys Acta* **1976**, *437* (1), 1-5.
5. Bergfeld, G. R.; Forrester, T., Release of ATP from human erythrocytes in response to a brief period of hypoxia and hypercapnia. *Cardiovascular Research* **1992**, *26* (1), 40-47.
6. Ellsworth, M. L.; Forrester, T.; Ellis, C. G.; Dietrich, H. H., The erythrocyte as a regulator of vascular tone. *Am. J. Physiol* **1995**, *269*, H2155-H2161.
7. Price, A. K.; Fischer, D. J.; Martin, R. S.; Spence, D. M., Deformation-Induced Release of ATP from Erythrocytes in a Poly(dimethylsiloxane)-Based Microchip with Channels That Mimic Resistance Vessels. *Analytical Chemistry* **2004**, *76* (16), 4849-4855.
8. Sprung, R.; Sprague, R.; Spence, D., Determination of ATP release from erythrocytes using microbore tubing as a model of resistance vessels in vivo. *Analytical Chemistry* **2002**, *74* (10), 2274-2278.
9. Fischer, D. J.; Torrence, N. J.; Sprung, R. J.; Spence, D. M., Determination of Erythrocyte Deformability and its Correlation to Cellular ATP Release using Microbore Tubing with Diameters that Approximate Resistance Vessels in vivo. *Analyst* **2003**, *128*, 1163-1168.
10. Sprague, R. S.; Ellsworth, M. L.; Stephenson, A. H.; Lonigro, A. J., ATP: the red blood cell link to NO and local control of the pulmonary circulation. *Am J Physiol* **1996**, *271* (6 Pt 2), H2717-H2722.
11. Sprague, R. S.; Stephenson, A. H.; Dimmit, R. A.; Weintraub, N. A.; Branch, C. A.; McMurdo, L.; Lonigro, A. J., Effect of L-NAME on pressure-flow relationships in isolated rabbit lungs: Role of red blood cells. *Am. J. Physiol* **1995**, *296*, H1941-H1948.

12. Kuchan, M. J.; Frangos, J. A., Role of calcium and calmodulin in flow-induced nitric oxide production in endothelial cells. *The American journal of physiology* **1994**, 266 (3 Pt 1), C628-C636.
13. Messana, I.; Misiti, F.; el-Sherbini, S.; Giardina, B.; Castagnola, M., Quantitative determination of the main glucose metabolic fluxes in human erythrocytes by ¹³C- and ¹H-MR spectroscopy. *J Biochem Biophys Methods* **1999**, 39 (1-2), 63-84.
14. GLUCOSE metabolism in the red blood cell. *Nutr Rev* **1960**, 18, 206-207.
15. Olson, A. L.; Pessin, J. E., Structure, function, and regulation of the mammalian facilitative glucose transporter gene family. *Annu Rev Nutr* **1996**, 16, 235-256.
16. Carruthers, A.; DeZutter, J.; Ganguly, A.; Devaskar, S. U., Will the original glucose transporter isoform please stand up! *Am J Physiol Endocrinol Metab* **2009**, 297 (4), E836-E848.
17. Wu, X.; Freeze, H. H., GLUT14, a duplicon of GLUT3, is specifically expressed in testis as alternative splice forms. *Genomics* **2002**, 80 (6), 553-557.
18. Salas-Burgos, A.; Iserovich, P.; Zuniga, F.; Vera, J. C.; Fischbarg, J., Predicting the three-dimensional structure of the human facilitative glucose transporter glut1 by a novel evolutionary homology strategy: insights on the molecular mechanism of substrate migration, and binding sites for glucose and inhibitory molecules. *Biophysical journal* **2004**, 87 (5), 2990-2999.
19. Liu, Q.; Vera, J. C.; Peng, H.; Golde, D. W., The predicted ATP-binding domains in the hexose transporter GLUT1 critically affect transporter activity. *Biochemistry* **2001**, 40 (26), 7874-7881.
20. Carruthers, A., Facilitated diffusion of glucose. *Physiol Rev* **1990**, 70 (4), 1135-1176.
21. Vrhovac, I.; Breljak, D.; Sabolic, I., Glucose transporters in the mammalian blood cells. *Period Biol* **2014**, 116 (2), 131-138.
22. Fisher, M. D.; Frost, S. C., Translocation of GLUT1 does not account for elevated glucose transport in glucose-deprived 3T3-L1 adipocytes. *J Biol Chem* **1996**, 271 (20), 11806-11809.
23. Egert, S.; Nguyen, N.; Schwaiger, M., Myocardial glucose transporter GLUT1: translocation induced by insulin and ischemia. *J Mol Cell Cardiol* **1999**, 31 (7), 1337-1344.
24. Baranano, K. W.; Hartman, A. L., The ketogenic diet: uses in epilepsy and other neurologic illnesses. *Curr Treat Options Neurol* **2008**, 10 (6), 410-419.

25. Sprung, R. J.; Sprague, R. S.; Spence, D. M., Determination of ATP release from erythrocytes using microbore tubing as a model of resistance vessels in vivo. *Anal. Chem.* **2002**, *74*, 2274-2278.
26. Bergfeld, G. R.; Forrester, T., Release of ATP from human erythrocytes in response to a brief period of hypoxia and hypercapnea. *Cardiovasc. Res.* **1992**, *26*, 40-47.
27. Ellsworth, M. L.; Sprague, R. S., Regulation of blood flow distribution in skeletal muscle: role of erythrocyte-released ATP. *The Journal of physiology* **2012**, *590* (Pt 20), 4985-4991.
28. Sprague, R. S.; Stephenson, A. H.; Bowles, E. A.; Stumpf, M. S.; Lonigro, A. J., Reduced expression of Gi in erythrocytes of humans with type 2 diabetes is associated with impairment of both cAMP generation and ATP release. *Diabetes* **2006**, *55* (12), 3588-3593.
29. Subasinghe, W.; Spence, D. M., Simultaneous determination of cell aging and ATP release from erythrocytes and its implications in type 2 diabetes. *Analytica Chimica Acta* **2008**, *618* (2), 227-233.
30. Sprague, R. S.; Ellsworth, M. L.; Stephenson, A. H.; Kleinhenz, M. E.; Lonigro, A. J., Deformation-induced ATP release from red blood cells requires CFTR activity. *American Journal of Physiology* **1998**, *275* (5, Pt. 2), H1726-H1732.
31. Goodwin, J. E.; Geller, D. S., Glucocorticoid-induced hypertension. *Pediatr Nephrol* **2012**, *27* (7), 1059-1066.
32. Letourneau, S.; Hernandez, L.; Faris, A. N.; Spence, D. M., Evaluating the effects of estradiol on endothelial nitric oxide stimulated by erythrocyte-derived ATP using a microfluidic approach. *Anal Bioanal Chem* **2010**, *397* (8), 3369-3375.
33. Burnstock, G., Purinergic signalling: from discovery to current developments. *Exp Physiol* **2014**, *99* (1), 16-34.
34. Burnstock, G., Discovery of purinergic signalling, the initial resistance and current explosion of interest. *Br J Pharmacol* **2012**, *167* (2), 238-255.
35. Minneci, P. C.; Deans, K. J.; Shiva, S.; Zhi, H.; Banks, S. M.; Kern, S.; Natanson, C.; Solomon, S. B.; Gladwin, M. T., Nitrite reductase activity of hemoglobin as a systemic nitric oxide generator mechanism to detoxify plasma hemoglobin produced during hemolysis. *American journal of physiology. Heart and circulatory physiology* **2008**, *295* (2), H743-H754.
36. Gow, A. J.; Stamler, J. S., Reactions between nitric oxide and haemoglobin under physiological conditions. *Nature* **1998**, *391* (6663), 169-173.
37. Jia, L.; Bonaventura, C.; Bonaventura, J.; Stamler, J. S., S-nitrosohaemoglobin: a dynamic activity of blood involved in vascular control. *Nature* **1996**, *380*, 221-226.

38. Stamler, J. S.; Jia, L.; Eu, J. P.; McMahon, T. J.; Demchenko, I. T.; Bonaventura, J.; Gernert, K.; Piantadosi, C. A., Blood flow regulation by S-nitrosohemoglobin in the physiological oxygen gradient. *Science* **1997**, *276* (5321), 2034-2037.
39. Navarro, X.; Sutherland, D. E.; Kennedy, W. R., Long-term effects of pancreatic transplantation on diabetic neuropathy. *Ann Neurol* **1997**, *42* (5), 727-736.
40. Fiorina, P.; Folli, F.; Zerbini, G.; Maffi, P.; Gremizzi, C.; Di Carlo, V.; Socci, C.; Bertuzzi, F.; Kashgarian, M.; Secchi, A., Islet transplantation is associated with improvement of renal function among uremic patients with type I diabetes mellitus and kidney transplants. *J Am Soc Nephrol* **2003**, *14* (8), 2150-2158.
41. Pinger, C. W.; Entwistle, K. E.; Bell, T. M.; Liu, Y.; Spence, D. M., C-Peptide replacement therapy in type 1 diabetes: are we in the trough of disillusionment? *Mol Biosyst* **2017**, *13* (8), 1432-1437.
42. Lockwood, S. Y.; Summers, S.; Eggenberger, E.; Spence, D. M., An In Vitro Diagnostic for Multiple Sclerosis Based on C-peptide Binding to Erythrocytes. *EBioMedicine* **2016**, *11*, 249-252.
43. Hach, T.; Forst, T.; Kunt, T.; Ekberg, K.; Pflutzner, A.; Wahren, J., C-peptide and its C-terminal fragments improve erythrocyte deformability in type 1 diabetes patients. *Exp Diabetes Res* **2008**, *2008*, 730594.
44. Clark, J. L.; Cho, S.; Rubenstein, A. H.; Steiner, D. F., Isolation of a proinsulin connecting peptide fragment (C-peptide) from bovine and human pancreas. *Biochem Biophys Res Commun* **1969**, *35* (4), 456-461.
45. Rigler, R.; Pramanik, A.; Jonasson, P.; Kratz, G.; Jansson, O. T.; Nygren, P.; Stahl, S.; Ekberg, K.; Johansson, B.; Uhlen, S.; Uhlen, M.; Jornvall, H.; Wahren, J., Specific binding of proinsulin C-peptide to human cell membranes. *Proc Natl Acad Sci U S A* **1999**, *96* (23), 13318-13323.
46. Henriksson, M.; Pramanik, A.; Shafqat, J.; Zhong, Z.; Tally, M.; Ekberg, K.; Wahren, J.; Rigler, R.; Johansson, J.; Jornvall, H., Specific binding of proinsulin C-peptide to intact and to detergent-solubilized human skin fibroblasts. *Biochem Biophys Res Commun* **2001**, *280* (2), 423-427.
47. Liu, Y.; Chen, C.; Summers, S.; Medawala, W.; Spence, D. M., C-peptide and zinc delivery to erythrocytes requires the presence of albumin: implications in diabetes explored with a 3D-printed fluidic device. *Integr Biol (Camb)* **2015**, *7* (5), 534-543.
48. Meyer, J. A.; Froelich, J. M.; Reid, G. E.; Karunaratne, W. K.; Spence, D. M., Metal-activated C-peptide facilitates glucose clearance and the release of a nitric oxide stimulus via the GLUT1 transporter. *Diabetologia* **2008**, *51* (1), 175-182.
49. Sprague, R. S.; Olearczyk, J. J.; Spence, D. M.; Stephenson, A. H.; Sprung, R. W.; Lonigro, A. J., Extracellular ATP signaling in the rabbit lung: Erythrocytes as

determinants of vascular resistance. *American Journal of Physiology* **2003**, 285 (2, Pt. 2), H693-H700.

50. Meyer, J. Successful and Reproducible Bioactivity with C-peptide via Activation with Zinc. Michigan State University, 2009.

51. Letourneau, S. Delivery of Zinc to Red Blood Cells and the Downstream Effects in Multiple Sclerosis. Dissertation, Michigan State University, 2013.

Chapter 2 – Red Blood Cell GLUT1 Levels in Autoimmune Diseases

2.1 Introduction to Autoimmune Diseases

Immune systems of healthy individuals neutralize invaders of the body by sending cells throughout the body to bind to and inactivate foreign antigens. Autoimmune diseases consist of abnormal innate and adaptive immune responses to a normal part of the body, often leading to inflammation. It is unclear what triggers an autoimmune attack; however, certain traits make individuals more susceptible. Women encounter certain autoimmune diseases almost twice as often as men do, while some autoimmune diseases are hereditary.¹⁻³ It is suspected that environmental factors such as infections, diet, and chemical exposure may be involved in triggering an autoimmune disease; however, to date little has been proven. Although there are over 80 different classified autoimmune diseases,⁴ the work in this dissertation will focus on type 1 diabetes (T1D) and multiple sclerosis (MS).

2.1.1 Overview of Diabetes Mellitus

It is estimated by the Centers for Disease Control and Prevention (CDC) that more than 23 million Americans are diagnosed with diabetes, and another 7.2 million people are affected but currently undiagnosed.⁵ Diabetes mellitus, commonly referred to as diabetes, is a metabolic disease resulting from either low insulin production from damaged

pancreatic β -cells, or an improper response to the insulin produced by the body. The result of the disease is improper glucose utilization, leading to elevated blood glucose levels.

Insulin is a hormone produced by the islets of Langerhans in pancreatic β -cells that regulates the amount of glucose in the bloodstream. Glucose absorption into skeletal muscle, liver, and fat cells is accomplished through the activation of the glucose transporter 4 (GLUT4) protein by insulin.⁶⁻⁸ As insulin activates the translocation of GLUT4 to the cell membrane, glucose is transported through the protein, down the concentration gradient.⁷ If glucose is unable to be cleared from the bloodstream, hyperglycemic conditions arise, leading to long-term complications such as cardiovascular disease, retinopathy, neuropathy, and nephropathy.⁹

In healthy individuals, fasting plasma glucose levels fall between 70 and 100 mg/dL, or 3.8 and 5.6 mM. If fasting plasma glucose levels are greater than or equal to 126 mg/dL, or 7.0 mM, the person is termed hyperglycemic and diagnosed with diabetes.¹⁰ There are four main types of diabetes, T1D, Type 2 diabetes (T2D), gestational diabetes, and other types of diabetes. Each type of diabetes is characterized by differing mechanisms, but all involve hyperglycemia. Management of the disease focuses on maintaining healthy blood glucose levels, with specific treatments dependent on each patient. The following sections will describe the specific diagnoses of diabetes in greater detail.

2.1.1.1 Classifications and Diagnoses of Diabetes

T2D is the most common form of diabetes in the United States (about 90% of all diabetes cases) and is characterized by insulin resistance in the body.⁵ Occurring mostly in adults, T2D is primarily caused by lifestyle choices and genetics. Obesity, poor diet, stress, and lack of physical activity are the main factors in the development of T2D, and prior to a T2D diagnosis, most people are termed prediabetic. It is estimated that 84.1 million adults who are 18 and older are already in the prediabetic stage, which indicates a high risk for developing T2D; however, prediabetes is often reversible with strict diet and lifestyle changes.⁵ Specific ethnic groups, such as African Americans, Latinos, Native Americans, Alaskan natives, Asian Americans, and Native Hawaiians are more susceptible to T2D.⁹

The insulin resistance in T2D patients means that the insulin produced in the body is not as effective at stimulating glucose transport as it would be in a healthy person. Insulin resistance often leads to a reduction in insulin secretion in T2D, and a leading hypothesis for insulin resistance involves defective responses of insulin receptors.⁹

Medications such as metformin are often utilized to lower blood sugar in T2D patients. Metformin works by decreasing the production of glucose in the liver, leading to decreased overall blood sugar.¹¹ Similar medications increase insulin release, decrease the absorption of sugar, or make the body more sensitive to insulin.¹²⁻¹⁴ Insulin is not always used to treat T2D; however when it is, a long-acting form is used to supplement

the oral medications previously mentioned. In extreme cases, weight loss surgery in obese patients is an effective measure. After surgery, patients often have success maintaining healthy blood glucose levels, and long-term mortality is decreased.⁹

T1D, commonly referred to as juvenile diabetes, is classified as an autoimmune disease and involves the loss of insulin production through the destruction of pancreatic β -cells. Insulin and β -cells are destroyed by autoimmune processes involving β -cell autoantigens, macrophages, dendritic cells, B lymphocytes, and T lymphocytes, and this type of diabetes accounts for about 5% of all diabetes cases.^{5, 15} The exact etiology of the disease is incomplete; however, the leading hypothesis involves a genetic predisposition coupled with environmental factors such as viral infections or diet.⁹ Insulin supplementation is the main treatment for T1D, and frequent blood glucose monitoring must accompany insulin administration in order to verify that proper blood glucose levels are achieved.

Gestational diabetes occurs in about 2-10% of all pregnancies, and may disappear postpartum.^{5, 9} Resembling T2D, gestational diabetes involves a combination of inadequate insulin secretion and insulin resistance. Medical supervision is required throughout pregnancy; however, gestational diabetes is fully treatable with a proper diet, blood glucose monitoring, and in some cases insulin supplementation. Untreated gestational diabetes may risk the health of the mother or fetus. Risks to the mother include high blood pressure and preeclampsia, while risks to the fetus include high birth weight

and skeletal muscle malformations. After experiencing gestational diabetes, women have an approximately 7-fold increased risk of developing T2D postpartum.¹⁶

Along with the three previously mentioned diabetes diagnoses, there are many other specific forms of diabetes related to diseases where the pancreas becomes damaged, or the insulin levels within the body are altered due to certain hormones. The pancreas may become damaged in diseases such as pancreatitis, cystic fibrosis, or damage caused by trauma.¹⁷ Hormones that alter the insulin levels within the body include cortisol, growth hormone, and epinephrine. These hormones decrease the insulin sensitivity of cells, and cortisol increases the glucose production of the liver from glucagon, all of which lead to insulin resistance in the body.⁹ Table 2.1 summarizes the four types of diabetes described here.

Table 2.1 - Overview of the four main classifications of diabetes.

	Cause	Treatment
Type 1 Diabetes	A loss of insulin production through the destruction of pancreatic β -cells	Insulin administration
Type 2 Diabetes	Lifestyle choices and genetics causing insulin resistance in the body	Medications to increase insulin sensitivity and decrease blood glucose levels, along with a healthy lifestyle
Gestational Diabetes	Buildup of glucose in the bloodstream during pregnancy	Healthy lifestyle
Other forms of Diabetes	Damaged pancreas	Insulin administration and/or medications to increase insulin sensitivity and decrease blood glucose levels

When patients present with diabetic symptoms of hyperglycemia, physicians must distinguish between T1D and T2D before determining the most effective treatment process. Since the main difference between T1D patients and T2D patients is the functionality of the pancreatic β -cells, β -cell activity is tested to determine the correct diagnosis. Insulin has a half-life of about 10 minutes in the bloodstream, making it difficult to measure. However, C-peptide, a peptide secreted in equimolar amounts as insulin, has a half-life of about 30 minutes in the bloodstream, and is thus a more ideal candidate to measure and ultimately diagnose T1D or T2D.¹⁸ T1D patients will have very low (or nonexistent) concentrations of C-peptide due to their damaged β -cells, while T2D patients will have a significantly higher C-peptide concentration in their bloodstream.

2.1.1.2 Diabetic Complications

Complications are experienced by most people with diabetes, including retinopathy, neuropathy, and nephropathy. Retinopathy is any damage to the retina of the eye, which may lead to vision impairment or blindness. This will often occur due to retinal vascular disease or damage caused by insufficient blood flow.¹⁹ Insufficient blood flow results in a lack of oxygen delivered to the tissue, leading to the experienced symptoms. Diabetic retinopathy is the leading cause of blindness, and accounts for about 12% of blindness worldwide.²⁰⁻²¹ Within 20 years of a confirmed diabetic diagnoses, T1D patients will most likely experience retinopathy, while T2D patients usually experience retinopathy complications within 7 years of diagnosis.²⁰

Most diabetic patients also experience neuropathy to some degree. Neuropathy is classified as damage to the nervous system, which may affect various aspects of the body, depending on the nerves impacted; however, the legs and feet are most commonly affected.²² Similar to retinopathy, neuropathy is thought to be caused by hindered blood flow along with hyperglycemia. Duration of hyperglycemia along with genetic predisposition contribute to the extent of neuropathy experienced. Weakness and loss of sensation often occur in neuropathy, which lead to the majority of the non-traumatic amputations in the United States when combined with other poor blood flow conditions.²³

The greatest mortality rate among diabetic patients involves complications of nephropathy, or kidney dysfunction.²⁴ In the body, the kidneys are responsible for filtering blood and removing waste from the body via urine. Diabetic patients experience nephropathy due to microvasculature complications leading to altered pressure within the kidneys. This pressure change causes the common blood protein, albumin, to be secreted into the urine, leading to albuminuria.²⁵ As diabetic nephropathy persists in patients, it is the leading cause of kidney failure in the United States.²⁶ A summary of the diabetic complications discussed here is shown in Table 2.2.

Table 2.2 – Overview of common diabetic complications.

	Definition	Result	Cause
Retinopathy	Damage to the retina of the eye	Vision impairment or blindness	Insufficient blood flow
Neuropathy	Damage to the nervous system	Impaired movement or sensation to various parts of the body	Insufficient blood flow and hyperglycemia
Nephropathy	Kidney dysfunction	Albuminuria and eventual kidney failure	Insufficient blood flow

Although the three complications described above affect different organs or systems *in vivo*, each are thought to be derived from poor blood flow.²⁷⁻³⁰ These complications cannot be avoided in diabetic patients; however, it is thought that enhancing blood flow will help to alleviate some of these complications. Previous work has reported that red blood cells (RBCs) from T2D patients release significantly less adenosine triphosphate (ATP) compared to control RBCs,³¹ and as mentioned in Chapter 1, RBC-derived ATP

stimulates vasodilation through the production of endothelial nitric oxide (NO) (Figure 1.2). A treatment to enhance RBC ATP release from diabetic RBCs is predicted to greatly enhance the quality of life for diabetic patients by decreasing the symptoms of retinopathy, neuropathy, and nephropathy.

Long-term glucose monitoring is accomplished by measuring glycated hemoglobin (A1C) in the bloodstream, and A1C levels have been shown to be related to disease complications.³² Although A1C tests are the accepted method to determine long-term glucose levels, conditions such as anemia, pregnancy, and uremia may interfere with the test.³³ Researchers have since recommended glycated albumin as a measure of short-term glucose levels, and even potentially as a biomarker in diabetes.³³⁻³⁶ The glycation of bloodstream molecules and cells may be a cause of the decreased RBC deformability and sequential ATP release in diabetic patients, ultimately leading to the diabetic microvasculature complications. Studies have reported that diabetic RBCs are less deformable than control RBCs, which is related to RBC ATP release.³⁷⁻³⁹ This effect is proposed to be caused by hyperglycemic conditions in the bloodstream. However, this is not the case with all autoimmune diseases, as will be discussed in the next section.

2.1.2 Overview of Multiple Sclerosis

MS is an inflammatory autoimmune disease of the central nervous system. Debate on an autoimmune or immune-mediated classification of the disease is ongoing due to the lack

of an identified specific antigen; however, most experts believe it to be an autoimmune disease.⁴⁰ It is the most widespread disabling neurological condition of young adults, and while disease development can happen at any age, most people are diagnosed between the ages of 20 and 40.⁴¹ Hallmark features of the disease are blood brain barrier (BBB) breakdown and brain lesions.⁴²⁻⁴³ Lesions form as the myelin sheath covering the axons of nerve cells becomes damaged causing nerve signals to slow, leading to impaired coordination, motor skills, and cognition.^{42, 44} The myelin sheath is made up of lipids and proteins, such as myelin basic protein and proteolipid protein. The main function of the myelin sheath is to increase the speed of nerve signal propagation through nerve cells by inhibiting the electric current from leaving the axon. Figure 2.1 depicts a myelinated nerve cell, which make up the “white matter” of the brain due to their white color, while the “dark matter” of the brain is composed of mainly cell bodies and glial cells. Oligodendrocytes are the cells that make myelin, and their presence allows for remyelination in the central nervous system.

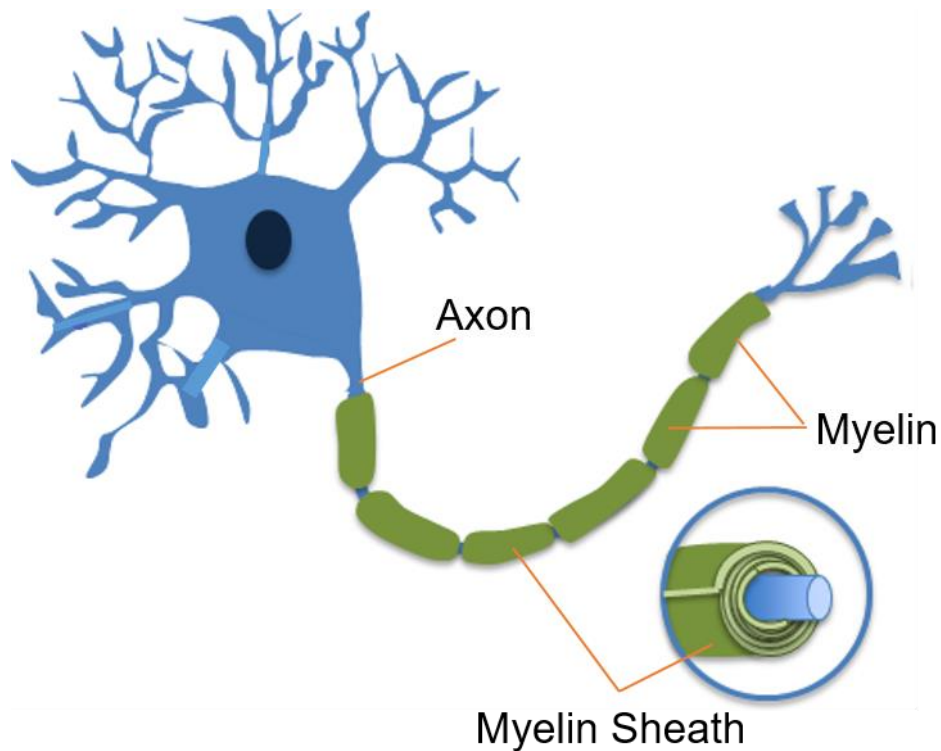


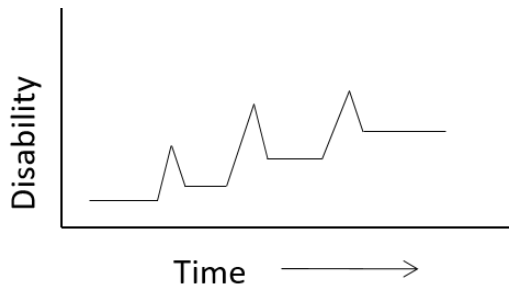
Figure 2.1 – Myelinated Nerve Cell. Axons of nerve cells are coated in myelin to increase the speed of nerve signal propagation from cell bodies to the axon terminals. This is done by inhibiting the electric current from leaving the axon while it propagates. When axons become demyelinated, lesions form and nerve signals are compromised, which is seen in MS.

It is estimated that 2.5 million people worldwide, and over 400,000 people in the United States are diagnosed with MS, and the total cost of MS in the United States alone is approaching \$12 billion per year.⁴⁵ The origin of MS is currently unknown; however, the incidence of MS is higher farther from the equator, and women are diagnosed almost twice as frequently as men.^{41, 46} People of Northern European descent have the highest risk of developing MS, regardless of where they live, and Native Americans, people of African descent, and people of Asian descent, appear to have the lowest risk.⁴⁷⁻⁴⁸

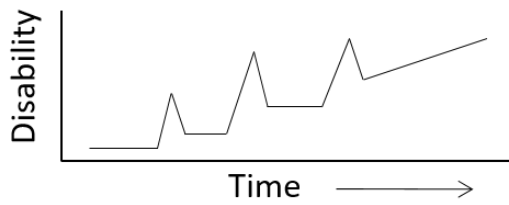
While MS is not an inherited disorder, research suggests a genetic predisposition to developing the disease. The offspring of an MS patient has a 2-3% risk of getting MS, and there is a 300-fold increase in instance of the disease if an identical twin has the disease.⁴⁹⁻⁵⁰ Oksenberg and colleagues found that the HLA-DRB1 and IL7R genes are associated with disease susceptibility, and although the etiology of MS is still unknown, a leading hypothesis involves the combination of a genetic predisposition and an environmental or viral factor.⁵¹ Certain infections such as Epstein-Barr, herpes, and varicella-zoster have been studied and are thought to possibly be part of the viral factor associated with MS onset.⁵²⁻⁵⁵ Because MS is an autoimmune disease, people with other autoimmune diseases such as T1D, thyroid disease, and inflammatory bowel disease, are found to have a slightly higher risk of developing MS.⁵⁶⁻⁵⁹

2.1.2.1 Diagnosis of Multiple Sclerosis

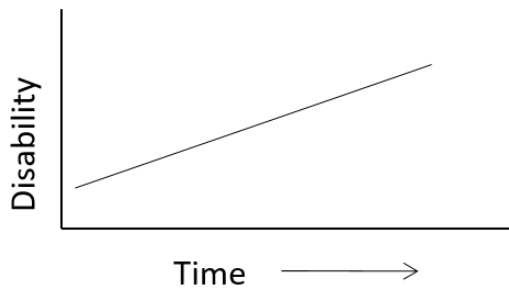
Many people who are diagnosed with MS originally present with a clinically isolated syndrome (CIS), which is a first episode of neurologic symptoms caused by inflammation and demyelination of the central nervous system (CNS).⁶⁰ By definition, the episode must last for at least 24 hours; however, a confirmed CIS diagnosis does not necessarily lead to a MS diagnosis. Results show that individuals with CIS who are treated with a MS disease-modifying therapy are seen to have a delayed onset of MS compared to CIS patients without early treatment.⁶¹



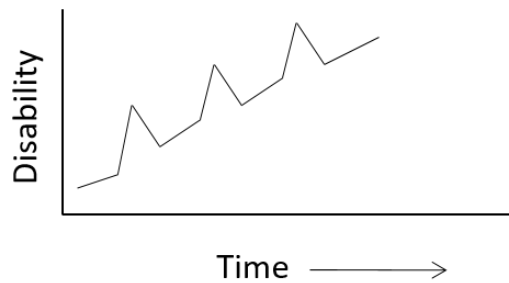
Relapsing-Remitting MS



Secondary-Progressive MS



Primary-Progressive MS



Progressive-Relapsing MS

Figure 2.2 – Depiction of the Four Types of MS. Relapsing-remitting MS (RRMS) consists of relapses followed by periods of disease remission. Secondary-progressive MS (SPMS) originally presents as RRMS and suddenly begins to decline without periods of remission. Primary-progressive MS (PPMS) consists of a steady increase in disability without attacks, and progressive-relapsing MS (PRMS) consists of a steady decline of health along with relapses.

There are four main types of MS, and the disease progression of each is shown in Figure 2.2. Relapsing-remitting MS (RRMS) is the most common type of MS diagnosed after a

CIS diagnosis, with approximately 80% of MS patients initially diagnosed with RRMS, and is characterized by relapses of increased disease activity followed by remissions where the disease does not progress.⁶⁰ Following a relapse, new symptoms may disappear without causing any increased disability, or they may only partially disappear, leading to an increase in overall disability.

Following a diagnosis of RRMS, if left untreated, about 50% of people transition to a diagnosis of secondary-progressive MS (SPMS) within 10 years of the initial diagnosis.^{43,60} SPMS is characterized by a progressive worsening of neurologic function and increased disability over time. Relapses do not necessarily occur during this course, but instead the disease worsens gradually. Approximately 15% of MS patients are originally diagnosed with primary-progressive MS (PPMS), which consists of a steady progression of the disease without early relapses or remissions.^{44, 63}

The final type of MS is progressive-relapsing MS (PRMS), and it is the rarest form of MS (about 5% of MS patients at onset).⁴³ PRMS is a combination of both RRMS and PPMS in that it consists of clear relapses along with a steady progression of the disease. Interestingly, about 10-20% of people with MS do not experience any symptoms and experience very little disease progression, while about 1% of patients develop a form of the disease that progresses very rapidly.⁴³

The disease progresses differently for each individual, which makes it a difficult disease to predict and diagnose, but there are common symptoms seen for most patients: fatigue,

blurred vision, numbness, dizziness, coordination problems, and muscle weakness. Less common symptoms experienced by patients include mood swings, depression, difficulty walking, and bladder dysfunction. Although MS causes painful and debilitating symptoms, studies conflict on whether the symptoms lead to a 10-12 year decreased life expectancy,⁶² or do not reduce life expectancy significantly compared to the general population.⁶³

2.1.2.2 Remyelination in Multiple Sclerosis

Lesions are repaired in the brain through remyelination. Studies have measured the reappearance of oligodendrocytes in active lesions of patients with early MS, indicating remyelination.⁶⁴ Oligodendrocyte presence may lead to partially or fully remyelinated lesions, termed 'shadow plaques', and studies report restoration of conduction due to remyelination in some lesions.⁶⁴⁻⁶⁵ Remyelination in later stages of MS is suggested to be scarce and not penetrate throughout the entire lesion well. Unfortunately, there is not yet a noninvasive method to measure remyelination, and studies must rely on histopathological analysis postmortem to determine the extent of remyelination. Patrikios *et al.* measured lesion remyelination in 51 autopsied MS patients, and found extensive remyelination in patients with both relapsing and progressive disease courses.⁶⁴ Extensive remyelination was found in 20% of the patients studied, and disease duration, along with age, were found to be associated with significantly more remyelinated lesions.⁶⁴ Work is ongoing to better understand spontaneous remyelination, and hopefully develop it into a therapy.

2.2 Glucose Metabolism in Autoimmune Diseases

Autoimmune diseases are characterized by T-cell mediated attacks throughout the body, and the metabolism of T-cells plays a large role in their ability to function. In the immune system, glucose serves as the primary source for the generation of ATP, which is essential for the survival of both resting and active T-cells.⁶⁶ GLUT1 is the primary glucose transporter in T-cells, and without its transport of glucose, T-cells would not be able to respond to foreign antigens properly. Glucose metabolism is of great importance in autoimmune diseases because cells involved in autoimmune attacks generally require an increased amount of energy due to their hyperactive nature. An overview of potential glucose metabolism pathways is depicted in Figure 2.3. The following sections will focus on the overall glucose metabolism of both diabetes and MS.

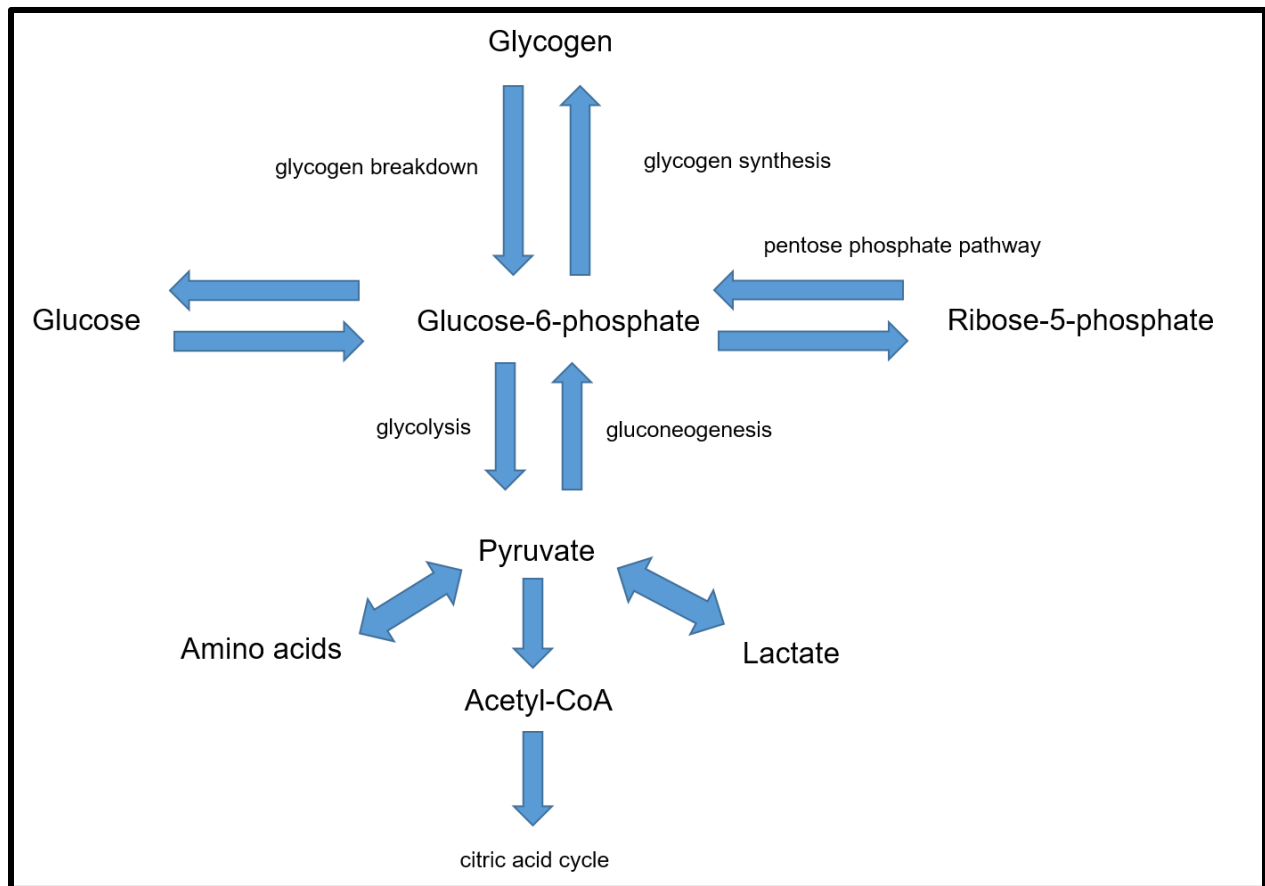


Figure 2.3 – Overview of Glucose Metabolism in the Body. Glucose can be metabolized in the body to glucose-6-phosphate which has three distinct fates: glycogen synthesis, glycolysis, or the pentose phosphate pathway. Glycogen is a form of glucose that is stored until required for energy. Glycolysis produces pyruvate which is involved in the synthesis of certain amino acids, is a precursor for the citric acid cycle, and is also involved in fermentation processes. The pentose phosphate pathway produces ribose-5-phosphate, and also protects cells against oxidative stress. Machinery of the cell dictates which method of glucose metabolism is required for cells at a given time for survival.

2.2.1 Glucose Metabolism in Diabetes

Diabetes consists of ineffective glucose metabolism within the body, contributing to the elevated blood glucose levels experienced with the disease. The disease also encompasses an improper balance of hormones. Without the proper balance of

hormones in the body, glucose is not metabolized properly.⁶⁷ It is essential to treat diabetes with a healthy lifestyle, medications, and/or insulin to maintain proper glucose metabolism *in vivo* and keep blood glucose levels within the healthy range. Although a very different disease, improper glucose metabolism has also been implicated in MS.

2.2.2 Glucose Metabolism in Multiple Sclerosis

RBCs do not contain mitochondria, and use glycolysis to produce ATP. Glycolysis begins with glucose entering the cell, and ends with the products of two ATP molecules and two pyruvate molecules. Various studies report defective pyruvate metabolism in MS patients,⁶⁸⁻⁷⁰ and Jones *et al.* reported an elevated blood pyruvate level in MS patients.⁶⁸ These reports suggest a mitochondrial dysfunction in MS patients, which may be significant with regard to the RBC. If there is mitochondria dysfunction within MS patients, the result may lead to an increased glucose metabolism within the RBC to compensate for the experienced dysfunction, or contrary to that, the RBCs may metabolize too much glucose, thereby hindering the amount metabolized by cells containing mitochondria, causing the elevated pyruvate level. It has been reported that MS RBCs release an elevated amount of ATP compared to control RBCs, which is thought to directly correlate to glucose metabolism within the cell.⁷¹ In addition to these results, a significant increase in the ATP content of RBCs from MS patients was measured compared to control RBCs after patients consumed 50 g of glucose.⁷² The work presented in this chapter

investigates the basal RBC GLUT1 content in the diseases of both T1D and MS, hoping to give insight as to characteristics of each disease with regard to the RBC.

2.3 Experimental

2.3.1 Isolation and Purification of Red Blood Cells

Whole blood was obtained through venipuncture into heparnized tubes from consented adults. The whole blood was centrifuged at 500g for 10 minutes, and the plasma and buffy coat were removed via aspiration. The remaining RBCs were resuspended and washed three times in a physiological salt solution (PSS) containing 4.7 mM KCl, 2.0 mM CaCl₂, 140.5 mM NaCl, 12 mM MgSO₄, 21.0 mM tris(hydroxymethyl) aminomethane, 5.5 mM dextrose and 0.5% bovine serum albumin at pH 7.4. RBCs were prepared on the day of experiment and used within 8 hours of collection. To determine the percentage of RBCs in the final sample, the hematocrit of the washed RBCs was measured using a hematocrit centrifuge (StatSpin CritSpin, Beckman Coulter, Brea, CA).

2.3.2 Preparation of Reagents

Distilled deionized water (DDW, 18.2 MΩ) was used for all experiments. 1 mL samples were prepared with 7% RBCs by volume in PSS. Tris buffered saline (TBS) was prepared by dissolving 2.4 g of Tris-hydrochloride and 29.2 g of sodium chloride in 1 L of water at a pH of 7.5, and tris buffered saline with tween (TBST) was prepared by mixing 500 mL of TBS with 250 μL of Tween-20 (Sigma Aldrich, St. Louis, MO). Bicarbonate buffer was

prepared by dissolving 4.1 g of sodium bicarbonate and 0.2 g of magnesium chloride in 500 mL of DDW. 10x running buffer was prepared by dissolving 144 g glycine, 30 g Tris, and 10 g SDS in 1 L of water, and 10x transfer buffer was prepared by dissolving 3 g Tris and 14.4 g glycine in 200 mL of methanol and 800 mL water at a pH of 8.3. Running buffer and transfer buffer were reused six times before disposal, and 500 mL of lysis buffer was prepared with 10 mM Tris HCl and 0.2 mM EDTA at a pH of 7.2 in DDW.

2.3.3 Preparing RBC Ghost Samples

To assess the membrane protein content of the RBC, the cytosolic contents of the cell was removed, and the remaining sample was termed a RBC ghost. After incubation and centrifugation, the supernatant of each sample was removed, and the remaining pelleted RBCs were lysed with 1 mL of lysis buffer. The samples were then placed on ice for 30 minutes and then centrifuged at 22,000g for 15 minutes at 4°C. The resulting supernatant was removed, and the pellet resuspended in 1 mL of lysis buffer. Once again, the samples were centrifuged at 22,000g and 4°C for 5 minutes, the supernatant was removed, and the RBCs were resuspended in lysis buffer. This process was repeated three times total or until no more hemoglobin (red color) was visible. Once all hemoglobin was removed, the remaining lysis buffer was removed, and the pellets were stored at -20°C.

2.3.4 SDS-PAGE and Coomassie Blue Staining

Sodium dodecyl sulfate polyacrylamide gel electrophoresis (SDS-PAGE) was used to separate the proteins of the RBC membrane prior to analysis. RBC ghosts diluted 1:200 in 2x Laemmli Sample Buffer (Bio-Rad, Hercules, CA) were loaded onto a 10% polyacrylamide gel. The gel was subjected to 80 V for 20 minutes, and then 120 V for about 90 minutes or until the buffer reached the bottom of the gel by visual inspection. Subsequent analysis consisted of either Coomassie Blue staining or Western Blot analysis.

Coomassie staining of the resulting gel was utilized to visualize all proteins. After separation, the gel was covered with 20 mL of Coomassie Brilliant Blue R-250 (Bio-Rad) and microwaved on high for 1 minute. The stain was discarded and 20 mL of destaining solution (Water/methanol/acetic acid: 50/40/10 v/v/v) was added to the gel to remove all nonspecifically bound stain. The gel was microwaved for 1 minute, and the destaining solution was removed. This process was repeated twice, and the resulting gel was allowed to incubate overnight in the destaining solution. A picture of the final gel was captured on a Gel Imaging System (Bio-Rad).

2.3.5 Western Blot Analysis

To specifically probe the GLUT1 content of the RBCs, Western Blot analysis was utilized. Once the proteins were separated by SDS-PAGE, all proteins were transferred to a polyvinylidene difluoride (PVDF) transfer membrane (EMD Millipore, Burlington, MA) overnight at 15 V for Western Blot analysis the following day. After transfer, the PVDF membrane was blocked for nonspecific binding for 1 hour with 5% dry milk in TBST. Primary antibodies for GLUT1 (Abcam, Cambridge, MA) and Spectrin Beta 1 (Novus Biological, Littleton, CO) (diluted 1:1000 in TBS with 0.75 g dry milk) were added and allowed to incubate for 1 hour at room temperature. After rinsing in TBST, anti-rabbit and anti-mouse secondary antibodies conjugated with alkaline phosphatase (Sigma Aldrich) (diluted 1:3000 in TBST with 0.75 g dry milk) were added and allowed to incubate an additional hour. Following a final rinsing step with TBST, incubation with 4.5 mg NBT (nitro-blue tetrazolium chloride) (Sigma Aldrich) and 2 mg BCIP (5-bromo-4-chloro-3'-indolyphosphate p-toluidine salt) (Sigma Aldrich) in 500 μ L N-dimethylformamide and 15 mL bicarbonate buffer produced a colorimetric indication of the GLUT1 and Beta Spectrin present. After color development, the membranes were rinsed in water and allowed to dry. Once dried, the membrane was scanned using an office scanner, and ImageJ software was used to quantify band thickness and intensity. GLUT1 band intensities were normalized to Beta Spectrin band intensities, and all samples were normalized to the control sample on each membrane.

2.4 Results

RBC GLUT1 content was evaluated initially by SDS-PAGE separation followed by Coomassie blue staining. A Coomassie blue stained gel is shown in Figure 2.4 and the proposed GLUT1 (54 kDa) and Beta Spectrin (246 kDa) bands are labeled.

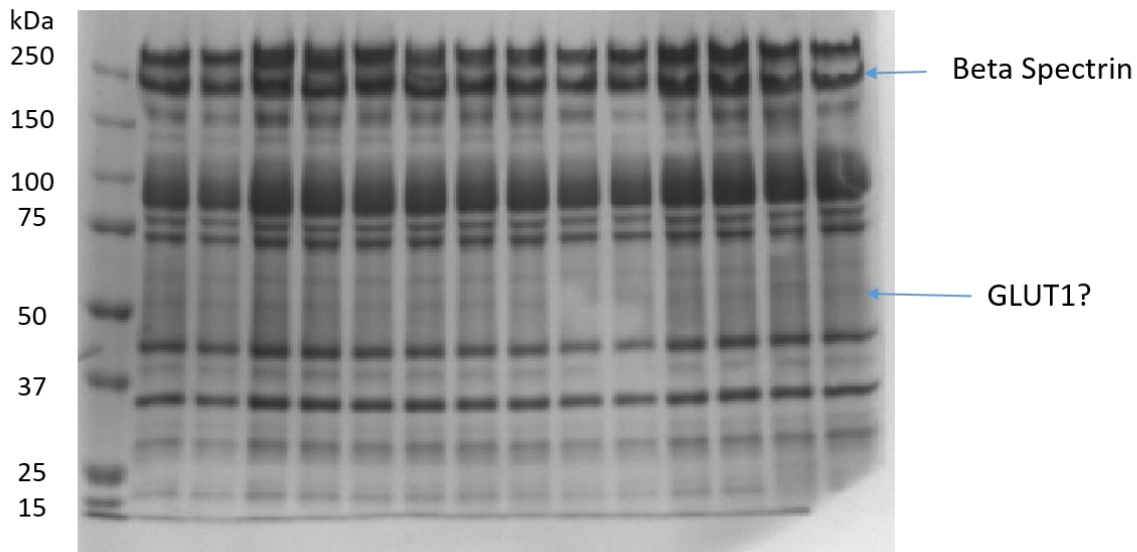


Figure 2.4 – RBC Membranes Separated by SDS-PAGE and Stained with Coomassie Blue. After the cytosolic contents was removed from the RBCs using lysis buffer, the resulting ghosts were subject to SDS-PAGE to separate the remaining proteins. Coomassie Blue staining was used to visualize all proteins present, and a molecular weight ladder was used to evaluate the mass of each protein band. Bands that are thought to be GLUT1 and Beta Spectrin are labeled above.

Although the labels are appropriate based on molecular weight, if any other proteins in the RBC membrane have the same or similar molecular weight, the analysis of GLUT1 would be compromised. Western Blot analysis was utilized to specifically probe only

GLUT1 and Beta Spectrin proteins (Figure 2.5). To verify that the GLUT1 and Beta Spectrin antibodies did not interfere with each other, probing the membrane with each antibody individually (Beta Spectrin: Figure 2.5A, GLUT1: Figure 2.5B) was performed and compared to a membrane probed with both antibodies simultaneously (Figure 2.5C). No interference between the two antibodies was detected, and all analyses consisted of both antibodies mixed and incubated together on the same membrane.

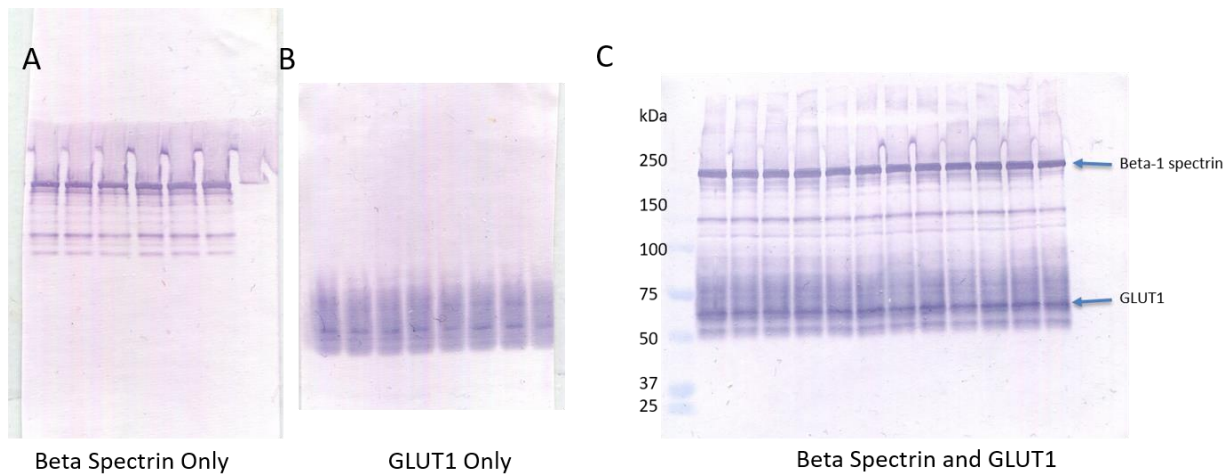


Figure 2.5 – Resulting Western Blots. Western Blot analysis was utilized to probe for Beta Spectrin and GLUT1. To confirm that the antibodies for Beta Spectrin and GLUT1 did not interfere with each other, they were initially probed on a membrane alone, and then probed simultaneously on the same membrane for comparison. A. Membrane probed for Beta Spectrin only. B. Membrane probed for GLUT1 only. C. Membrane probed for both Beta Spectrin and GLUT1 simultaneously. The resulting bands are labeled.

A significant difference in the RBC membrane GLUT1 content was measured in both MS and T1D RBCs compared to control RBCs when Western Blot analysis was used, shown in Figure 2.6. MS RBCs contain $23.3 \pm 4.8\%$ more GLUT1 at basal levels compared to control RBCs ($n = 12$ MS donors and 7 control donors), and T1D RBCs contained $23.6 \pm 4.2\%$ less GLUT1 than control RBCs ($n = 8$ T1D donors and 7 control donors).

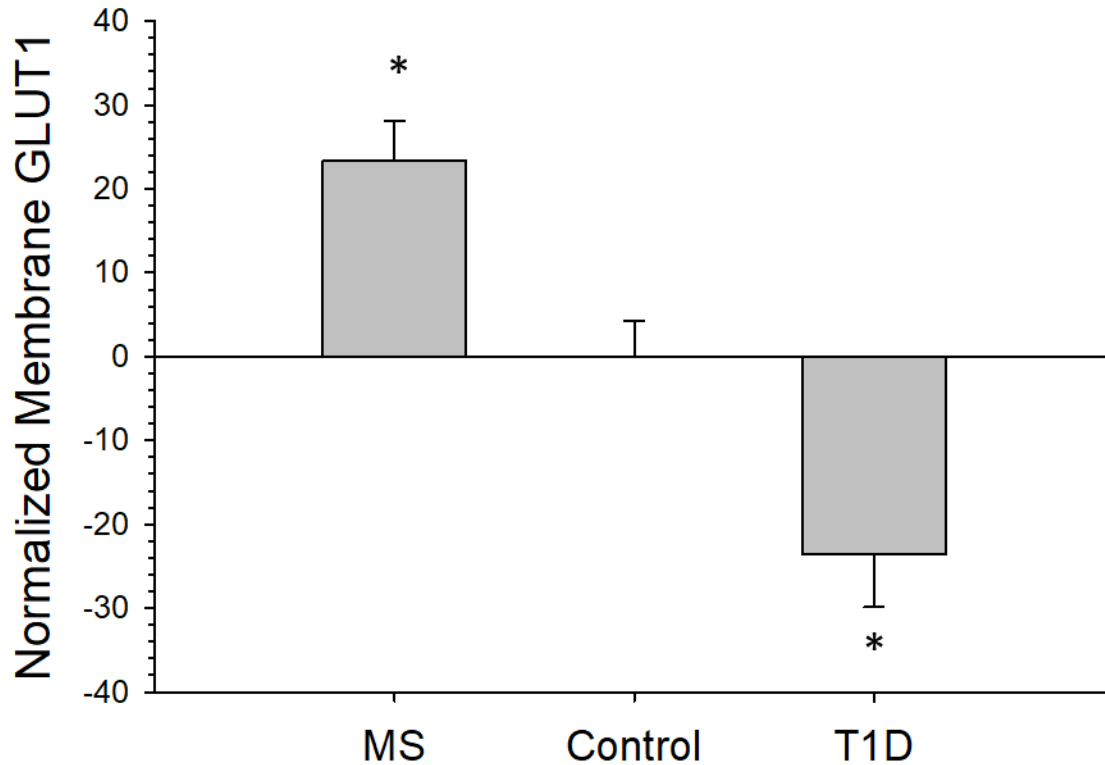


Figure 2.6 – Normalized RBC Membrane GLUT1 Content of MS, Control, and T1D RBCs. When the GLUT1 content of control and MS RBS were probed, a significant 23.3% increase in the RBC membrane GLUT1 content was measured by Western Blot analysis. Contrary to the MS RBCs, a significant 23.6% decrease in RBC GLUT1 content was measured in T1D RBCs compared to control RBCs. n = 12 MS donors, 7 control donors, and 8 T1D donors, error bars = SEM, * p < 0.05 to Control.

2.5 Discussion

Patients with autoimmune diseases have overactive immune systems, and glucose is the primary molecule that supplies energy for the immune system. It is thought that the

glucose transporter content of cells directly correlates with glucose transport into those cells and eventual cell metabolism. With that in mind, this work focused on the GLUT1 content of RBCs from control, MS, and T1D patients. GLUT1 is the primary glucose transporter on RBCs, and it follows that the amount of GLUT1 present on the RBC membrane correlates to overall cell metabolism.

Although both T1D and MS are autoimmune diseases, the RBC GLUT1 content of each disease were contradictory. While MS RBCs contained significantly more GLUT1 than control RBCs, T1D RBCs contained significantly less GLUT1. These results give insight to the amount of cell metabolism occurring within the RBCs of each disease. Even though both diseases have autoimmune classifications, T-cells are the main cells that are known to be overactive in autoimmune diseases, and less is known about RBC metabolism. The elevated GLUT1 measured in MS RBCs is thought to correlate with elevated ATP production and release by the cells. An increase in RBC ATP release was previously measured from MS RBCs by Letourneau *et al*,⁷¹ and literature reports that ATP stimulates the production of NO from endothelial cells *in vivo*.⁷³⁻⁷⁴ NO is damaging to the BBB at high concentrations, and NO metabolites have been found at elevated concentrations in the spinal fluid and urine of MS patients.⁷⁵⁻⁷⁷ Elevated RBC metabolism may be a key link to the BBB disruption experienced by MS patients, and methods to decrease RBC metabolism may prove to also decrease BBB damage.

Contrary to MS RBCs, T1D RBCs contain less GLUT1 than control RBCs, which may be associated with reports of decreased deformability of diabetic RBCs.^{38-39, 78} A decrease in RBC deformability has been reported to be related to a decrease in RBC ATP release, which has also been previously measured from diabetic RBCs.⁷⁹⁻⁸² As less GLUT1 is present on the diabetic RBC membrane, it is thought that less glucose will be able to enter the cell and undergo glycolysis to produce ATP within the cell. If less ATP is produced within the RBC, insufficient ATP will likely be released, and blood flow may be hindered due to a decrease in the endothelial NO production;⁸³⁻⁸⁴ leading to the experienced microvasculature complications in diabetes. A therapy to enhance microvasculature blood flow by enhancing the RBC GLUT1 content may prove successful at ameliorating the diabetic microvasculature complications previously described.

Even though MS and T1D RBCs contain different basal levels of GLUT1, it is clear that RBCs from both diseases have altered cell metabolism when compared to control RBCs. The rest of the work presented in this dissertation aims to more fully understand the RBCs of MS and T1D patients, and hopefully determine methods to manipulate the GLUT1 levels to more closely reflect levels of healthy individuals to better study and treat each disease.

REFERENCES

REFERENCES

1. Lockshin, M. D., Sex differences in autoimmune disease. *Lupus* **2006**, 15 (11), 753-756.
2. Ngo, S. T.; Steyn, F. J.; McCombe, P. A., Gender differences in autoimmune disease. *Front Neuroendocrinol* **2014**, 35 (3), 347-369.
3. Whitacre, C. C., Sex differences in autoimmune disease. *Nat Immunol* **2001**, 2 (9), 777-780.
4. Autoimmune Diseases - National Institute of Environmental Health Sciences. https://www.niehs.nih.gov/health/materials/autoimmune_diseases_508.pdf.
5. National Diabetes Statistics Report, 2017.
6. Kono, T.; Suzuki, K.; Dansey, L. E.; Robinson, F. W.; Blevins, T. L., Energy-dependent and protein synthesis-independent recycling of the insulin-sensitive glucose transport mechanism in fat cells. *J Biol Chem* **1981**, 256 (12), 6400-6407.
7. Brewer, P. D.; Habtemichael, E. N.; Romenskaia, I.; Mastick, C. C.; Coster, A. C., Insulin-regulated Glut4 translocation: membrane protein trafficking with six distinctive steps. *J Biol Chem* **2014**, 289 (25), 17280-17298.
8. Karnieli, E.; Zarnowski, M. J.; Hissin, P. J.; Simpson, I. A.; Salans, L. B.; Cushman, S. W., Insulin-stimulated translocation of glucose transport systems in the isolated rat adipose cell. Time course, reversal, insulin concentration dependency, and relationship to glucose transport activity. *J Biol Chem* **1981**, 256 (10), 4772-4777.
9. Poretsky, L., *Principles of diabetes mellitus*. 2nd ed.; Springer: New York, 2010; p xviii, 887.
10. Inzucchi, S. E., Clinical practice. Diagnosis of diabetes. *N Engl J Med* **2012**, 367 (6), 542-550.
11. Magalhaes, F. O.; Gouveia, L. M.; Torquato, M. T.; Paccola, G. M.; Piccinato, C. E.; Foss, M. C., Metformin increases blood flow and forearm glucose uptake in a group of non-obese type 2 diabetes patients. *Horm Metab Res* **2006**, 38 (8), 513-517.
12. Madison, L. L.; Combes, B.; Unger, R. H.; Kaplan, N., The relationship between the mechanism of action of the sulfonylureas and the secretion of insulin into the portal circulation. *Ann N Y Acad Sci* **1959**, 74 (3), 548-556.
13. Flemmer, M.; Scott, J., Mechanism of action of thiazolidinediones. *Curr Opin Investig Drugs* **2001**, 2 (11), 1564-1567.

14. American Diabetes, A., 7. Approaches to Glycemic Treatment. *Diabetes Care* **2016**, *39 Suppl 1*, S52-S59.
15. Yoon, J. W.; Jun, H. S., Autoimmune destruction of pancreatic beta cells. *Am J Ther* **2005**, *12* (6), 580-591.
16. Melchior, H.; Kurch-Bek, D.; Mund, M., The Prevalence of Gestational Diabetes. *Dtsch Arztebl Int* **2017**, *114* (24), 412-418.
17. American Diabetes, A., Diagnosis and classification of diabetes mellitus. *Diabetes Care* **2010**, *33 Suppl 1*, S62-S69.
18. Polonsky, K. S.; Rubenstein, A. H., C-peptide as a measure of the secretion and hepatic extraction of insulin. Pitfalls and limitations. *Diabetes* **1984**, *33* (5), 486-494.
19. Icks, A.; Trautner, C.; Haastert, B.; Berger, M.; Giani, G., Blindness due to diabetes: population-based age- and sex-specific incidence rates. *Diabet Med* **1997**, *14* (7), 571-575.
20. Keenan, H. A.; Costacou, T.; Sun, J. K.; Doria, A.; Cavallerano, J.; Coney, J.; Orchard, T. J.; Aiello, L. P.; King, G. L., Clinical factors associated with resistance to microvascular complications in diabetic patients of extreme disease duration: the 50-year medalist study. *Diabetes Care* **2007**, *30* (8), 1995-1997.
21. Sheetz, M. J.; King, G. L., Molecular understanding of hyperglycemia's adverse effects for diabetic complications. *JAMA* **2002**, *288* (20), 2579-2588.
22. Sugimoto, K.; Murakawa, Y.; Sima, A. A., Diabetic neuropathy--a continuing enigma. *Diabetes Metab Res Rev* **2000**, *16* (6), 408-433.
23. Boulton, A. J., Guidelines for diagnosis and outpatient management of diabetic peripheral neuropathy. European Association for the Study of Diabetes, Neurodiab. *Diabetes Metab* **1998**, *24 Suppl 3*, 55-65.
24. Nathan, D. M., Long-term complications of diabetes mellitus. *N Engl J Med* **1993**, *328* (23), 1676-1685.
25. Helal, I.; Fick-Brosnahan, G. M.; Reed-Gitomer, B.; Schrier, R. W., Glomerular hyperfiltration: definitions, mechanisms and clinical implications. *Nat Rev Nephrol* **2012**, *8* (5), 293-300.
26. Aoun, S.; Blacher, J.; Safar, M. E.; Mourad, J. J., Diabetes mellitus and renal failure: effects on large artery stiffness. *J Hum Hypertens* **2001**, *15* (10), 693-700.
27. McVeigh, G. E.; Brennan, G. M.; Johnston, G. D.; McDermott, B. J.; McGrath, L. T.; Henry, W. R.; Andrews, J. W.; Hayes, J. R., Impaired endothelium-dependent and independent vasodilation in patients with type 2 (non-insulin-dependent) diabetes mellitus. *Diabetologia* **1992**, *35* (8), 771-776.

28. Low, P. A.; Schmelzer, J. D.; Ward, K. K.; Curran, G. L.; Poduslo, J. F., Effect of Hyperbaric Oxygenation on Normal and Chronic Streptozotocin Diabetic Peripheral-Nerves. *Exp Neurol* **1988**, 99 (1), 201-212.
29. Pierce, E. A.; Avery, R. L.; Foley, E. D.; Aiello, L. P.; Smith, L. E. H., Vascular Endothelial Growth-Factor Vascular-Permeability Factor Expression in a Mouse Model of Retinal Neovascularization. *Proceedings of the National Academy of Sciences of the United States of America* **1995**, 92 (3), 905-909.
30. Craven, P. A.; Caines, M. A.; DeRubertis, F. R., Sequential alterations in glomerular prostaglandin and thromboxane synthesis in diabetic rats: relationship to the hyperfiltration of early diabetes. *Metabolism: clinical and experimental* **1987**, 36 (1), 95-103.
31. Subasinghe, W.; Spence, D. M., Simultaneous determination of cell aging and ATP release from erythrocytes and its implications in type 2 diabetes. *Anal Chim Acta* **2008**, 618 (2), 227-233.
32. Khaw, K. T.; Wareham, N.; Bingham, S.; Luben, R.; Welch, A.; Day, N., Association of hemoglobin A1c with cardiovascular disease and mortality in adults: the European prospective investigation into cancer in Norfolk. *Ann Intern Med* **2004**, 141 (6), 413-420.
33. Freitas, P. A. C.; Ehlert, L. R.; Camargo, J. L., Glycated albumin: a potential biomarker in diabetes. *Arch Endocrinol Metab* **2017**, 61 (3), 296-304.
34. Peacock, T. P.; Shihabi, Z. K.; Bleyer, A. J.; Dolbare, E. L.; Byers, J. R.; Knovich, M. A.; Calles-Escandon, J.; Russell, G. B.; Freedman, B. I., Comparison of glycated albumin and hemoglobin A(1c) levels in diabetic subjects on hemodialysis. *Kidney Int* **2008**, 73 (9), 1062-1068.
35. Inaba, M.; Okuno, S.; Kumeda, Y.; Yamada, S.; Imanishi, Y.; Tabata, T.; Okamura, M.; Okada, S.; Yamakawa, T.; Ishimura, E.; Nishizawa, Y.; Osaka, C. K. D. E. R. G., Glycated albumin is a better glycemic indicator than glycated hemoglobin values in hemodialysis patients with diabetes: effect of anemia and erythropoietin injection. *J Am Soc Nephrol* **2007**, 18 (3), 896-903.
36. Roohk, H. V.; Zaidi, A. R., A review of glycated albumin as an intermediate glycation index for controlling diabetes. *J Diabetes Sci Technol* **2008**, 2 (6), 1114-1121.
37. Sprague, R. S.; Ellsworth, M. L.; Stephenson, A. H.; Kleinhenz, M. E.; Lonigro, A. J., Deformation-induced ATP release from red blood cells requires CFTR activity. *Am J Physiol-Heart C* **1998**, 275 (5), H1726-H1732.
38. Brown, C. D.; Ghali, H. S.; Zhao, Z.; Thomas, L. L.; Friedman, E. A., Association of reduced red blood cell deformability and diabetic nephropathy. *Kidney Int* **2005**, 67 (1), 295-300.

39. McMillan, D. E.; Utterback, N. G.; La Puma, J., Reduced erythrocyte deformability in diabetes. *Diabetes* **1978**, 27 (9), 895-901.
40. Gulcher, J. R.; Vartanian, T.; Stefansson, K., Is Multiple-Sclerosis an Autoimmune-Disease. *Clin Neurosci* **1994**, 2 (3-4), 246-252.
41. Gorman, M. P.; Healy, B. C.; Polgar-Turcsanyi, M.; Chitnis, T., Increased relapse rate in pediatric-onset compared with adult-onset multiple sclerosis. *Arch Neurol* **2009**, 66 (1), 54-59.
42. Stadelmann, C.; Wegner, C.; Bruck, W., Inflammation, demyelination, and degeneration - recent insights from MS pathology. *Biochim Biophys Acta* **2011**, 1812 (2), 275-282.
43. Stuve, O.; Oksenberg, J., Multiple Sclerosis Overview. In *GeneReviews((R))*, Pagon, R. A.; Adam, M. P.; Ardinger, H. H.; Wallace, S. E.; Amemiya, A.; Bean, L. J. H.; Bird, T. D.; Ledbetter, N.; Mefford, H. C.; Smith, R. J. H.; Stephens, K., Eds. Seattle (WA), 1993.
44. Marrie, R. A.; Cohen, J.; Stuve, O.; Trojano, M.; Sorensen, P. S.; Reingold, S.; Cutter, G.; Reider, N., A systematic review of the incidence and prevalence of comorbidity in multiple sclerosis: overview. *Mult Scler* **2015**, 21 (3), 263-281.
45. Whetten-Goldstein, K.; Sloan, F. A.; Goldstein, L. B.; Kulas, E. D., A comprehensive assessment of the cost of multiple sclerosis in the United States. *Mult Scler* **1998**, 4 (5), 419-425.
46. Vukusic, S.; Confavreux, C., Pregnancy and multiple sclerosis: the children of PRIMS. *Clin Neurol Neurosurg* **2006**, 108 (3), 266-270.
47. Handel, A. E.; Giovannoni, G.; Ebers, G. C.; Ramagopalan, S. V., Environmental factors and their timing in adult-onset multiple sclerosis. *Nat Rev Neurol* **2010**, 6 (3), 156-166.
48. Pugliatti, M.; Sotgiu, S.; Rosati, G., The worldwide prevalence of multiple sclerosis. *Clin Neurol Neurosurg* **2002**, 104 (3), 182-191.
49. Sadovnick, A. D.; Ebers, G. C.; Dyment, D. A.; Risch, N. J., Evidence for genetic basis of multiple sclerosis. The Canadian Collaborative Study Group. *Lancet* **1996**, 347 (9017), 1728-1730.
50. Stuve, O.; Oksenberg, J., Multiple Sclerosis Overview. In *GeneReviews(R)*, Pagon, R. A.; Adam, M. P.; Ardinger, H. H.; Wallace, S. E.; Amemiya, A.; Bean, L. J. H.; Bird, T. D.; Fong, C. T.; Mefford, H. C.; Smith, R. J. H.; Stephens, K., Eds. Seattle (WA), 1993.

51. Oksenberg, J. R.; Baranzini, S. E.; Sawcer, S.; Hauser, S. L., The genetics of multiple sclerosis: SNPs to pathways to pathogenesis. *Nat Rev Genet* **2008**, 9 (7), 516-526.
52. Ascherio, A.; Munger, K. L.; Lennette, E. T.; Spiegelman, D.; Hernan, M. A.; Olek, M. J.; Hankinson, S. E.; Hunter, D. J., Epstein-Barr virus antibodies and risk of multiple sclerosis: a prospective study. *JAMA : the journal of the American Medical Association* **2001**, 286 (24), 3083-3088.
53. Felgenhauer, K.; Reiber, H., The diagnostic significance of antibody specificity indices in multiple sclerosis and herpes virus induced diseases of the nervous system. *Clin Investig* **1992**, 70 (1), 28-37.
54. Sospedra, M.; Martin, R., Immunology of Multiple Sclerosis. *Semin Neurol* **2016**, 36 (2), 115-127.
55. Sotelo, J.; Martinez-Palomo, A.; Ordonez, G.; Pineda, B., Varicella-zoster virus in cerebrospinal fluid at relapses of multiple sclerosis. *Annals of neurology* **2008**, 63 (3), 303-311.
56. Dorman, J. S.; Steenkiste, A. R.; Burke, J. P.; Songini, M., Type 1 diabetes and multiple sclerosis: together at last. *Diabetes Care* **2003**, 26 (11), 3192-3193.
57. International Multiple Sclerosis Genetics, C., The expanding genetic overlap between multiple sclerosis and type I diabetes. *Genes Immun* **2009**, 10 (1), 11-14.
58. Broadley, S. A.; Deans, J.; Sawcer, S. J.; Clayton, D.; Compston, D. A., Autoimmune disease in first-degree relatives of patients with multiple sclerosis. A UK survey. *Brain* **2000**, 123 (Pt 6), 1102-1111.
59. Kimura, K.; Hunter, S. F.; Thollander, M. S.; Loftus, E. V., Jr.; Melton, L. J., 3rd; O'Brien, P. C.; Rodriguez, M.; Phillips, S. F., Concurrence of inflammatory bowel disease and multiple sclerosis. *Mayo Clin Proc* **2000**, 75 (8), 802-806.
60. Miller, D.; Barkhof, F.; Montalban, X.; Thompson, A.; Filippi, M., Clinically isolated syndromes suggestive of multiple sclerosis, part I: natural history, pathogenesis, diagnosis, and prognosis. *Lancet Neurol* **2005**, 4 (5), 281-288.
61. Kappos, L.; Polman, C. H.; Freedman, M. S.; Edan, G.; Hartung, H. P.; Miller, D. H.; Montalban, X.; Barkhof, F.; Bauer, L.; Jakobs, P.; Pohl, C.; Sandbrink, R., Treatment with interferon beta-1b delays conversion to clinically definite and McDonald MS in patients with clinically isolated syndromes. *Neurology* **2006**, 67 (7), 1242-1249.
62. Bronnum-Hansen, H.; Koch-Henriksen, N.; Stenager, E., Trends in survival and cause of death in Danish patients with multiple sclerosis. *Brain* **2004**, 127 (Pt 4), 844-850.
63. Sadovnick, A. D.; Ebers, G. C.; Wilson, R. W.; Paty, D. W., Life expectancy in patients attending multiple sclerosis clinics. *Neurology* **1992**, 42 (5), 991-994.

64. Patrikios, P.; Stadelmann, C.; Kutzelnigg, A.; Rauschka, H.; Schmidbauer, M.; Laursen, H.; Sorensen, P. S.; Bruck, W.; Lucchinetti, C.; Lassmann, H., Remyelination is extensive in a subset of multiple sclerosis patients. *Brain* **2006**, *129* (Pt 12), 3165-3172.
65. Kriss, A.; Francis, D. A.; Cuendet, F.; Halliday, A. M.; Taylor, D. S.; Wilson, J.; Keast-Butler, J.; Batchelor, J. R.; McDonald, W. I., Recovery after optic neuritis in childhood. *J Neurol Neurosurg Psychiatry* **1988**, *51* (10), 1253-1258.
66. Yang, Z.; Matteson, E. L.; Goronzy, J. J.; Weyand, C. M., T-cell metabolism in autoimmune disease. *Arthritis Res Ther* **2015**, *17*, 29.
67. Yiu, K. H.; Tse, H. F., Specific role of impaired glucose metabolism and diabetes mellitus in endothelial progenitor cell characteristics and function. *Arterioscler Thromb Vasc Biol* **2014**, *34* (6), 1136-1143.
68. Jones, H. H.; Jones, H. H.; Bunch, L. D., Biochemical Studies in Multiple Sclerosis. *Ann Intern Med* **1950**, *33* (4), 831-840.
69. Jeanes, A. L.; Cumings, J. N., Some laboratory investigations in multiple sclerosis. *Confin Neurol* **1958**, *18* (6), 397-404.
70. Mathur, D.; Lopez-Rodas, G.; Casanova, B.; Marti, M. B., Perturbed glucose metabolism: insights into multiple sclerosis pathogenesis. *Front Neurol* **2014**, *5*.
71. Letourneau, S.; Hernandez, L.; Faris, A. N.; Spence, D. M., Evaluating the effects of estradiol on endothelial nitric oxide stimulated by erythrocyte-derived ATP using a microfluidic approach. *Anal Bioanal Chem* **2010**, *397* (8), 3369-3375.
72. Raczkiew.J; Leyko, W., Adenine Nucleotide Content of Erythrocytes of Multiple Sclerosis Patients. *Clin Chim Acta* **1966**, *14* (3), 408-409.
73. Smith, K. J.; Lassmann, H., The role of nitric oxide in multiple sclerosis. *Lancet Neurol* **2002**, *1* (4), 232-241.
74. Minagar, A.; Alexander, J. S., Blood-brain barrier disruption in multiple sclerosis. *Mult Scler* **2003**, *9* (6), 540-549.
75. Giovannoni, G., Cerebrospinal fluid and serum nitric oxide metabolites in patients with multiple sclerosis. *Mult Scler* **1998**, *4* (1), 27-30.
76. Giovannoni, G.; Heales, S. J. R.; Land, J. M.; Thompson, E. J., The potential role of nitric oxide in multiple sclerosis. *Multiple Sclerosis* **1998**, *4*, 212-216.
77. Giovannoni, G.; Silver, N. C.; O'Riordan, J.; Miller, R. F.; Heales, S. J.; Land, J. M.; Elliot, M.; Feldmann, M.; Miller, D. H.; Thompson, E. J., Increased urinary nitric oxide metabolites in patients with multiple sclerosis correlates with early and relapsing disease. *Mult Scler* **1999**, *5* (5), 335-341.

78. McMillan, D. E.; Gion, K. M., Glucosylated hemoglobin and reduced erythrocyte deformability in diabetes. *Horm Metab Res Suppl* **1981**, 11, 108-112.
79. Sprague, R. S.; Ellsworth, M. L.; Stephenson, A. H.; Kleinhenz, M. E.; Lonigro, A. J., Deformation-induced ATP release from red blood cells requires CFTR activity. *American Journal of Physiology* **1998**, 275 (5, Pt. 2), H1726-H1732.
80. Ellsworth, M. L.; Sprague, R. S., Regulation of blood flow distribution in skeletal muscle: role of erythrocyte-released ATP. *The Journal of physiology* **2012**, 590 (Pt 20), 4985-4991.
81. Meyer, J. A.; Subasinghe, W.; Sima, A. A. F.; Keltner, Z.; Reid, G. E.; Daleke, D.; Spence, D. M., Zinc-activated C-peptide resistance to the type 2 diabetic erythrocyte is associated with hyperglycemia-induced phosphatidylserine externalization and reversed by metformin. *Mol. BioSyst.* **2009**, 5 (10), 1157-1162.
82. Meyer, J. A.; Froelich, J. M.; Reid, G. E.; Karunarathne, W. K. A.; Spence, D. M., Metal-activated C-peptide facilitates glucose clearance and the release of a nitric oxide stimulus via the GLUT1 transporter. *Diabetologia* **2008**, 51 (1), 175-182.
83. Ellsworth, M. L.; Forrester, T.; Ellis, C. G.; Dietrich, H. H., The erythrocyte as a regulator of vascular tone. *The American journal of physiology* **1995**, 269 (6 Pt 2), H2155-H2161.
84. Sprague, R. S.; Ellsworth, M. L.; Stephenson, A. H.; Lonigro, A. J., ATP: the red blood cell link to NO and local control of the pulmonary circulation. *Am J Physiol* **1996**, 271 (6 Pt 2), H2717-H2722.

Chapter 3 – Effects of Multiple Sclerosis Therapies

3.1 Multiple Sclerosis Therapies

Although there is no current biomarker or cure for multiple sclerosis (MS), various medications are used to treat the disease, modify the disease course, and manage symptoms. Disease modifying therapies are the most common long-term MS treatment method, and have been shown to delay progression of the disease, reduce relapses, and limit new disease activity.¹ To date, there are 18 medications approved by the food and drug administration (FDA), including injectable, oral, and intravenous medications.²⁻⁴ The first MS disease modifying therapy was approved in 1993, and is in the interferon (IFN) drug class. IFNs are cytokines, and although their mechanism of action is not completely understood, it is thought that they inhibit the proliferation of T-cells and decrease the production of pro-inflammatory cytokines.¹

Although naturally present in all humans, IFNs used to treat MS are manufactured using recombinant DNA. There are currently four FDA-approved medications made from IFNs (Betaseron, Avonex, Rebif, and Extavia), all of which are injectable. IFN- β , the specific IFN utilized in each listed medication, is a protein comprised of two identical subunits and has three associated ligands: beta-D-glucose, 6-deoxy- α -d-glucose, and zinc ion. Avonex and Rebif are specifically IFN- β -1a, while Betaseron and Extavia are IFN- β -1b, the difference being the type of cell from which it is produced (IFN- β -1a, mammalian cells, IFN- β -1b, *E. coli*). Overall, IFNs reduce the relapse rate of patients with RRMS by about 30%.²⁻⁴

Glatiramer acetate (Copaxone) is the most commonly prescribed MS medication, and its treatment requires an injection three times per week or every day, depending on dosage. Approved by the FDA in 1996, this drug mimics myelin basic protein. The drug's effectiveness was discovered while treating experimental autoimmune encephalomyelitis (EAE), the animal model for MS.⁵ Glatiramer acetate reduced the severity of EAE in mice, which lead to its development for human use. Clinical trials have shown a 33% reduction in relapse rates, a reduction in disability, and a reduction in the number of enhancing lesions in RRMS patients treated with glatiramer acetate.⁵

Oral medications used to treat MS were introduced in 2010; the first was fingolimod (Gilenya). Fingolimod has been shown to reduce peripheral blood lymphocytes in both animal models and humans, and multiple studies report that the mechanism of action of fingolimod is correlated to G protein-coupled receptors (GPCRs) and altered lymphocyte trafficking.⁶⁻⁸ Teriflunomide (Aubagio) and dimethyl fumarate (Tecfidera) are the other FDA-approved oral medications to treat MS, and while their mechanisms of action are not identical, they both involve inhibiting immune cells.⁹⁻¹⁰

Although not thought to have any long-term benefit on MS, corticosteroids are commonly prescribed to MS patients to more quickly end exacerbations of the disease. Steroids are thought to end exacerbations by acting on the nucleus of cells to alter the inflammatory gene expression and decrease the pro-inflammatory protein expression in cells.¹¹⁻¹³ At high concentrations, steroids activate the expression of anti-inflammatory proteins such as I κ B and annexin I, leading to decreased overall inflammation.¹¹⁻¹³ These mechanisms

are depicted in Figure 3.1. High doses of intravenous steroid treatments for three to five days are commonly prescribed to reduce inflammation, and the main medications used are methylprednisolone (Soul-Medrol), prednisone (Deltasone), and adrenocorticotrophic hormone (ACTH Gel). Steroids are not exclusively prescribed to MS patients; other diseases such as asthma, rheumatoid arthritis, and lupus require steroid use to decrease inflammation and pain. Although beneficial at decreasing inflammation and pain, serious side effects such as hypertension, osteoporosis, weight gain, and hyperglycemia are experienced by patients being treated with steroids.¹⁴⁻¹⁶

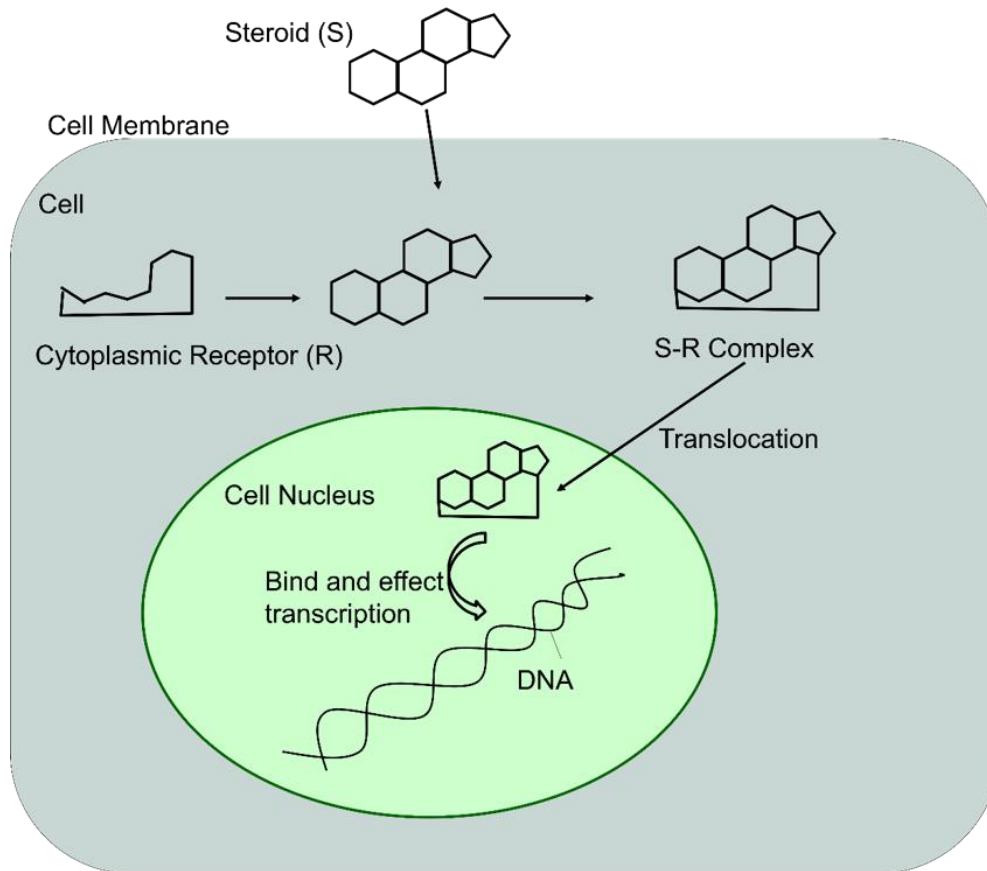


Figure 3.1 – Steroid Mechanism of Action. Steroids act on cells by binding to a cytoplasmic receptor within the cell, and the steroid-receptor complex is subsequently translocated to the nucleus of the cell. Once in the nucleus, the steroid-receptor complex binds to the promoter region of the target genes, resulting in regulation of gene expression. At low concentrations steroids decrease the expression of pro-inflammatory genes, and at high concentrations, steroids active the expression of anti-inflammatory genes.¹¹⁻¹³

Alternative treatments for MS are also widely used, such as herbal medicines, massage, acupuncture, and certain diets. Studies report that up to 70% of MS patients have tried one or more complementary and alternative medicine (CAM) treatment.¹⁷⁻¹⁹ To date there has been little research investigating the efficacy of CAM treatments, however many MS patients using CAMs report benefit from their usage.¹⁷ Most MS patients who use CAM

treatments combine them with conventional therapy instead of substituting conventional therapies altogether. One of the most promising CAM for MS treatment is a low-fat diet, or 'Swank diet'.¹⁷ The diet consists of consuming no more than 10-15 g of saturated fats per day, and was widely used before disease-modifying therapies were introduced. Literature reports a 50-year study beginning in 1953 that followed 144 MS patients; 70 consumed less than 20 g/day of fat ('good dieters'), and 74 consumed more than 20 g/day of fat ('bad dieters'). The study reported in the year 2000 there were only 15 survivors from the beginning 144 patients, and most of whom were currently healthy MS patients who were originally from the 'good dieters' group.^{17, 20} Although criticized for lacking a control group, this work along with others supports a diet low in saturated fats contributing to reduced disease activity and disability.²¹

Recent work has linked a ketogenic diet (KD) to decreased MS disease activity.²²⁻²⁴ Known for being a low carbohydrate diet, the KD consists of high fats and low carbohydrates, which forces the body to produce ketones from the breakdown of fats in the liver, rather than carbohydrates, to be used as energy. Carbohydrates cause the body to produce glucose, which is the easiest molecule for your body to convert and use as energy, which is why the KD is often referred to as a carbohydrate fast. The KD is widely used in patients with epilepsy and has been found to have neuroprotective effects and be both clinically safe and effective.²²⁻²⁴ When the KD was used to treat EAE, motor disability improved and periventricular lesions were reversed.²³ A decrease in reactive oxygen species and inflammatory cytokines were also measured due to a KD in EAE.²³ Studies report a neuroprotective role of ketone bodies in animal models of neurodegeneration

and are thought to have beneficial effects by stabilizing neurons and allowing their potassium ion channels to open.²⁵ In order to more fully understand how various therapies are effective in MS patients, certain traits of the disease must be understood.

3.2 Multiple Sclerosis Traits

3.2.1 ATP and NO in Multiple Sclerosis

Various reports in the literature implicate adenosine triphosphate (ATP) as being toxic to oligodendrocytes, the cells that make myelin.²⁶⁻²⁸ Oligodendrocytes have extremely high metabolic rates, which allows them to properly myelinate, and a large amount of ATP is necessary for their success. The ATP receptor on oligodendrocytes is the P2X7 receptor, which is a Ca²⁺-permeable purinergic receptor. Healthy ATP levels will reversibly open the P2X7 cation channel, while higher ATP levels cause sustained activation of the receptors, leading to oligodendrocyte excitotoxic cell death and lesions that are similar to those found in MS patients.^{26, 28} Interestingly, Matute *et al.* reported that chronic EAE treated with P2X7 antagonists reduced demyelination and ameliorated neurological symptoms.²⁷ In the same study, elevated levels of P2X7 RNA and protein levels were measured in axon tracts of patients with MS, implying oligodendrocyte P2X7 receptor signaling is enhanced in MS, which has potential to be used as a diagnostic tool.²⁶⁻²⁷ An additional study of interest investigated EAE induction in P2X7 deficient mice.²⁹ Interestingly, the P2X7 deficient mice were 4-times less likely to experience EAE symptoms compared to wild type mice, and although activated T-cells were detected in the brains of the deficient mice, no clinical signs of EAE were observed.²⁹ These results

together are indicative of ATP playing a large role in MS, suggesting that MS symptoms decrease as the amount of available P2X7 receptors decrease.

T-cells also contain purinergic receptors that bind ATP to open Ca^{2+} ion channels. Increased Ca^{2+} flux activates T-cells, and as in autoimmune disease, MS is associated with overly active T-cells. When activated, T-cells proliferate and enhance inflammation through cytokine secretion. ATP is a known stimulus of T-cell activation, but only at elevated levels (such as ATP release due to cell death), and although the origin of the excess ATP is debated, it is clear that overactive T-cells lead to the demyelination seen in MS.³⁰⁻³¹

If ATP is a determinant in MS, finding sources of this extracellular ATP is a key step towards understanding disease etiology. The Spence group has reported that RBCs from MS patients, in comparison to control RBCs, release elevated amounts of ATP when subjected to flow-induced shear stress.³² RBC ATP release is triggered by RBC deformation, and while debate is ongoing as to whether or not MS RBCs are more or less deformable than control RBCs,³³ an increase in RBC deformability is thought to lead to increased RBC ATP release.³⁴

As shown in Figure 2.1, RBC ATP release in the bloodstream begins with activation of the heterotrimeric G protein (G_i) by mechanical deformation.³⁴⁻³⁶ It follows that if RBC deformation activates G_i , the more deformable a RBC is, the more often G_i will become activated, leading to elevated ATP release. This mechanism is of particular importance in

MS due to the fact that ATP is a stimulus of endothelial NO production, which is a determinate in MS.³⁷

The production of NO is often thought of as a positive event in the bloodstream due to its role as a vessel dilator leading to improved blood flow;³⁸ however, reports suggest that high levels of NO break down the BBB and are detected in lesions of MS patients.³⁹⁻⁴⁰ Elevated levels of NO metabolites, such as nitrate and nitrite, have also been measured in the CSF and urine of MS patients.⁴¹⁻⁴⁴ Smith *et al.* studied the effect of NO on axons, and discovered that the combination of NO in lesions and normal impulse traffic of axons may cause degeneration of axons, leading to permanent damage and disability that accompanies MS.⁴⁵ Also noteworthy, the inducible form of nitric oxide synthase (iNOS) is able to release low micromolar concentrations of NO, which can impair mitochondrial metabolism, and is often found at sites of inflammation (lesions in MS patients).⁴⁶ Collectively, it is clear that ATP and NO play a role in MS. Most MS studies focus on the central nervous system, where most of the damage occurs in the disease; however, events in the bloodstream may play a larger role than previously anticipated in the onset of MS.

3.2.2 Zinc and Multiple Sclerosis

The role of zinc in MS has been debated for over 30 years. As an essential element for all organisms, and secreted from pancreatic beta cells into the bloodstream at very high concentrations, the immune system and nervous system rely heavily on zinc to properly

function. T-cell count, function, and activity are affected by zinc concentrations. Interestingly, there exists cluster studies that investigated geographical clusters of increased MS diagnoses with respect to trace metal contamination, specifically zinc. Results found that areas exposed to zinc contamination were associated with higher than normal MS diagnoses in people living in that area, suggesting elevated zinc levels may play a role in the etiology of the disease.⁴⁷⁻⁴⁸

Other studies involving zinc and MS were reported in the mid 1980's by Dore-Duffy; she reported that RBCs obtained from people with MS contain three times more zinc when compared to RBCs from healthy controls.⁴⁹ Studies from the Spence lab have also measured similar results, strongly implicating zinc in MS, specifically with regard to the RBC.⁵⁰ Researchers suggest hypotheses implicating zinc carrier protein affinity to RBCs, RBC increased affinity for zinc carrier proteins, or increased receptors for the complex on RBCs.^{49, 51} Work presented in this dissertation, along with previous work, attempts to better understand the role of the bloodstream in MS disease onset, and mechanisms of action of certain MS therapies.

3.2.3 Pregnancy and Multiple Sclerosis

Overall, women are diagnosed with MS twice as frequently as men, although men tend to have a more progressive disease state compared to women.⁵² In accordance with these statistics, it has been suggested that the Y chromosome may contain genes that

produce protective effects on MS. Conversely, the X chromosome may have promoting effects that lead to the discrepancy of MS diagnoses; however there is no conclusive evidence to date.⁵³

Before 1950, women with MS were advised to avoid pregnancy. It was thought that the combination of pregnancy and MS might increase relapse rate. It is now understood that pregnancy has a protective effect on MS symptoms, and various explanations have been implicated in its mechanism.⁵⁴⁻⁵⁶ Pregnancy is known to have an immunosuppressive effect on the body, due to the necessity of compatibility between the maternal immune system and the fetomaternal unit,⁵⁵ and high levels of immunologically active substances such as IFN- β , estrogen, and cortisol have been found in the serum of pregnant women.⁵⁶ An important immune shift during pregnancy is from helper T-cell1 (Th1) dominance, to Th2 dominance. Because of this T-cell shift, it follows that pregnancy improves Th1-dominant immune diseases such as rheumatoid arthritis and MS. The shift in immune cells is thought to be caused by high levels of estrogen and progesterone associated with pregnancy. Estrogens downregulate the activity of microglia, have been found to decrease the negative effects associated with EAE, and inhibit cell-mediated immunity at high concentrations.⁵⁵

The pregnancy in MS (PRIMS) study was conducted in 1998 by Confavreux *et al.*, and followed 254 pregnant women with MS during their pregnancies and for up to 12 months postpartum, documenting experienced relapses.⁵⁷ Results from this study found that MS

relapses decreased in number during pregnancy, particularly during the third trimester; however, relapses increased during the first three months postpartum before returning to the rate experienced before pregnancy. MS relapse rate during pregnancy correlates to steroid hormone levels such as the estrogens, estradiol and estriol. Both steroid hormones are present during pregnancy, and are at their highest during the third trimester. Noteworthy, the levels of both estradiol and estriol dramatically decrease after delivery, suggesting a direct correlation between estrogen content in the body and relapse rate.⁵⁸

Following the PRIMS study, Vukusic *et al.* studied the treatment of MS patients with progestin and estradiol immediately postpartum (when relapses recur), in the Prevention of Post-Partum Relapses with Progestin and Estradiol in Multiple Sclerosis (POPART'MUS) trial. High doses of progestin (10 mg daily) or estradiol (100 µg transdermal patch weekly) were administered to MS patients immediately following delivery in a randomized, placebo-controlled and double-blind clinical trial. The trial consisted of 202 patients, and researchers anticipated a decrease in relapse rate.⁵⁹ Unfortunately, the trial was stopped early in October 2011 due to no significant difference in relapse rate between control and treated groups. A possible explanation could be that the dose of steroids used in the study was not sufficient. Regardless, researchers agree that the role of steroids should be further studied with respect to MS.⁵⁹⁻⁶⁰

Due to the sex discrepancy and results from the PRIMIS study, Sicotte *et al.* investigated the treatment of female MS patients with 8 mg/day of oral estriol.⁶⁰ The study reported a significant decrease in enhancing lesions with estriol treatment, and when treatment was stopped, the lesions increased to levels seen before treatment.⁶⁰ To investigate if estriol treatment is gender specific, Palaszynski *et al.* investigated the effect of estriol on male and female EAE in mice.⁶¹ Results concluded that a decrease in EAE severity was measured due to estriol treatment in both female and male mice.⁶¹ Proinflammatory cytokine production also decreased with estriol treatment in both male and female EAE, suggesting a significant role for the sex steroid in both males and females with MS.⁶¹

The Spence lab investigated the *in vitro* effects of estradiol on RBC ATP release and subsequent endothelial NO production from bovine pulmonary arterial endothelial cells (bPAECs).³² RBCs from MS patients release significantly more ATP (375 ± 51 nM) when subjected to flow induced shear stress compared to control RBCs (138 ± 21 nM). Furthermore, the ATP release, along with the subsequent endothelial NO production, was attenuated almost 40% when the controls RBCs were treated with estradiol.⁵⁰ Although estradiol-treated MS RBCs were not studied, a similar trend is hypothesized due to the suggested mechanism of action within the RBC.³²

Although estrogens are not currently an approved MS therapy, other steroids, such as prednisone, are commonly prescribed to alleviate MS symptoms. Avila-Ornelas *et al.* reported a statistically significant benefit of 1 g of the intravenous steroid methylprednisolone (used to treat acute MS relapses) in preventing MS relapses after

delivery.⁶² Although sex steroids were not used, sex steroids such as estradiol are similar in structure to methylprednisolone, suggesting their effect on cells may be similar, even though their structures are different.

Steroid treatments are successful in decreasing inflammation and pain; however, hypertension is known to be a common side effect.^{14-15, 63} Steroids reduce inflammation by decreasing the pro-inflammatory protein expression of cells, and at high concentrations activate the expression of anti-inflammatory proteins in cells.¹¹⁻¹² Although this is the accepted mechanism of action, it is only relevant to cells containing a nucleus, which does not include RBCs. Any effect steroids have on RBCs must be through a different mechanism of action.

To further investigate how steroids affect RBCs and the downstream mechanisms, studies involving cell-to-cell communication between RBCs and endothelial cells are necessary. Previous work utilized soft lithography and poly(dimethylsiloxane) (PDMS) to create microfluidic devices that allowed RBCs to flow in channels beneath bPAECs, separated by a membrane. This set-up allowed for an *in vitro* mimic of *in vivo* conditions within blood vessels; however, the devices proved to be difficult to produce and reuse, which led to alternate methods, discussed in the following section.

3.3 3D Printed Device and Design for Experimental Analysis

3D printing has been in existence for nearly 30 years, and is very popular in the fields of engineering and biomedical sciences.⁶⁴ The fabrication process involves using computer aided design (CAD) software to create models that are saved as .STL (Standard Tessellation Language) files and are compatible with a 3D printer. The .STL file triangulates the design and allows the 3D printer to read the design as coordinates, and the printing process uses additive manufacturing to build a 3D model one layer at a time.

After realizing the shortcomings of PDMS devices, the Spence group began utilizing 3D printing to create a device to mimic *in vivo* circulatory vessels. The Connex PolyJet 3D printer available in the Department of Electrical and Computer Engineering at Michigan State University was used for this research. The printer contains a nozzle that lays down a layer of monomer, and then cures that layer using UV light. This process occurs many times until the object is finished. As the object is built, support material can be utilized to create void spaces that can be cleared out using high-pressure water after printing. The ability to design all specifications of an object makes 3D printing is a preferable technique compared to soft polymer lithography.

Human resistance vessels range in size from about 10 – 200 μm in diameter, which cannot be created with this 3D printer. The resolution of the printer available for the work reported here is 100 μm in the x, y direction, and 16 μm in the z direction. In order to guarantee consistent and reproducible channels throughout the device, all channels were

created 2 mm in diameter. Although not directly mimicking microfluidic conditions, fluidic conditions simulating the *in vivo* shear stress experience by RBCs were still achieved.

The device printed for this work contains 6 channels to allow for high throughput, all with two detection wells containing a membrane for separation. RBCs were circulated through the channels using a peristaltic pump and tygon tubing, creating a closed-loop system, and as RBCs released ATP due to flow induced shear stress, the released ATP diffused into the buffer-filled detection wells to be measured.

bPAECs were also cultured in the detection well to allow for cell-to-cell communication between RBCs and the bPAECs. As the RBC-released ATP bound to the endothelial P2Y receptors, NO was produced and detected using a fluorescent probe. Although not the first device to allow for cell-to-cell communication, the ability for .STL files to be amenable to any 3D printer allows for standardization and more consistent results between various laboratories.

3.4 Experimental

3.4.1 Isolation and Purification of Red Blood Cells

Whole blood was obtained from consenting donors through venipuncture, and collected into heparinized tubes. The whole blood was centrifuged at 500g for 10 minutes, and the plasma and buffy coat removed via aspiration. The remaining RBCs were resuspended and washed three times in a physiological salt solution (PSS) containing 4.7 mM KCl, 2.0

mM CaCl₂, 140.5 mM NaCl, 12 mM MgSO₄, 21.0 mM tris(hydroxymethyl) aminomethane, 5.5 mM dextrose, and 0.5% bovine serum albumin at pH 7.4. RBCs were prepared the day of the experiment and used within 8 hours of collection. To determine the percentage of RBCs in the final sample, the hematocrit of the washed RBCs was measured using a StatSpin CritSpin hematocrit centrifuge (Beckman Coulter, Brea, CA).

3.4.2 Preparation of Reagents

18.2 MΩ distilled deionized water (DDW) was used for all experiments. Estriol (Sigma Aldrich, St. Louis, MO) stock solutions were prepared by dissolving 2.9 mg in 0.5 mL dimethyl sulfoxide (DMSO, EMD Chemicals, Gibbstown, NJ) and two serial dilutions were performed in PSS to make 50 μM (12.5 μL of the stock solution in 5 mL of PSS) and 0.5 μM (10 μL of the 50 μM solution in 990 μL of PSS) solutions. Prednisolone, the active form of prednisone, (Sigma Aldrich) stock solutions were prepared by dissolving 2.4 mg in 0.5 mL DMSO, and working solutions were made by diluting the stock to 0.5 mM in PSS (38 μL in 962 μL PSS). A stock solution of Zn²⁺ was prepared by dissolving 0.02 g Zinc (II) chloride (Jade Scientific, Canton, MI) in 100 nM DDW and diluting to 800 nM in DDW, and the initial ⁶⁵Zn²⁺ stock was prepared by diluting 500 μCi of ⁶⁵ZnCl₂ in 30 mL DDW (80 μM), and sequential dilutions were prepared in DDW (10 μL in 990 μL DDW).

Crude C-peptide (80% pure, Peptide 2.0, Chantilly, VA) was purified using reverse-phase high performance liquid chromatography (HPLC) and the parameters shown in Table 3.1. The purified C-peptide was subsequently lyophilized overnight prior to dissolution of 5 mg

in 5 mL DDW. The resulting C-peptide purity was verified using HPLC- mass spectrometry, and a final 8 μ M stock solution was prepared in DDW and used for all experiments (121 μ L in 5 mL DDW).

Hanks' balanced salt solution (HBSS) was prepared by dissolving Hanks' Balanced Salts (Sigma Aldrich) in 1.0 L DDW. A stock luciferin/luciferase solution was prepared by dissolving 20 mg of Luciferin (Golden Bio, Olivette, MO) and 100 mg firefly lantern extract (Sigma Aldrich) in 10 mL DDW. NO detection utilized a stock solution of 4-amino-5-methylamino-2',7'-difluorescein (DAF-FM, Life Technologies, Waltman, MO), prepared by dissolving 1 mg of DAF-FM in 288 μ L DMSO and diluting to 5 μ M in HBSS. A PPADS (pyridoxalphosphate-6-azophenyl-2', 4'-disulfonic acid, Abcam, Cambridge, MA) working solution of 10 mM was prepared by diluting a 100 mM stock (50 mg PPADS in 1 mL DMSO) in HBSS.

Table 3.1 – HPLC gradient method C-peptide purification.

Time (min)	Flow Rate (mL/min)	% Solvent A	%Solvent B
0	5	100	0
5	5	60	40
30	5	50	50
40	5	0	100
45	5	0	100
50	5	100	0
55	5	stop	stop

Solvent A: 0.1% HPLC-grade trifluoroacetic acid (TFA) in HPLC-grade water

Solvent B: 0.089% TFA + 60% HPLC-grade Acetonitrile in HPLC-grade water

Flow Rate: 5 mL/min

Column: Waters Atlantis T3 OBD Prep Column. 10 mm x 150 mm.

The following reagents were prepared and used for all Western Blot analysis: Tris buffered saline (TBS) was prepared by dissolving 2.4 g of Tris-hydrochloride and 29.2 g of sodium chloride in 1 L of water at a pH of 7.5, and Tris buffered saline with Tween (TBST) was prepared by mixing 500 mL of TBS with 250 μ L of Tween-20 (Sigma Aldrich). Bicarbonate buffer was prepared by dissolving 4.13 g of sodium bicarbonate and 0.24 g of magnesium chloride in 500 mL of water. 10x running buffer was prepared by dissolving 144 g glycine, 30.2 g UltraPure Tris, and 10 g SDS in 1 L of water, and 10x transfer buffer was prepared by dissolving 3.0 g UltraPure Tris and 14.4 g glycine in 200 mL of methanol and 800 mL water at a pH of 8.3. Running buffer and transfer buffer were reused six times before disposal, and 500 mL of lysis buffer were prepared with 10 mM UltraPure Tris HCl and 0.2 mM EDTA at a pH of 7.2 in DDW.

3.4.3 Red Blood Cell Prednisolone and Estriol Treatment

RBC samples (1 mL total volume) were prepared at 7% hematocrit with varying concentrations of estriol or prednisolone. The estriol concentrations reflect levels of estriol per RBC seen during pregnancy. Scaled to the 7% RBC samples used throughout these studies, estriol is present at 7 nM in a healthy female, 30 nM is present during early pregnancy, and up to 0.5 μM is present in late pregnancy.⁶⁰ Samples prepared throughout these studies reflected these estriol concentrations along with additional concentrations for resolution.

Prednisolone is the active form of prednisone, which is commonly prescribed to MS patients to help with symptoms of acute relapses. A common dosage prescribed is between 500 and 1000 mg once daily for three to five days total.⁶⁵ Scaling to proper steroid concentration per RBC, the appropriate physiologically relevant prednisolone concentrations fall within a range of 50 – 100 μM for a 7% RBC sample. Lower prednisolone concentrations were also examined in this work for full analysis.

Samples 1 mL in total volume were prepared by adding the steroid to a 1.6 mL sample vial, followed by PSS and then enough RBCs to result in a 7% RBC solution (about 7.8×10^8 cells) prior to a 45-minute incubation at 37°C before flowing through the 3D printed device. All NO experiments required a washing of the RBCs after the initial 45-minute incubation, which consisted of centrifugation at 500g at 25°C for 5 minutes followed by 850 μL of the supernatant replaced with fresh PSS.

When samples required C-peptide and Zn^{2+} addition, the samples were centrifuged at 500g for 5 minutes after the initial 45-minute incubation, and 840 μ L of the supernatant were replaced with 790 μ L of fresh PSS. 50 μ L of a 400 nM C-peptide and Zn^{2+} mixture were subsequently added to each sample, followed by a 2 hour incubation at 37°C prior to sample analysis.

3.4.4 3D Printed Device Preparation

Autodesk Inventor software was used to create a model prototype of the device. The model was then saved as a .STL file and sent to the 3D printer (Objet Connex 350) housed in the Department of Electrical and Computer Engineering. Once printed, a high-pressure water stream was used to remove support material before utilizing the device for experiments. The device was made of VeroClear material (Stratasys Ltd, Eden Prairie, MN), and a schematic drawing of the device along with dimensions is shown in Figure 3.2. While the exact composition of the VeroClear material is proprietary, it approximately contains isobornyl acrylate (15-30%), acrylic monomer (15-30%), urethane acrylate (10-30%), acrylic monomer (5-10; 10-15%), epoxy acrylate (5-10; 10-15%), acrylate oligomer (5-10; 10-15%), and photoinitiator (0.1-1; 1-2%). Samples were circulated by a peristaltic pump (IDEX Health & Science LLC, Oak Harbor, WA) below inserts containing a 0.4 μ m polyester membrane (Sterlitech, Kent, WA). All membranes were in direct contact with the flowing sample to aid in diffusion, and a unique feature of the device is that when finger tight fittings were attached to the end of each channel, the device was the exact size of a 96 well plate. This design allowed for ease of

measurements using a plate reader, as the device fit directly into the instrument for detection following flow.

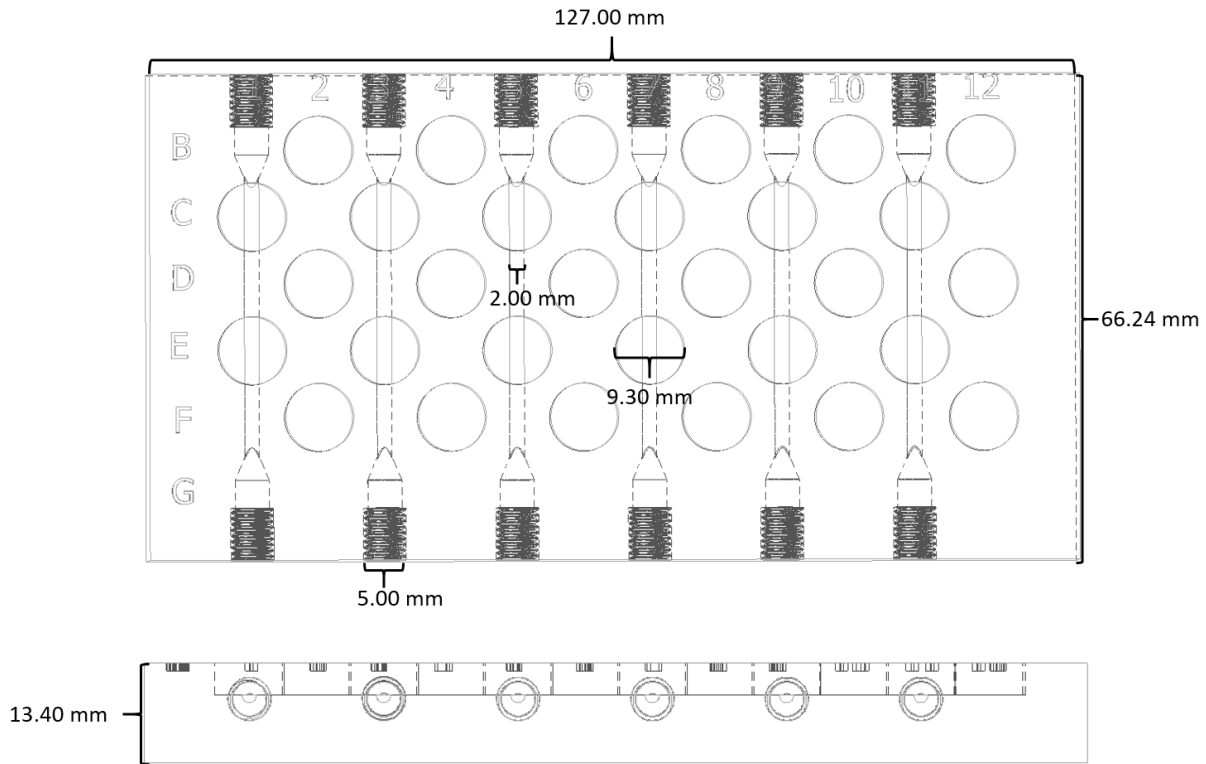


Figure 3.2 – 3D Printed Device Design and Dimensions. The device used for all ATP and NO measurements is shown above. Six channels allow for high throughput, and each channel can hold two membrane inserts. The dimensions of the device are 127.00 mm x 66.24 mm x 13.40 mm. Each channel is 2.00 mm in diameter, and a membrane insert with a diameter of 9.30 mm is compatible. The ends of each channel contain threads compatible with commercial finger tight fittings. When each channel contains two finger tight fittings, the device is the same size as a 96-well plate and can be integrated into a plate reader for detection.

3.4.5 ATP Detection Procedure

The luciferin/luciferase chemiluminescent assay was utilized to determine the amount of ATP released from RBCs. Samples were prepared and incubated prior to circulation through the 3D printed device at a rate of 250 $\mu\text{L}/\text{min}$. As the RBCs were subjected to shear stress, the released ATP diffused through the porous polyester membrane (0.4 μm pore size, Sterlitech, Kent, WA) into 100 μL of PSS loaded above the membrane. After 20 minutes of circulation, 10 μL of the luciferin/luciferase solution were added to the transwell insert, and the chemiluminescence intensity was detected exactly 20 seconds later using a Spectra Max M4 plate reader (Molecular Devices, San Jose, CA). The entire experimental set-up is shown in Figure 3.3, and the reaction measured is depicted in Figure 3.4. ATP standards were circulated under identical conditions in order to quantify the ATP release.

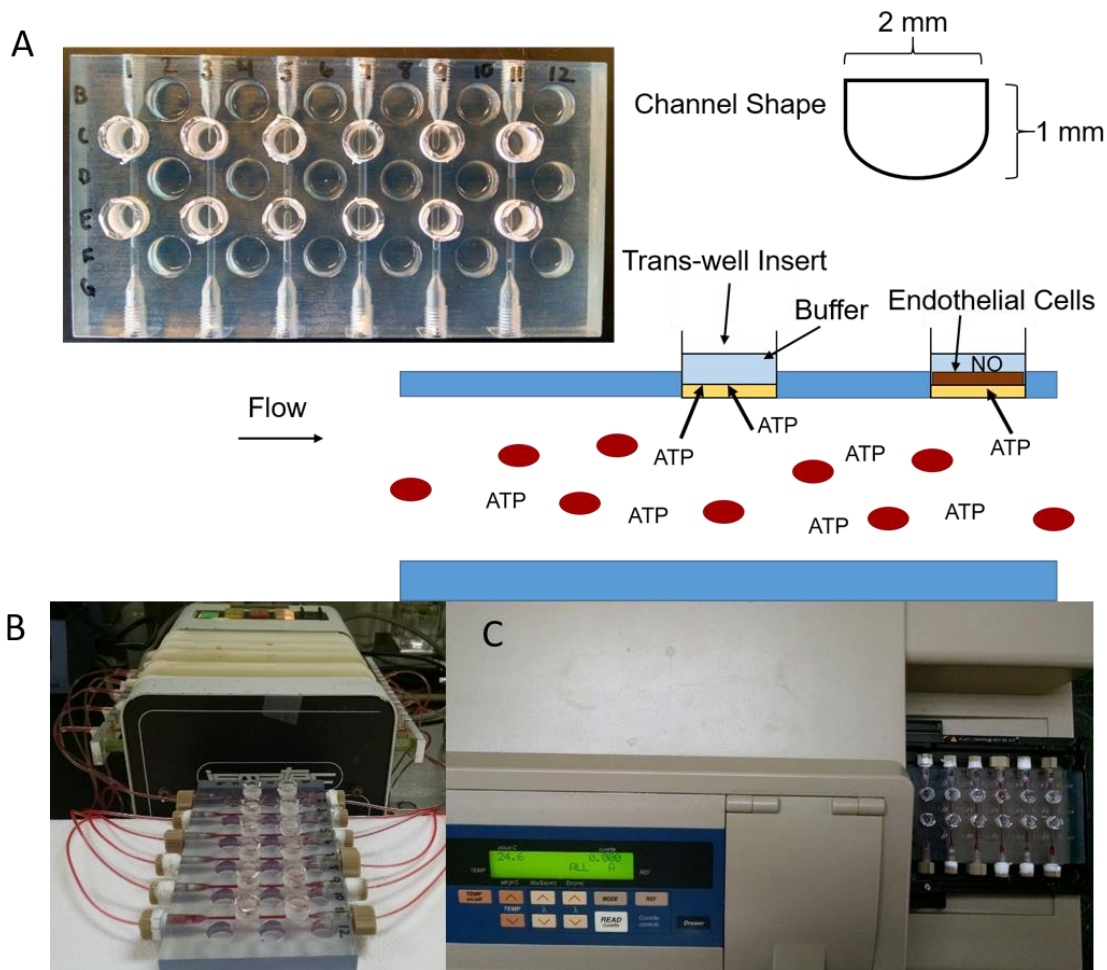


Figure 3.3 – Experimental Setup and Detection. A. The device used for all experiments. Each channel contains two transwell inserts with a $0.4 \mu\text{m}$ membrane. A schematic drawing shows that the device is diffusion based, and as RBCs release ATP, the ATP will diffuse into the detection wells. bPAECs can be cultured on one of the transwell insert to measure NO production. B. View of a flow experiment. The experimental set up utilizes a peristaltic pump and Tygon tubing to create a closed loop system mimicking *in vivo* vasculature. C. Luminescence or fluorescence is measured using a plate reader. The device is the size of a 96-well plate and fits into the detection compartment of the instrument.

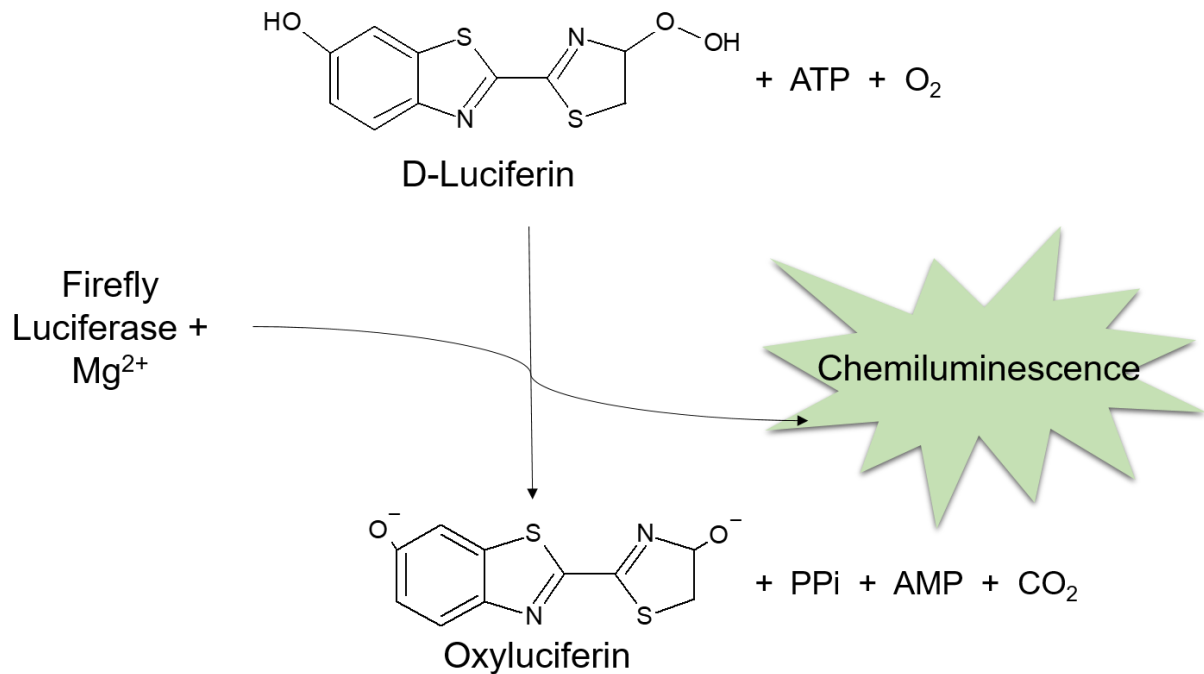


Figure 3.4 – Chemiluminescent Luciferin/Luciferase Reaction. As D-Luciferin mixes with Firefly Luciferase, Mg²⁺, and ATP in the presence of oxygen, oxyluciferin is generated along with inorganic phosphate (PPi), AMP, and carbon dioxide. The generated products produce a chemiluminescence intensity that can be measured by a photomultiplier tube (PMT), and standards are used to quantify the amount of ATP released.

3.4.6 Bovine Pulmonary Arterial Cell Culture

Bovine pulmonary arterial endothelial cells (bPAECs) were used as a mimic of a human endothelium and cultured in a T-75 culture flask in cell media (Endothelial Growth Media (EGM), which contains 5% fetal bovine serum with penicillin, streptomycin and phenol red). Once grown to confluence (confirmed using optical microscopy, shown in Figure 3.5A), the cells were harvested using a 0.25% trypsin solution to release them from the flask, and washed in EGM by centrifugation at 1500g for 5 minutes followed by aspiration

of the supernatant. After resuspension in EGM, the cells were ready to be immobilized to the detection well membranes.

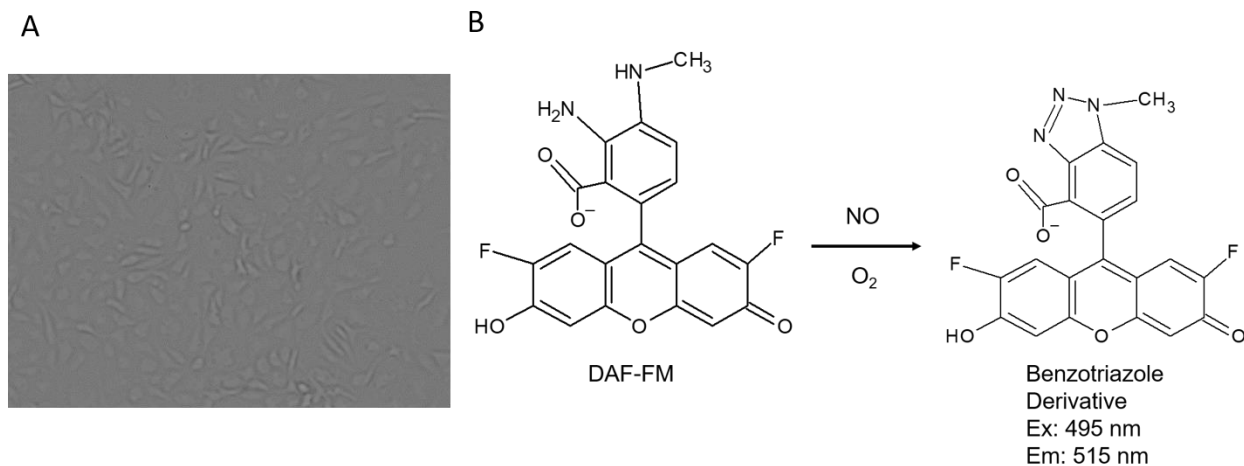


Figure 3.5 – Optical Microscopy bPAEC Picture and DAF-FM Reaction. A. Optical microscopy picture of confluent bPAECs grown in a tissue culture flask. B. As NO is produced and reacts with DAF-FM in the presence of oxygen, a benzotriazole derivative is produced. This product can be measured by fluorescence with an excitation wavelength of 495 nm and an emission wavelength of 515 nm.

To allow the cells to adhere and grow on the membranes, 50 μ L of a 32 μ g/mL fibronectin solution in DDW were added to the detection well and allowed to dry. Once fully dried, the device was exposed to a UV light for 15 minutes for sterilization purposes. 200 μ L of the bPAEC suspension solution (30,000 – 40,000 cells) were then added to the well and allowed to incubate at 37°C overnight before use in experiments.

3.4.7 NO Detection Procedure

To determine the amount of NO produced from endothelial cells, DAF-FM was used as a fluorescent probe. Similar to the ATP release protocol, samples were circulated underneath a porous membrane that contained a layer of cultured endothelial cells. Above the membrane, 200 μ L of a 5 μ M DAF-FM solution in HBSS were loaded onto the cultured cells, and the produced NO was allowed to react with the probe in total darkness (reaction shown in Figure 3.5B). After 60 minutes of circulation, a fluorescence measurement of the wells was performed (excitation: 488 nm, emission: 520 nm). Following the fluorescence measurement, the bPAECs were removed from the inserts using 0.25% trypsin, and counted using a hemacytometer (Reichert, Buffalo, NY). All fluorescence measurements were normalized to the cell count of each insert, and that ratio normalized to the control sample ratio.

The ATP receptor on endothelial cells (P2Y receptor) was inhibited to verify that the measured NO was produced from the endothelial cells due to ATP exposure. PPADS was used to inhibit the NO production of the endothelial cells, and if a similar amount of NO was detected after PPADS treatment, the results would suggest that NO was being produced by a source other than ATP stimulation of the endothelial cells. 50 μ L of the PPADS working solution were added to the inserts containing bPAECs and allowed to incubate for 30 minutes at 37°C before rinsing with HBSS prior to use in experiments.

3.4.8 Deformability Procedure

The deformability of RBCs was assessed using a 3D-printed cell filter containing a porous membrane. Samples of 5% RBCs were forced through the deformability device utilizing a peristaltic pump, and collected. The number of RBCs that passed through the filter in 10 minutes were counted on a hemacytometer (Reichert, Buffalo, NY) and compared relative to other samples as a measure of deformability.

The device was created by a previous member of the Spence group, and is shown in Figure 3.6.⁶⁶ As shown, the two main parts of the filter were printed in VeroClear material with rubber-like TangoBlack material (Stratasys Ltd,) O-rings that sandwiched a 5 μ m polycarbonate membrane. Binder clips held the device together, and a peristaltic pump delivered the cells via tygon tubing screwed into the device by a finger tight adapter. All RBCs that passed through the membrane after 10 minutes were collected and the number of cells counted.⁶⁶

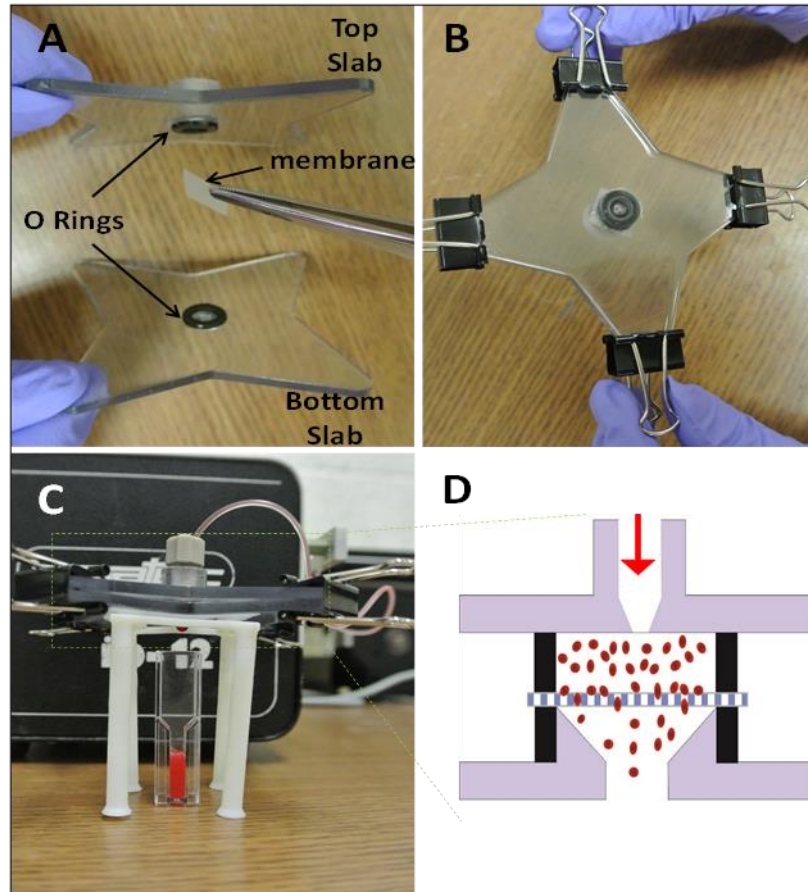


Figure 3.6 – 3D Printed Deformability Device Design and Experimental Setup. A. O-rings on each slab sandwich a 5 μm polycarbonate membrane which acts as a filter for this device. B. The assembled device with binder clips to hold the membrane and two slabs in place. C. View of a deformability experiment. As RBCs are forced through the device and membrane, the cells that pass through are collected and later counted. Comparing the number of RBCs that pass through the membrane in a given time is used as the measure of deformability. D. A schematic view of the filtration process. RBCs are forced through the device using a peristaltic pump, and the cells are required to deform to fit through the membrane. Cells that are deformable enough to fit through the membrane pass through and are collected, while cells that are not deformable enough will not pass through the membrane. The device was created by a former Spence lab member.⁶⁶

3.4.9 Red Blood Cell Radioactive $^{65}\text{Zn}^{2+}$ Binding

Zn^{2+} binding to RBCs was measured with radiolabeled $^{65}\text{ZnCl}_2$ using a scintillation counter. Samples were prepared with and without prednisone as described in section 3.4.3 with one exception; the Zn^{2+} added was 800 nM $^{65}\text{Zn}^{2+}$. After the addition of C-peptide and $^{65}\text{Zn}^{2+}$, all samples were incubated for 2 hours at 37°C followed by centrifugation at 500g for 5 minutes. $^{65}\text{Zn}^{2+}$ binding was determined by analysis of the amount of $^{65}\text{Zn}^{2+}$ left in the supernatant, which was subtracted from the initially added 20 nM $^{65}\text{Zn}^{2+}$. A Micro Beta scintillation counter (Perkin Elmer, Boston, MA) was used for detection of 200 μL of the sample supernatant mixed with 100 μL of Ultima Gold scintillation cocktail (Perkin Elmer, Boston, MA) in a 96-well plate and allowed to incubate for 30 minutes prior to detection.

3.4.10 Red Blood Cell C-peptide Binding

RBC C-peptide binding was measured with a commercially available C-peptide enzyme linked immunosorbent assay (ELISA) kit (ALPCO, Salem, NH). After treatment with prednisolone, 50 μL of the 400 nM C-peptide and Zn^{2+} stock were added to the samples before a 2 hour incubation at 37°C. After the incubation, all samples were centrifuged and the supernatant was removed for analysis. The amount of C-peptide bound to the RBCs was calculated by subtracting the amount left in the supernatant from the amount initially added (20 nM, as described in section 3.4.3). Prior to analysis, all samples were diluted

1:50 in DDW to assure final values within the dynamic range of the assay. The ELISA kit assay consists of wells coated with primary C-peptide antibodies to capture the C-peptide molecules in the sample. After the initial capture, secondary antibodies conjugated with an enzyme were added to each well. Before detection, a substrate that produced a colorimetric reaction when combined with the enzyme was added. A final addition of the stop solution halted the ongoing reaction and an absorbance measurement was taken at 450 nm by a Spectra Max M4 plate reader (Molecular Devices).

3.4.11 Preparing Red Blood Cell Ghost Samples

RBC samples were prepared as described in sections 3.4.3 and 3.4.5. After the 2 hour incubation with C-peptide and Zn^{2+} , the samples were centrifuged at 500g for 5 minutes and the supernatant removed. The remaining pelleted RBCs were lysed with 1 mL lysis buffer. All samples were then stored at 4°C for 30 minutes before centrifugation at 22,000g for 15 minutes at 4°C. The supernatant was removed and the pellet resuspended in 1 mL of lysis buffer. After mixing, the samples were centrifuged again at 22,000g and 4°C for 5 minutes, the supernatant removed, and fresh lysis buffer added. This process was repeated three times total or until no more hemoglobin was visible (red color). Once all hemoglobin and cytosolic content were removed; the remaining pelleted ghosts were stored at -20°C until use.

3.4.12 SDS-PAGE and Western Blot Analysis

Sodium dodecyl sulfate polyacrylamide gel electrophoresis (SDS-PAGE) was used to separate the proteins of the RBC membrane prior to analysis. RBC ghosts diluted 1:200 in 2x Laemmli Sample Buffer (Bio-Rad, Hercules, CA) were loaded onto a 10% polyacrylamide gel. The gel was subjected to 80 V for 20 minutes, and then 120 V for about 90 minutes or until the buffer reached the bottom of the gel by visual inspection. Subsequent analysis consisted of Western Blot analysis.

Western Blot analysis was utilized to specifically probe the GLUT1 content of the RBCs. Once the proteins were separated by SDS-PAGE, all proteins were transferred to a polyvinylidene difluoride (PVDF) transfer membrane (EMD Millipore, Burlington, MA) overnight at 15 V for Western Blot analysis the following day. After transfer, the PVDF membrane was blocked for nonspecific binding for 1 hour with 5% dry milk in TBST. Primary antibodies for GLUT1 (Abcam, Cambridge, MA) and Spectrin Beta 1 (Novus Biological, Littleton, CO) (15 μ L in 15 mL of TBS and 0.75 g dry milk) were added and allowed to incubate for one hour at room temperature. After rinsing in TBST, anti-rabbit and anti-mouse secondary antibodies conjugated with alkaline phosphatase (Sigma Aldrich,) (5 μ L in 15 mL of TBST and 0.75 g dry milk) were added and allowed to incubate an additional hour. Following a final rinsing step, incubation with 4.5 mg NBT (nitro-blue tetrazolium chloride) (Sigma Aldrich,) and 2.0 mg BCIP (5-bromo-4-chloro-3'-indolyphosphate p-toluidine salt) (Sigma Aldrich,) in 500 μ L N-dimethylformamide and 15 mL bicarbonate buffer produced a colorimetric indication of the GLUT1 and Beta Spectrin

present. Once dried, the membrane was scanned and ImageJ software was used to quantify band thickness and intensity. GLUT1 band intensities were normalized to Beta Spectrin band intensities, and all samples were normalized to the control sample on each membrane.

3.5 Results

Prior to measuring ATP release from flowing RBCs, the effect of estriol and prednisolone on the chemiluminescence was assessed. Table 3.2 depicts no significant difference in chemiluminescence intensity when 1 μM estriol, or 100 μM prednisolone is added to an ATP standard of 200 nM and flowed under conditions described in section 3.4.5.

Table 3.2 – The Effect of Estriol and Prednisolone on Luminescence Detection.

	Luminescence (Intensity)		Luminescence (Intensity)
200 nM ATP in Buffer	152.6 \pm 24.3	200 nM ATP in Buffer	151.0 \pm 17.3
200 nM ATP in Buffer + 1 μM Estriol*	169.3 \pm 9.1	200 nM ATP in Buffer + 100 μM Prednisolone*	158.4 \pm 9.1

* $p > 0.2$ to 200 nM ATP in Buffer
 $n = 3$, error = standard deviation

A significant decrease in RBC-derived ATP release from both control and MS RBCs treated with estriol is shown in Figure 3.7. While healthy RBCs release 216 ± 11 nM ATP at basal level, when treated with estriol, the ATP release measured decreased to $108 \pm$

12 nM. The 3 nM treated reduction was not statistically significant, however, when treated with 7 nM, 30 nM, or 1 μ M estriol, a significant decrease in RBC ATP release was measured. Due to flow induced shear stress, MS RBCs release 105 nM more ATP than control RBCs, as seen in Figure 3.7. Interestingly, when MS RBCs were treated with the same estriol concentrations as the control RBCs, the measured ATP release decreased to statistically the same level as control RBCs when treated with 7 nM estriol, and a significant decrease in ATP release was measured at all estriol concentrations.

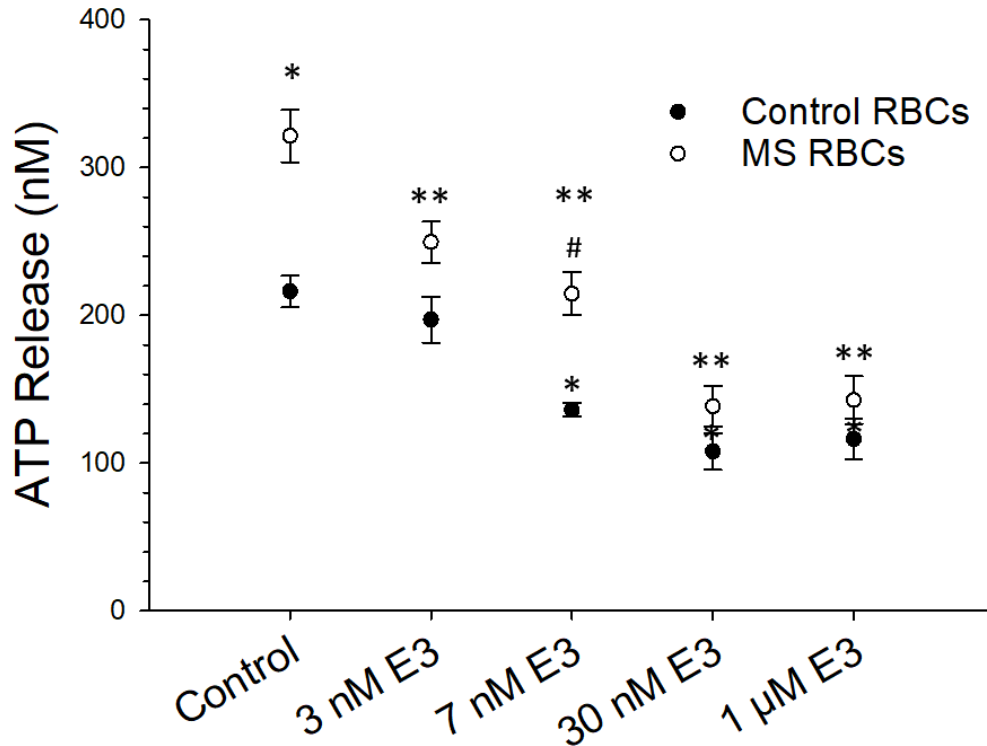


Figure 3.7 – RBC ATP Release from Control and MS RBCs Treated with Estriol. When both control and MS RBCs were treated with estriol, the measured ATP release significantly decreased. Control RBCs are depicted in the black circles, and MS RBCs are depicted in the white circles. At basal level, control RBCs release 216 ± 11 nM ATP, and MS RBCs release 321 ± 18 nM ATP. As higher estriol concentrations were incubated with RBCs, the ATP release continued to decrease until reaching a plateau level. Noteworthy, when MS RBCs are treated with 7 nM estriol, the RBC ATP release decreased to statistically the same level as the untreated control RBC ATP release. $n \geq 4$ donors, * $p < 0.05$ to control RBCs, ** $p < 0.05$ to MS RBCs, # $p > 0.4$ to control RBCs, E3 = estriol, error bars = SEM.

Similar to estriol treated RBCs, a decrease in RBC ATP release was also measured due to the presence of prednisolone, from both control and MS RBCs. Shown in Figure 3.8, when control RBCs (closed circles) are treated with prednisolone, the measured ATP release decreased from 226 ± 9 nM to 146 ± 17 nM and a significant decrease in ATP release was measured at all prednisolone concentrations tested. MS RBCs responded

similarly to prednisolone, also shown in Figure 3.8 (open circles). MS RBCs released 330 ± 22 nM ATP when subjected to flow induced shear stress, which decreased to 178 ± 15 nM ATP release when the cells were treated with $100 \mu\text{M}$ prednisolone. As with the estriol treated MS RBCs, treatment with prednisolone decreased RBC ATP release to statistically the same level as control RBCs for prednisolone concentrations of 5 and $50 \mu\text{M}$, and interestingly, 5, 50, and $100 \mu\text{M}$ prednisolone-treated MS RBCs all released significantly less ATP than the untreated MS RBCs.

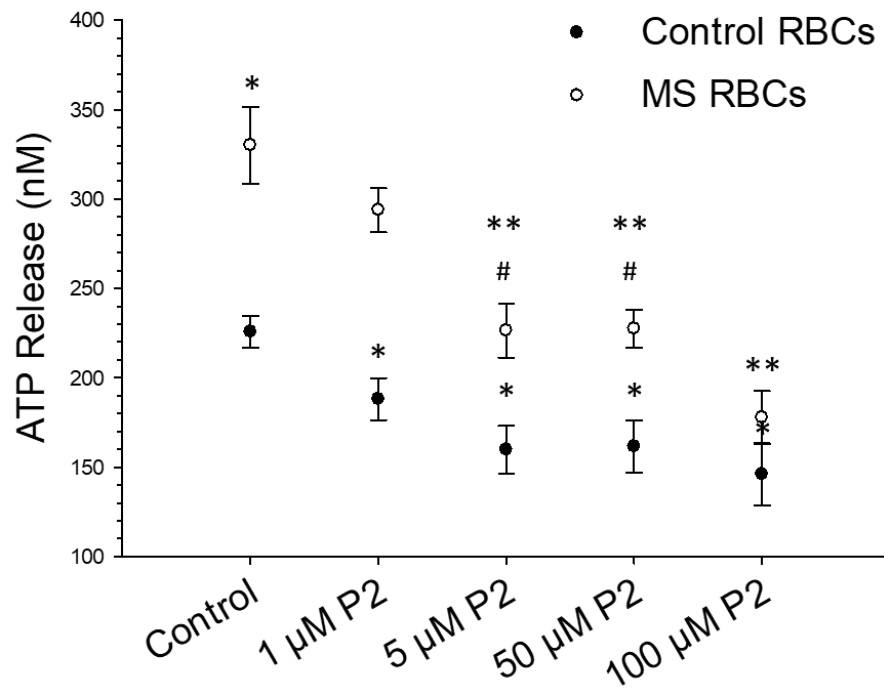


Figure 3.8 – RBC ATP Release from Control and MS RBCs Treated with Prednisolone. When both control and MS RBCs were treated with prednisolone, the measured ATP release significantly decreased. Control RBCs are depicted in the black circles, and MS RBCs are depicted in the white circles. As higher prednisolone concentrations were incubated with RBCs, the ATP release continued to decrease. Noteworthy: when MS RBCs were treated with 5 or $50 \mu\text{M}$ prednisolone, the RBC ATP release decreased to statistically the same level as the untreated control RBC ATP release. $n \geq 4$ donors, * $p < 0.05$ to control RBCs, ** $p < 0.05$ to MS RBCs, # $p > 0.4$ to control RBCs, P2 = prednisolone, error bars = SEM.

Diamide was used as a control to verify that the ATP release measured was not due to cell lysis while the RBCs traversed through the printed channels. Literature reports that diamide stiffens cells,⁶⁷ which has a direct correlation to ATP release from RBCs.⁶⁸ As shown in Figure 3.9, 40 μ M diamide treatment on samples of 7% RBCs decreased the measured ATP release from 189 ± 25 nM, to 57 ± 17 nM. This result suggests the RBCs are not lysing during the time of the experiment. If cell lysis did occur, the ATP release would increase greatly due to the large ATP pool within the RBC. Reports that cell stiffening leads to decreased ATP release also support the conclusion that the cells are not lysing during the experiments.⁶⁹

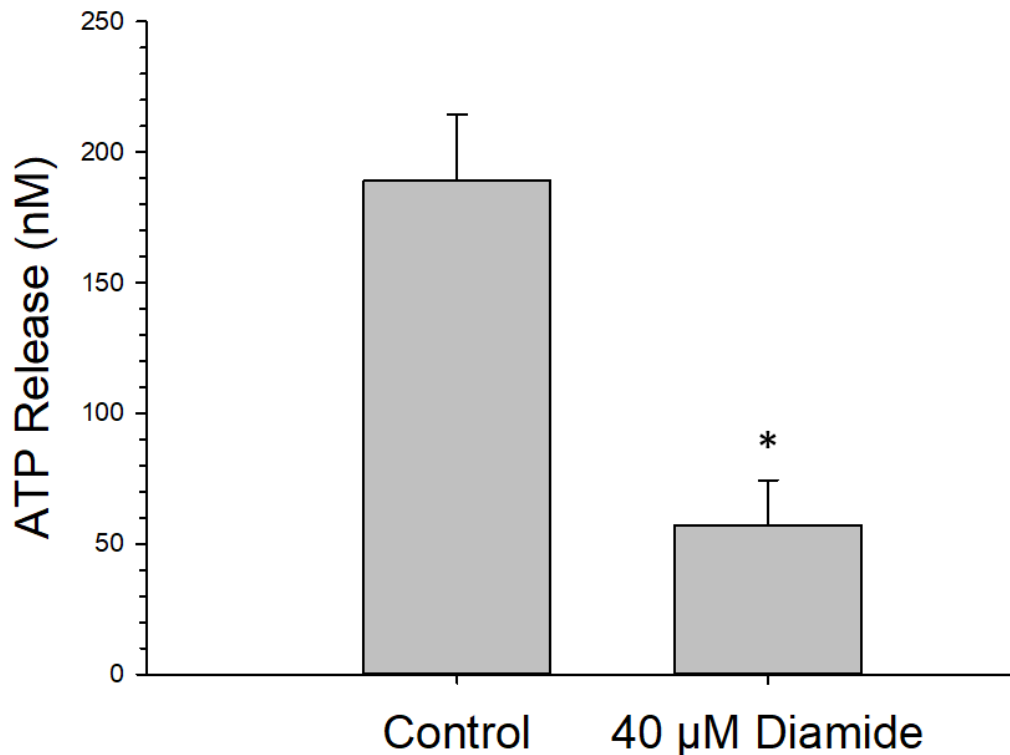


Figure 3.9 – RBC ATP Release from Control Cells Treated with Diamide. As a control, diamide was used to verify that the measured ATP was not due to cell lysis. Diamide stiffens cells, which has a direct correlation to ATP release from RBCs. When RBCs were treated with diamide, the measured ATP release decreases from 189 ± 25 nM, to 57 ± 17 nM. This result confirms that the RBCs are not lysing during the time of the experiment, as diamide would not decrease the ATP release from lysed RBCs. $n = 4$ donors, $*p < 0.05$ to control, error bars = SEM.

To study the direct relationship between RBC ATP release and endothelial NO production, NO production from bPAECs in contact with RBCs treated with either estriol or prednisolone was measured. To avoid any interference from excess steroid in the sample, all samples were washed with fresh PSS after incubation, prior to flowing for NO measurements. This ensured that NO production was from the RBCs and their secretions, instead of excess steroid that may have been in the sample.

7% RBC samples were treated with varying concentrations of estriol and allowed to incubate at 37°C for 45 minutes prior to centrifugation at 500g for 5 minutes. The resulting fluorescence intensities, summarized in Figure 3.10, were normalized to the number of bPAECs on the membrane insert and also to the control untreated RBC samples. When treated with 3 nM, 7 nM, 30 nM, or 1 µM estriol, the fluorescence intensities decreased up to $31 \pm 4\%$ compared to the control sample. Although the highest concentration of estriol (1 µM) elicited statistically the same NO produced as control cells, 3 nM, 7 nM, and 30 nM estriol-treated RBCs elicited a significant decrease in NO production compared to control, untreated RBCs.

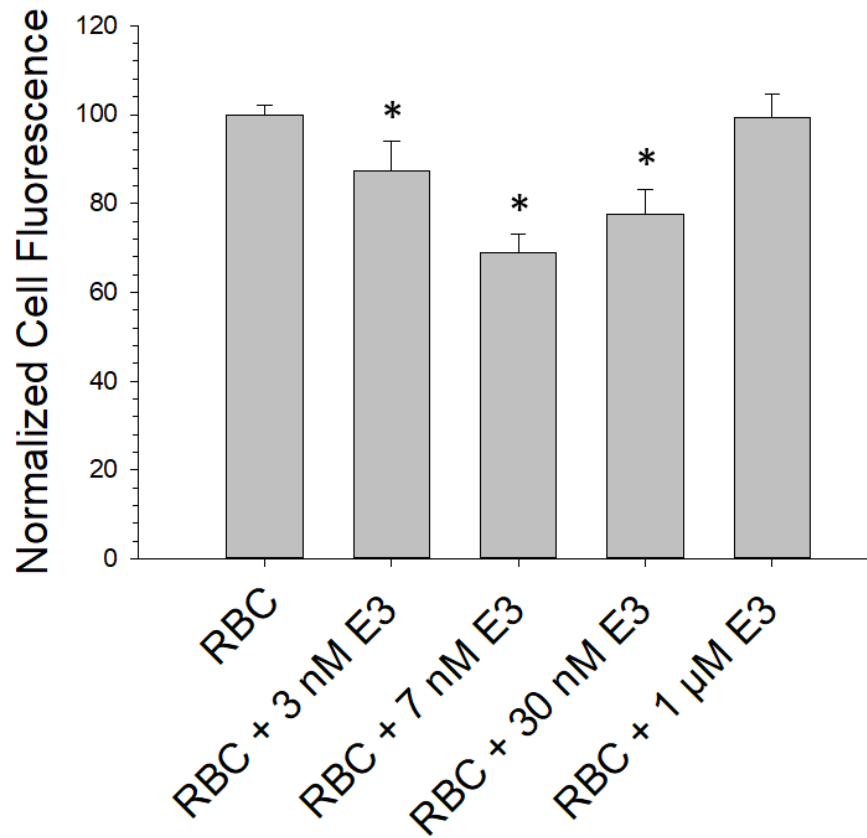


Figure 3.10 – Normalized Cell Fluorescence from bPAECs in Contact with RBCs Treated with Estriol. When the bPAEC NO production was measured as RBCs treated with estriol were flowed beneath, the NO production significantly decreased compared to bPAECs in contact with control RBCs. Shown above, the normalized bPAEC fluorescence when RBCs were treated with 3 nM, 7 nM, 30 nM, or 1 μM estriol resulted in a decrease in fluorescence intensity up to $31 \pm 4\%$ compared to the control sample. All fluorescence intensities are normalized to the number of cells in each well, and also to the untreated control RBCs. $n \geq 5$ donors, $*p < 0.05$ to control, E3 = estriol, error bars = SEM.

Similar to the NO production of bPAECs in contact with estriol treated RBCs, bPAECs in contact with RBCs treated with 1, 3, 5, 50, or 100 μM prednisolone were also evaluated. An extra prednisolone concentration of 3 μM was added to this data set to add resolution to the study. The data in Figure 3.11 shows the resulting fluorescence intensities normalized to both the number of bPAECs on each membrane, and the control untreated

RBC NO stimulation. Fluorescence intensities decreased up to $31 \pm 5\%$ compared to the control sample when bPAECs were in contact with flowing RBCs treated with prednisolone. While no significant difference was measured with RBCs treated with $1 \mu\text{M}$ prednisolone, RBCs treated with 3, 5, 50, and $100 \mu\text{M}$ prednisolone all elicited a significant decrease in bPAEC NO production.

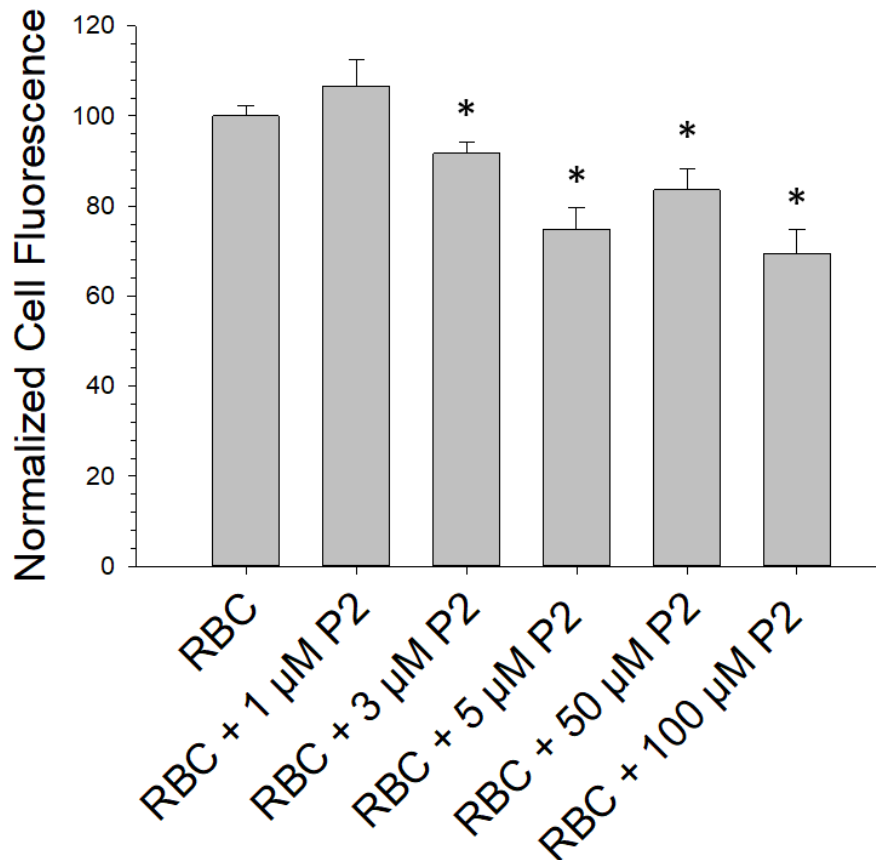


Figure 3.11 – Normalized Cell Fluorescence from bPAECs in Contact with RBCs Treated with Prednisolone. When the bPAEC NO production was measured as RBCs treated with prednisolone were flowed beneath, the NO production significantly decreased compared to bPAECs in contact with control RBCs. Shown above, the normalized bPAEC fluorescence when RBCs were treated with various prednisolone concentrations resulted in a decrease in fluorescence intensity up to $31 \pm 5\%$ compared to the control sample. All fluorescence intensities were normalized to the number of cells in each well, and also the untreated control RBCs. $n \geq 4$ donors, * $p < 0.05$ to control, P2 = prednisolone, error bars = SEM.

To assure the measured NO was due to its production by the bPAECs and not from cell lysis or from RBCs directly, PPADS was used to inhibit the P2Y receptors on bPAECs as RBCs flowed through the device. Shown in Figure 3.12, a significant decrease in fluorescence ($30 \pm 1\%$) was measured when bPAECs were treated with PPADS. This result suggests the NO measured by fluorescence through DAF-FM is the product of NO synthesis, activated by the P2Y receptor on the bPAECs, and not from another method such as cell lysis or from the RBCs directly.

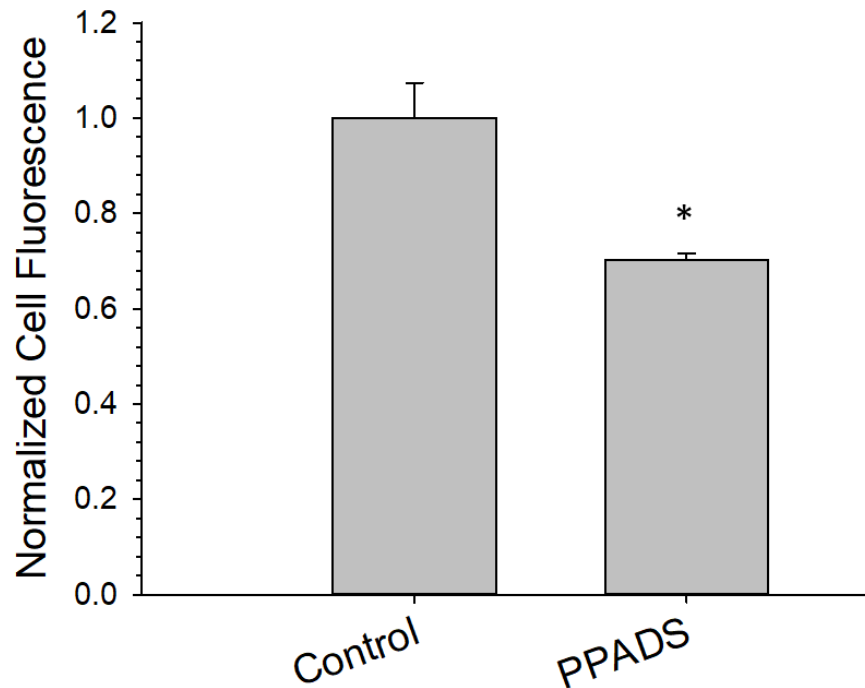


Figure 3.12 – Normalized Cell Fluorescence from PPADS Treated bPAECs in Contact with Control RBCs. PPADS inhibit P2Y receptors on bPAECs, and was used as a control to verify that the measured NO was due to bPAEC production. A 30% decrease in the normalized cell fluorescence was measured from PPADS treated bPAECs when control RBCs were flowed beneath the cells. This decrease suggests the NO measured by fluorescence through DAF-FM is the product of NO synthesis activated by the P2Y receptor on the bPAECs. $n = 3$ donors, $*p < 0.05$ to control, error bars = SEM.

Literature suggests that RBC ATP release is related to RBC deformability.^{68, 70} In order to evaluate how estriol and prednisolone lead to a decrease in RBC ATP release, the deformability of RBCs treated with estriol or prednisolone was evaluated. The data in Figure 3.13 shows a decrease in RBC deformability in the presence of 21.4 nM and 0.74 μ M estriol. Because deformability measurements had previously been optimized to contain 5% RBCs, the estriol and prednisolone concentrations were scaled appropriately to contain a consistent concentration of steroid per RBC. When treated with estriol, the RBC deformability decreased up to $13 \pm 2\%$ compared to the untreated control RBC sample.

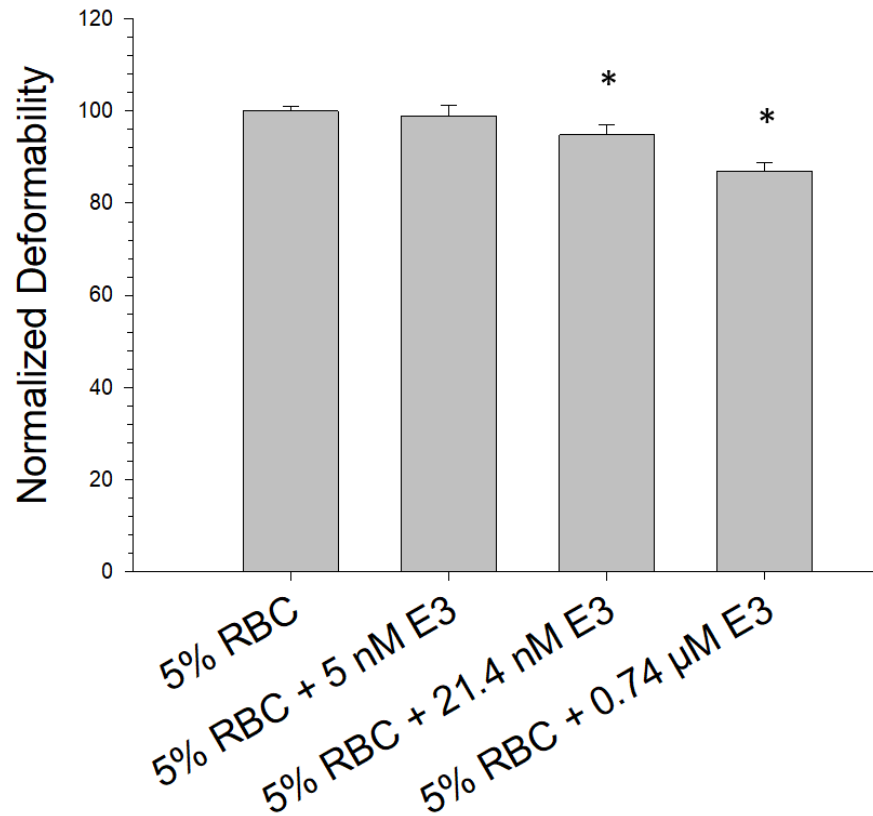


Figure 3.13 – The Deformability of RBCs Treated with Estriol. Deformability is reported to be directly correlated with ATP release, and a significant decrease of 5% and 13% in RBC deformability was measured when RBCs were treated with 21.4 nM or 0.74 μM estriol, respectively. This decrease in RBC deformability is thought to correlate to a decrease in RBC ATP release (Figure 3.7). $n \geq 4$ donors, $*p < 0.05$ to 5% RBC, E3 = estriol, error bars = SEM.

Shown in Figure 3.14, when RBCs were treated with various concentrations of prednisolone, the RBC deformability decreased to $75 \pm 2\%$ of the untreated control RBCs. While 3.6 μM treatment of prednisolone did not significantly decrease the RBC deformability, a significant decrease in RBC deformability was measured with treatment of 35.7 and 71.4 μM prednisolone. Surprisingly, results shown in Figure 3.15 report a $21 \pm 5\%$ decrease in deformability of MS RBCs compared to control RBCs, which may be

due to a difference in MS RBC diameter.^{33, 71} To date, methods to evaluate MS RBC deformability along with the validity of reported results have come into question, which may also call into question results presented in Figure 3.15.³³ This result will be discussed further in section 3.6.

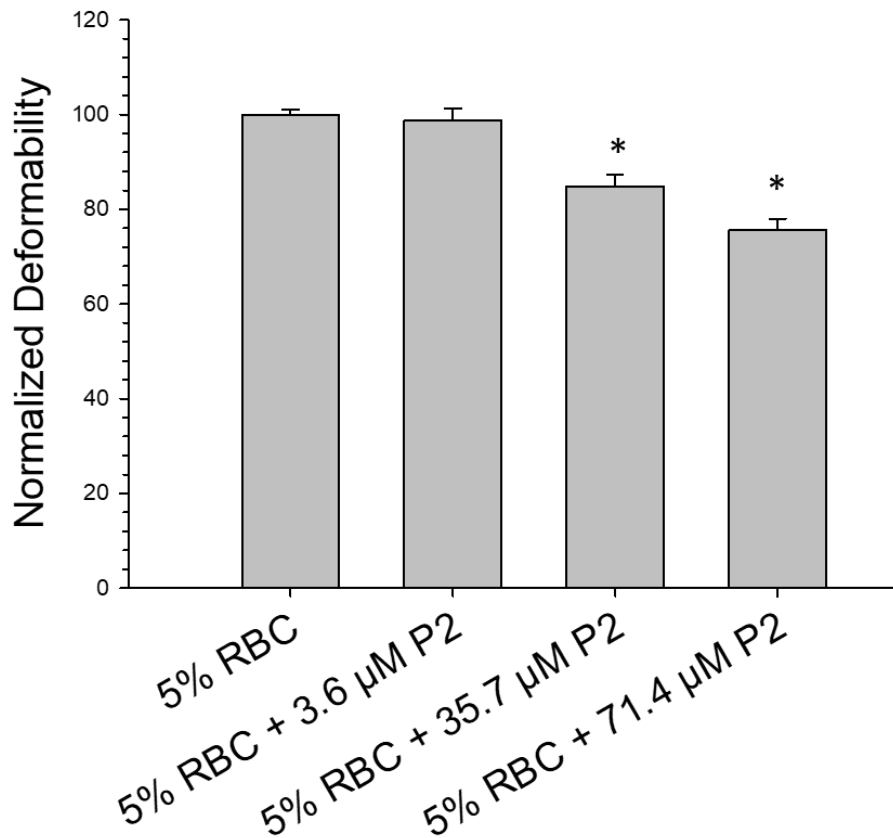


Figure 3.14 – The Deformability of RBCs Treated with Prednisolone. Deformability is reported to be directly correlated with ATP release, and a significant decrease in RBC deformability of 15% and 25% was measured when RBCs were treated with 35.7 and 71.4 µM prednisolone, respectively. This decrease in RBC deformability is thought to correlate to a decrease in RBC ATP release (Figure 3.8). $n \geq 4$ donors, * $p < 0.05$ to 5% RBC, P2 = prednisolone, error bars = SEM.

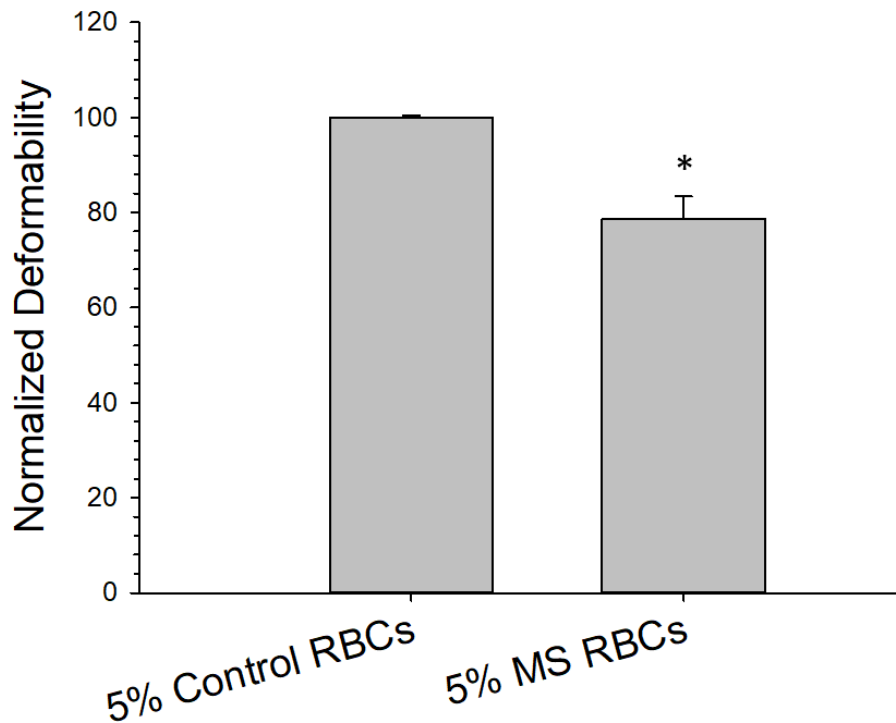


Figure 3.15 – The Deformability of Control and MS RBCs. Reported above, MS RBCs are $21 \pm 5\%$ less deformable than control RBCs. A possible explanation for this result could involve the size of MS RBCs compared to control RBCs. Reports suggest MS RBCs may be larger than control RBCs, and due to the membrane used in the device to measure deformability, different RBC sizes may skew results obtained. $n \geq 6$ donors, $*p < 0.05$ to 5% control RBCs, error bars = SEM.

In addition to RBC deformation, chemical stimulus is also a method resulting in RBC ATP release.³⁶ Previous work suggests that the complex of C-peptide, Zn^{2+} , and albumin is able to elicit an increase in RBC ATP release,⁷² and evaluation of the ability of prednisolone to disrupt the binding of the complex may be a mechanism of action leading to the measured decrease in RBC ATP release. Figure 3.16 shows the $^{65}Zn^{2+}$ binding from RBCs treated with varying amounts of prednisolone. A significant decrease in the RBC $^{65}Zn^{2+}$ binding was measured when RBCs were treated with as little as $0.1 \mu M$

prednisolone. Untreated, control RBCs bind an average of 1.99 ± 0.12 nM $^{65}\text{Zn}^{2+}$; however, with the addition of prednisolone the RBC $^{65}\text{Zn}^{2+}$ binding decreased to 0.18 ± 0.30 nM, and statistics report that the $^{65}\text{Zn}^{2+}$ binding significantly decreased for all prednisolone concentrations evaluated.

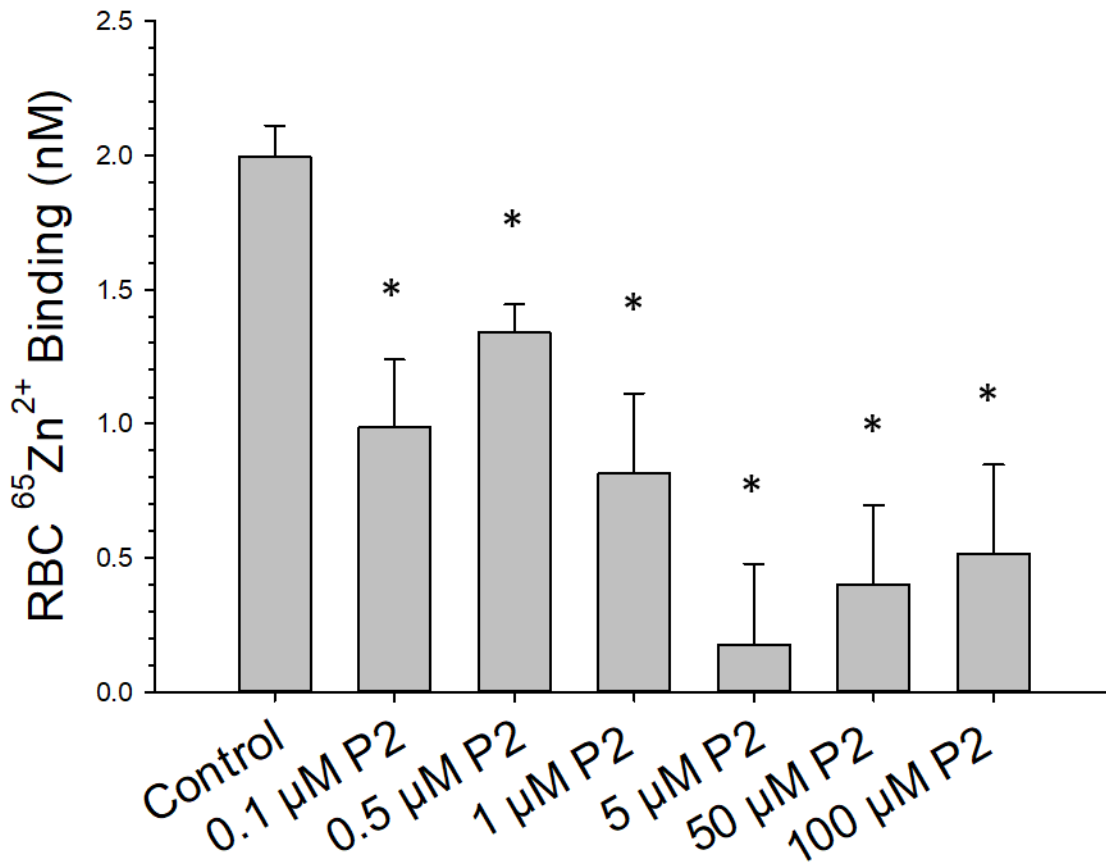


Figure 3.16 – RBC $^{65}\text{Zn}^{2+}$ Binding in the Presence of Prednisolone. When the RBC $^{65}\text{Zn}^{2+}$ binding was measured after treatment with prednisolone, a significant decrease in RBC $^{65}\text{Zn}^{2+}$ binding was measured at all concentrations of prednisolone tested. The evaluated concentrations of prednisolone were 0.1, 0.5, 1, 5, 50, and 100 μM , and all samples contained 20 nM C-peptide and $^{65}\text{Zn}^{2+}$. P2 = prednisolone, C+Z = C-peptide and $^{65}\text{Zn}^{2+}$, $n \geq 4$ donors, error bars = SEM, * $p < 0.05$ to Control.

The amount of C-peptide binding to RBCs treated with prednisolone was also measured, and shown in Figure 3.17. When RBCs were treated with varying amounts of prednisolone, C-peptide binding decreased from 2.02 ± 0.22 nM (untreated cells) to -0.47 ± 0.27 nM when treated with $100 \mu\text{M}$ prednisolone. All treatments with prednisolone resulted in a statistically significant decrease in RBC C-peptide binding compared to untreated RBCs.

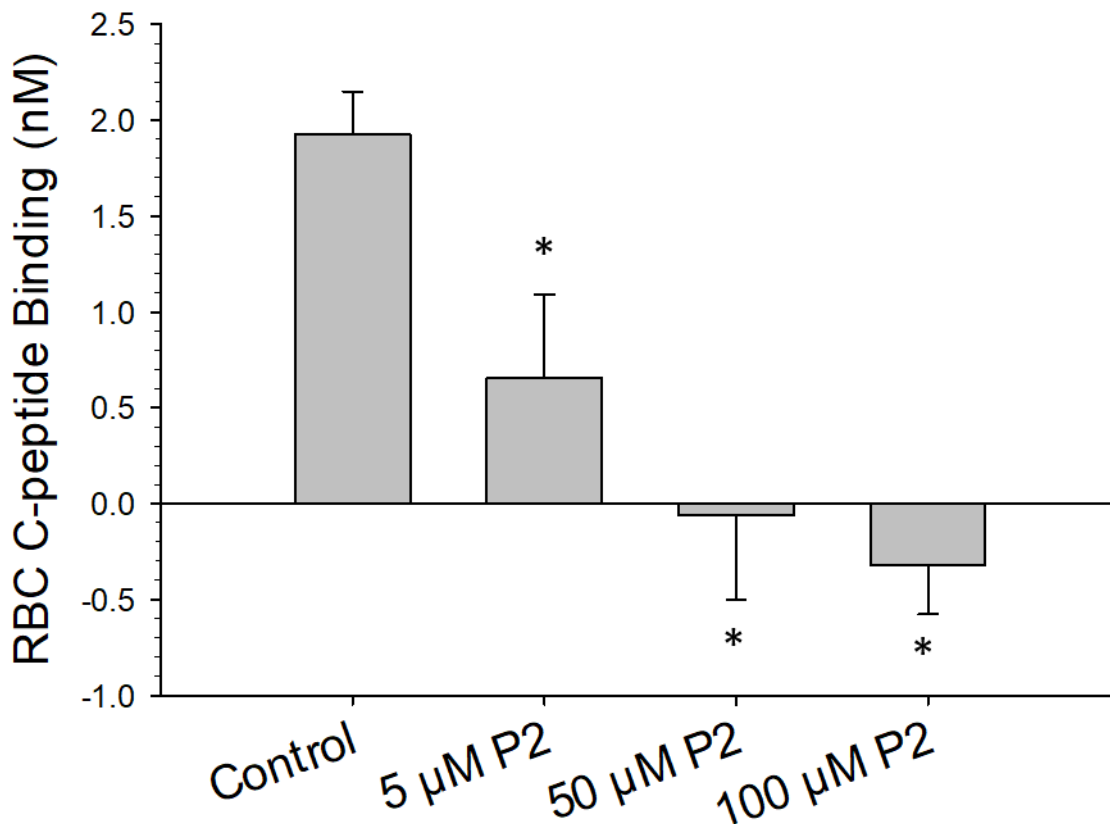


Figure 3.17 – RBC C-peptide Binding in the Presence of Prednisolone. When the RBC C-peptide binding was measured after treatment with prednisolone, a significant decrease in RBC C-peptide binding was measured at all concentrations of prednisolone tested. The evaluated concentrations of prednisolone were 5, 50, and $100 \mu\text{M}$, and all samples contained 20 nM C-peptide and Zn^{2+} . P2 = prednisolone, C+Z = C-peptide and Zn^{2+} , $n \geq 7$ donors, error bars = SEM, * $p < 0.05$ to Control.

Because ATP is produced through glycolysis within RBCs, GLUT1 content is proposed to be associated with RBC metabolism. RBC GLUT1 content was measured on cells treated with 20 nM C-peptide and Zn^{2+} and shown in Figure 3.18. When control RBCs were treated with 20 nM C-peptide and Zn^{2+} , a statistically significant $25.0 \pm 1.9\%$ increase in GLUT1 content was measured compared to control, untreated RBCs. As previously stated in Chapter 2, a significant increase in the RBC membrane GLUT1 content was also measured in MS RBCs compared to control RBCs, shown in Figure 2.6. MS RBCs contain $23.3 \pm 4.8\%$ more GLUT1 at basal levels compared to control RBCs, which may reflect altered cell metabolism within MS RBCs.

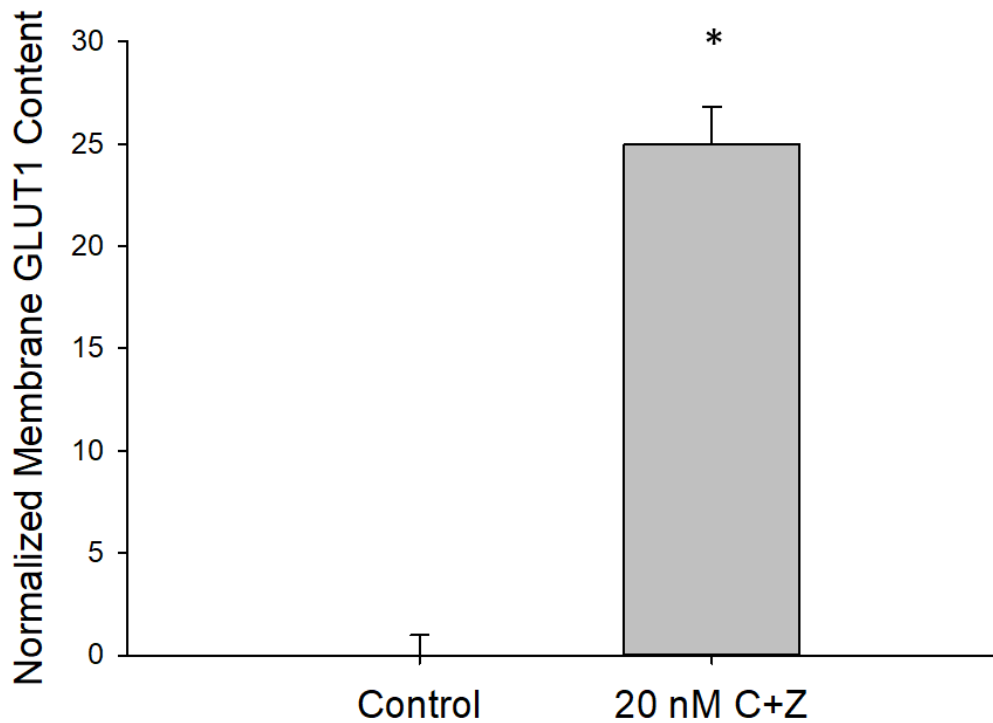


Figure 3.18 – Normalized RBC Membrane GLUT1 Content of RBCs treated with 20 nM C-peptide and Zn^{2+} . When samples of 7% RBCs were treated with 20 nM C-peptide and Zn^{2+} , a significant 25% increase in the RBC membrane GLUT1 content was measured by Western Blot analysis. This increase correlates with previous work suggesting that C-peptide and Zn^{2+} alter the cell metabolism of the RBC. C+Z = C-peptide and Zn^{2+} , $n \geq 8$ donors, error bars = SEM, * $p < 0.05$ to Control.

The GLUT1 content of control RBCs treated with varying amounts of prednisolone is shown in Figure 3.19. An increase in GLUT1 content is measured with the addition of increasing amounts of prednisolone. Compared to untreated RBCs, the RBC GLUT1 content increased up to $23.1 \pm 2.6\%$ when treated with prednisolone. This increase in GLUT1 may give insight as to how prednisolone affects RBCs, and ultimately the entire body.

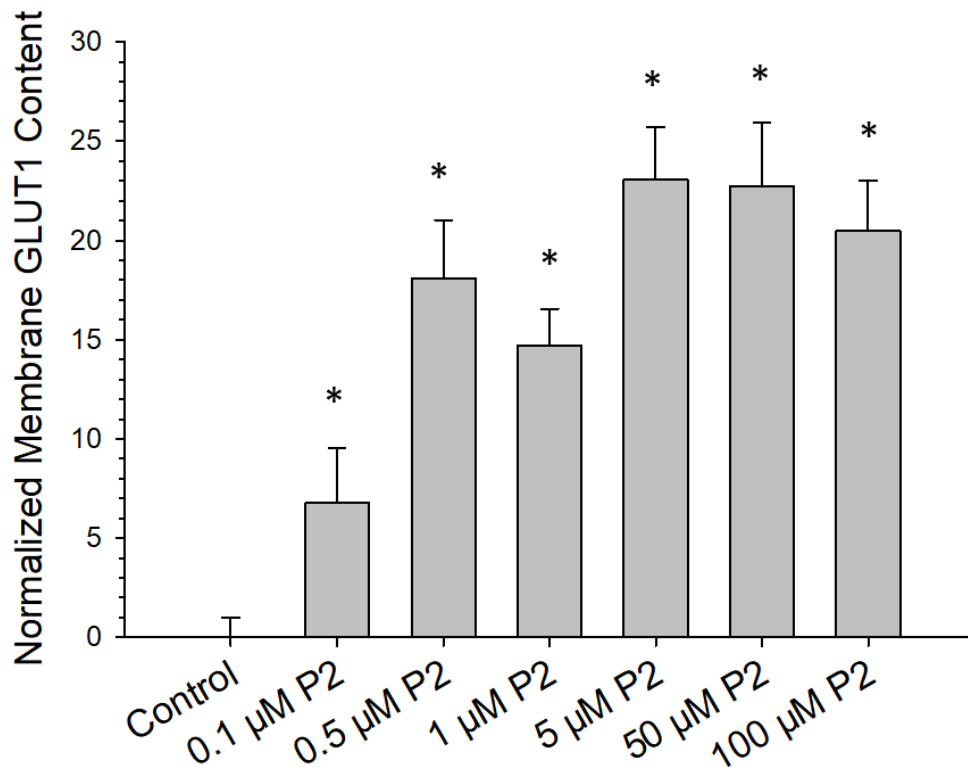


Figure 3.19 – Normalized RBC Membrane GLUT1 Content of RBCs Treated with Prednisolone. When control RBCs were treated with varying concentrations of prednisolone and the resulting RBC GLUT1 content evaluated, a significant increase in GLUT1 content was measured at prednisolone concentrations of 0.1, 0.5, 1, 5, 50, and 100 μM . P2 = prednisolone, $n \geq 6$ donors, error bars = SEM, * $p < 0.05$ to Control.

The blood protein albumin has been present in all of the experiments previously described. To further investigate the mechanism of action of prednisolone on RBCs, albumin was removed from the samples and the GLUT1 content evaluated. After treatment with prednisolone, no measureable change in GLUT1 content was observed when albumin was absent from the samples (Figure 3.20). Also noteworthy, compared to control RBCs without albumin, control RBCs with albumin contain $6.2 \pm 3.7\%$ more GLUT1 at basal levels.

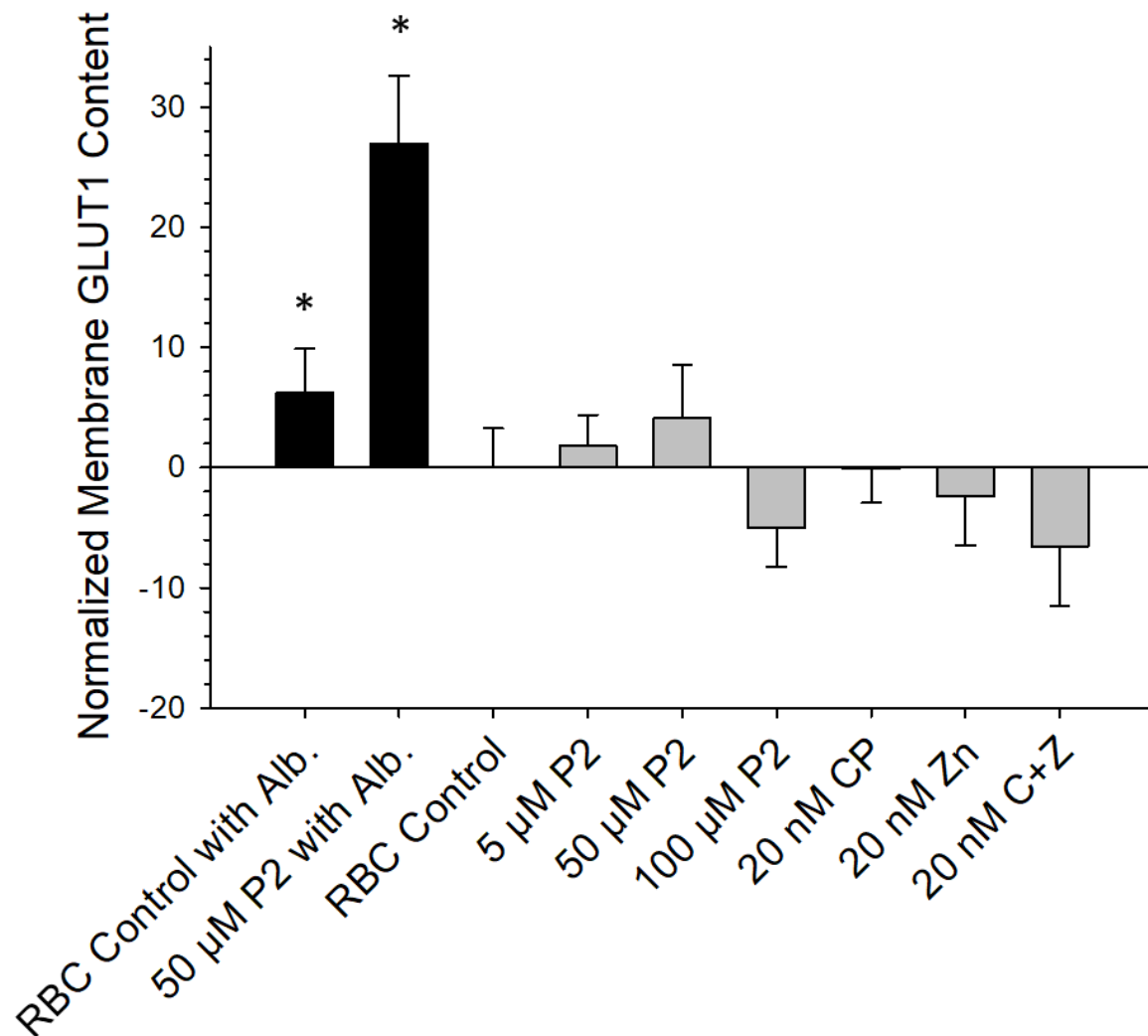


Figure 3.20 – Normalized RBC Membrane GLUT1 Content of RBCs Treated with Prednisolone, with and without Albumin. A significant increase in RBC GLUT1 content was measured after treatment with 50 μM prednisolone in the presence of albumin. When albumin was absent, there was no measureable change in RBC GLUT1 content due to prednisolone treatment, or due to C-peptide only, Zn^{2+} only, or the combination of the two. The prednisolone concentrations evaluated were 5, 50, and 100 μM . This results suggests that prednisolone requires albumin to specifically bind to RBCs and elicit an effect. P2 = prednisolone, Alb = albumin, CP = C-peptide, C+Z = C-peptide and Zn^{2+} , $n \geq 6$ donors, error bars = SEM, * $p < 0.05$ to RBC Control.

When treated with varying amounts of prednisolone, RBC GLUT1 content increases when albumin is present; however, when albumin is absent there is no significant measurable GLUT1 change due to the presence of prednisolone. There was also no significant increase in GLUT1 content measured due to 20 nM C-peptide, 20 nM Zn²⁺, or 20 nM C-peptide and Zn²⁺ in the absence of albumin. Final results were obtained from normalizing GLUT1 bands to Beta Spectrin bands of each lane, and normalizing each sample to the control sample on each membrane.

3.6 Discussion

MS is often thought of as a strictly neurological disease involving the brain and spinal cord and until recently, RBCs were not implicated in the disease.⁷³ The progress of the disease is difficult to understand and predict, but it is reported that NO is found at high concentrations in various fluids and is thought to contribute by breaking down the BBB and infiltrating MS lesions.⁷⁴⁻⁷⁹ NO may be a major factor in the disease, beginning in the bloodstream with RBCs.

Although the mechanism of action of steroids is known in nucleated cells, the exact mechanism of action on RBCs is unknown. Interestingly, treatment with steroids is correlated with hypertension,^{15, 63} and may be caused by decreased endothelial NO production.³⁶ Steroid treatment also alters blood glucose levels to the point that insulin often needs to be co-administered.⁸⁰ These two facts may further indicate that steroids affect cell metabolism, specifically for the RBC.

Literature reports RBC deformability has a direct effect on RBC ATP release.^{68, 70} Results presented here show RBC deformability slightly decreases after treatment with estriol or prednisolone, although not as predominately as expected from the ATP release results (Figures 3.7 and 3.8), which may be due to low sensitivity of the deformability measurement device. As steroids affect the deformability of RBCs, a proposed mechanism of this may include the hydrophobic steroids intercalating with the RBC membrane, leading to a stiffened cell and decreased deformability. This would lead to downstream hypertension through pathways investigated by this work.

Surprisingly, MS RBCs were found to be less deformable than control RBCs. Looking to the literature, a possible explanation for this result could be that MS RBCs are larger than control RBCs ($p < 0.001$).^{71, 81} It would inherently be more difficult for the larger cells to pass through the 5 μm membrane, hindering the amount of RBCs able to pass through the membrane in the given amount of time. Size discrepancy is an inherent problem with this measurement device, and although the deformability results suggest otherwise, due to the RBC size difference, these results are not reliable and prove to be inconclusive. Alternative deformability methods that are not subjective to RBC size must be implemented to better understand the deformability of MS RBCs.

Coupled with deformability studies, RBC ATP release was measured. Comparable to previously reported results, MS RBCs released significantly more ATP compared to control RBCs,⁸² and as anticipated, RBC ATP release decreased in both control and MS

RBCs when treated with either steroid. Interestingly, the MS RBC ATP release decreased to statistically the same level as control RBCs with treatment of physiologically relevant concentrations of 7 nM estriol, 5 μ M prednisolone, and 50 μ M prednisolone. As MS RBC ATP release is decreased to statistically the same level as control RBCs due to steroid treatment, a potential mechanism of action of these steroids on RBCs may involve the reduction of RBC deformability, hindering the activation of the heterotrimeric G protein, leading to a reduction in the amount of ATP released from the RBCs.

Sequential to RBC ATP release *in vivo* is NO production from endothelial cells. As the treated RBCs were flowed through the tubing and 3D printed device, the ATP released due to shear stress would bind to bPAECs and stimulate the production of NO. Although successful at decreasing bPAEC NO production at low concentrations, estriol-treated RBCs did not alter the NO production of bPAECs at the highest concentration studied, 1 μ M. This may be explained by the high levels of excess estriol not being removed during a single washing step, and the excess estriol itself stimulating NO production. The concentration of 1 μ M estriol is also higher than levels experienced in the third trimester of pregnancy, and was only studied as an extreme case to fully understand the effects of estriol.

A decrease in bPAEC NO production was also measured when RBCs were treated with increasing concentrations of prednisolone. Although MS RBCs were not used for any of the NO measurements, the data presented here along with the mechanism being

proposed leads to the hypothesis that the basal NO production level would be higher from bPAECs in contact with MS RBCs compared to control RBCs. The same trends of decreased NO production measured due to each steroid is also hypothesized with MS RBCs, due to a decrease in the amount of RBC ATP release, supporting our hypothesis of bloodstream cells having a large impact in MS.

To further investigate the mechanism of action of prednisolone on RBCs, the binding of C-peptide and $^{65}\text{Zn}^{2+}$, along with the GLUT1 content of RBCs, were investigated when the cells were treated with prednisolone. Literature suggests that the binding of C-peptide and Zn^{2+} to RBCs increases cell metabolism, which is what this research aimed to evaluate more fully.⁷² When healthy control RBCs were initially treated with varying amounts of prednisolone, a significant decrease in $^{65}\text{Zn}^{2+}$ binding was observed. If less Zn^{2+} is able to bind to RBCs after prednisolone treatment, any effect that Zn^{2+} has on the RBC should also be attenuated, which is hypothesized through this work to be glucose internalization leading to cell metabolism.

Following the $^{65}\text{Zn}^{2+}$ measurements, the amount of C-peptide binding to RBCs treated with varying amounts of prednisolone was also measured. As with the $^{65}\text{Zn}^{2+}$ results, prednisolone treatment significantly decreased the amount of C-peptide binding to RBCs. These results, combined with the $^{65}\text{Zn}^{2+}$ results, suggest that prednisolone affects the binding of both C-peptide and Zn^{2+} to RBCs, and is thought to cause a decrease in the cell metabolism, ATP release, and subsequent NO production by the endothelium.⁷² A

possible mechanism of action may involve prednisolone binding the $^{65}\text{Zn}^{2+}$ or C-peptide to itself before they are able to bind to the RBCs, or prednisolone is possibly binding to RBCs in the same location as $^{65}\text{Zn}^{2+}$ or C-peptide, thereby causing a decrease in the measured binding.

Lacking mitochondria, the only way for RBCs to produce ATP is through glycolysis, which begins with glucose. GLUT1 is the primary glucose transporter on RBCs, and GLUT1 content in the RBC membrane may correlate to glucose flux into the cell and overall cell metabolism. Initial studies investigated the changes in the GLUT1 content of RBCs treated with C-peptide and Zn^{2+} , and a significant 25% increase compared to control, untreated cells was measured. This increase was expected, as RBC C-peptide and Zn^{2+} treatment has previously been shown to increase RBC ATP release,⁷² which is thought to be caused by an overall increased cell metabolism.

Chapter 2 showed a significant 23% increase in GLUT1 content on MS RBCs compared to control RBCs, and this increase is in agreement with the increase in RBC ATP release measured from MS RBCs compared to control RBCs (Control: 226 nM, MS: 330 nM). A proposed mechanism involves the increased GLUT1 content of MS RBCs leading to an increase in glucose flux into the cells, causing an increase in the RBC ATP production and release. This increase in cell metabolism of MS patients may be an initiation of the disease, or a cause of the experienced symptoms of the disease.

To evaluate if prednisolone has a similar effect on the RBC GLUT1 content as its effect on RBC ATP release, the GLUT1 content of control RBCs treated with prednisolone was assessed. Surprisingly, an increase in the RBC GLUT1 content was measured with treatment of prednisolone. While this does not correlate with the RBC ATP release results from prednisolone treated RBCs, a possible explanation may involve prednisolone inhibiting glucose transport through GLUT1. Studies report that steroids competitively inhibit glucose transporters,⁸³ which may cause RBCs to translocate elevated amounts of GLUT1 to the cell membrane to compensate for the inhibited glucose transport. This theory may explain the discrepancy between decreased RBC ATP release and increased RBC GLUT1 content due to the presence of prednisolone.

To further investigate how prednisolone specifically interacts with RBCs, the carrier molecule albumin was removed from the samples to evaluate its effect. Albumin is the most abundant blood protein, and aids in specific delivery of molecules to certain cells. Albumin was present in all of the experiments discussed above, but to evaluate the ability of prednisolone to bind to RBCs and elicit an effect, samples were prepared without albumin. Albumin and prednisolone have an affinity constant of $4.32 \times 10^2 \text{ M}^{-1}$,⁸⁴ and when albumin was absent from the samples, prednisolone had no effect on the amount of GLUT1 on the RBC membrane, suggesting that albumin must be present for prednisolone to specifically bind to RBCs and elicit an effect. Also noteworthy, a statistically significant 6% decrease in RBC GLUT1 content was measured in RBCs in buffer without albumin compared to RBCs in albumin-containing buffer. These results suggest that albumin content alone effects the RBC GLUT1 content, which may be due

to oncotic pressure exerted by albumin, or albumin itself stimulating an increase in the GLUT1 content of the cell.

In summary of the findings from these studies, RBC derived ATP may play a large role in MS. RBCs from MS patients release significantly more ATP than control RBCs, and RBC released ATP stimulates endothelial NO production.^{36, 68} The excess ATP released from MS RBCs is thought to lead to excess NO production from endothelial cells, which can be detrimental to the BBB.³⁹⁻⁴⁰ Although the mechanism of action of steroids in MS is well established, it only applies to cells containing a nucleus, which does not include RBCs.¹¹⁻¹² Any effect that steroids have on RBCs must be in a manner that has yet to be established. Here, further studies were performed to more fully investigate that mechanism. Estriol and prednisolone were both shown to decrease RBC deformability, ATP release, and sequential bPAEC NO production; and prednisolone was found to decrease the amount of both C-peptide and ⁶⁵Zn²⁺ binding to RBCs, while increasing the RBC GLUT1 content. C-peptide and Zn²⁺ stimulate RBC ATP release,⁷² and this work supports the hypothesis that MS RBCs have an increased cell metabolism at basal level, which estriol and prednisolone decrease. This may be a mechanism of action for steroids in the bloodstream, and ultimately help to better understand the disease of MS.

REFERENCES

REFERENCES

1. Dhib-Jalbut, S.; Marks, S., Interferon-beta mechanisms of action in multiple sclerosis. *Neurology* **2010**, *74 Suppl 1*, S17-24.
2. Kappos, L.; Polman, C. H.; Freedman, M. S.; Edan, G.; Hartung, H. P.; Miller, D. H.; Montalban, X.; Barkhof, F.; Bauer, L.; Jakobs, P.; Pohl, C.; Sandbrink, R., Treatment with interferon beta-1b delays conversion to clinically definite and McDonald MS in patients with clinically isolated syndromes. *Neurology* **2006**, *67* (7), 1242-1249.
3. Comi, G.; Filippi, M.; Barkhof, F.; Durelli, L.; Edan, G.; Fernandez, O.; Hartung, H.; Seeldrayers, P.; Sorensen, P. S.; Rovaris, M.; Martinelli, V.; Hommes, O. R.; Early Treatment of Multiple Sclerosis Study, G., Effect of early interferon treatment on conversion to definite multiple sclerosis: a randomised study. *Lancet* **2001**, *357* (9268), 1576-1582.
4. Reuss, R., PEGylated interferon beta-1a in the treatment of multiple sclerosis - an update. *Biologics* **2013**, *7*, 131-138.
5. Comi, G.; Filippi, M.; Wolinsky, J. S., European/Canadian multicenter, double-blind, randomized, placebo-controlled study of the effects of glatiramer acetate on magnetic resonance imaging--measured disease activity and burden in patients with relapsing multiple sclerosis. European/Canadian Glatiramer Acetate Study Group. *Ann Neurol* **2001**, *49* (3), 290-297.
6. Brinkmann, V., FTY720 (fingolimod) in Multiple Sclerosis: therapeutic effects in the immune and the central nervous system. *Br J Pharmacol* **2009**, *158* (5), 1173-1182.
7. Brinkmann, V.; Billich, A.; Baumruker, T.; Heining, P.; Schmouder, R.; Francis, G.; Aradhye, S.; Burtin, P., Fingolimod (FTY720): discovery and development of an oral drug to treat multiple sclerosis. *Nat Rev Drug Discov* **2010**, *9* (11), 883-897.
8. Matloubian, M.; Lo, C. G.; Cinamon, G.; Lesneski, M. J.; Xu, Y.; Brinkmann, V.; Allende, M. L.; Proia, R. L.; Cyster, J. G., Lymphocyte egress from thymus and peripheral lymphoid organs is dependent on S1P receptor 1. *Nature* **2004**, *427* (6972), 355-360.
9. Bar-Or, A., Teriflunomide (Aubagio(R)) for the treatment of multiple sclerosis. *Exp Neurol* **2014**, *262 Pt A*, 57-65.
10. Bompreszi, R., Dimethyl fumarate in the treatment of relapsing-remitting multiple sclerosis: an overview. *Ther Adv Neurol Disord* **2015**, *8* (1), 20-30.
11. Thompson, E. B.; Lippman, M. E., Mechanism of action of glucocorticoids. *Metabolism* **1974**, *23* (2), 159-202.

12. Rhen, T.; Cidlowski, J. A., Antiinflammatory action of glucocorticoids--new mechanisms for old drugs. *N Engl J Med* **2005**, *353* (16), 1711-1723.
13. Edelman, I. S., Mechanism of action of steroid hormones. *J Steroid Biochem* **1975**, *6* (3-4), 147-159.
14. Whitworth, J. A.; Mangos, G. J.; Kelly, J. J., Cushing, cortisol, and cardiovascular disease. *Hypertension* **2000**, *36* (5), 912-916.
15. Goodwin, J. E.; Geller, D. S., Glucocorticoid-induced hypertension. *Pediatr Nephrol* **2012**, *27* (7), 1059-1066.
16. Schacke, H.; Docke, W. D.; Asadullah, K., Mechanisms involved in the side effects of glucocorticoids. *Pharmacol Ther* **2002**, *96* (1), 23-43.
17. Yadav, V.; Shinto, L.; Bourdette, D., Complementary and alternative medicine for the treatment of multiple sclerosis. *Expert Rev Clin Immunol* **2010**, *6* (3), 381-395.
18. Nayak, S.; Matheis, R. J.; Schoenberger, N. E.; Shiflett, S. C., Use of unconventional therapies by individuals with multiple sclerosis. *Clin Rehabil* **2003**, *17* (2), 181-191.
19. Berkman, C. S.; Pignotti, M. G.; Cavallo, P. F.; Holland, N. J., Use of alternative treatments by people with multiple sclerosis. *Neurorehab Neural Re* **1999**, *13* (4), 243-254.
20. Swank, R. L.; Goodwin, J., Review of MS patient survival on a swank low saturated fat diet. *Nutrition* **2003**, *19* (2), 161-162.
21. Das, U. N., Is there a role for saturated and long-chain fatty acids in multiple sclerosis? *Nutrition* **2003**, *19* (2), 163-166.
22. Choi, I. Y.; Piccio, L.; Childress, P.; Bollman, B.; Ghosh, A.; Brandhorst, S.; Suarez, J.; Michalsen, A.; Cross, A. H.; Morgan, T. E.; Wei, M.; Paul, F.; Bock, M.; Longo, V. D., A Diet Mimicking Fasting Promotes Regeneration and Reduces Autoimmunity and Multiple Sclerosis Symptoms. *Cell Rep* **2016**, *15* (10), 2136-2146.
23. Kim, D. Y.; Hao, J.; Liu, R.; Turner, G.; Shi, F. D.; Rho, J. M., Inflammation-mediated memory dysfunction and effects of a ketogenic diet in a murine model of multiple sclerosis. *PLoS One* **2012**, *7* (5), e35476.
24. Neal, E. G.; Chaffe, H.; Schwartz, R. H.; Lawson, M. S.; Edwards, N.; Fitzsimmons, G.; Whitney, A.; Cross, J. H., The ketogenic diet for the treatment of childhood epilepsy: a randomised controlled trial. *Lancet Neurol* **2008**, *7* (6), 500-506.
25. Storoni, M.; Plant, G. T., The Therapeutic Potential of the Ketogenic Diet in Treating Progressive Multiple Sclerosis. *Mult Scler Int* **2015**, *2015*, 681289.

26. Matute, C., Glutamate and ATP signalling in white matter pathology. *J Anat* **2011**, 219 (1), 53-64.
27. Matute, C.; Torre, I.; Perez-Cerda, F.; Perez-Samartin, A.; Alberdi, E.; Etxebarria, E.; Arranz, A. M.; Ravid, R.; Rodriguez-Antiguedad, A.; Sanchez-Goomez, M. V.; Domercq, M., P2X(7) receptor blockade prevents ATP excitotoxicity in oligodendrocytes and ameliorates experimental autoimmune encephalomyelitis. *J Neurosci* **2007**, 27 (35), 9525-9533.
28. Bradl, M.; Lassmann, H., Oligodendrocytes: biology and pathology. *Acta Neuropathol* **2010**, 119 (1), 37-53.
29. Sharp, A. J.; Polak, P. E.; Simonini, V.; Lin, S. X.; Richardson, J. C.; Bongarzone, E. R.; Feinstein, D. L., P2x7 deficiency suppresses development of experimental autoimmune encephalomyelitis. *J Neuroinflammation* **2008**, 5, 33.
30. Trautmann, A., Extracellular ATP in the immune system: more than just a "danger signal". *Sci Signal* **2009**, 2 (56), pe6.
31. Trabanelli, S.; Ocadlikova, D.; Gulinelli, S.; Curti, A.; Salvestrini, V.; Vieira, R. P.; Idzko, M.; Di Virgilio, F.; Ferrari, D.; Lemoli, R. M., Extracellular ATP exerts opposite effects on activated and regulatory CD4+ T cells via purinergic P2 receptor activation. *J Immunol* **2012**, 189 (3), 1303-1310.
32. Letourneau, S.; Hernandez, L.; Faris, A. N.; Spence, D. M., Evaluating the effects of estradiol on endothelial nitric oxide stimulated by erythrocyte-derived ATP using a microfluidic approach. *Anal Bioanal Chem* **2010**, 397 (8), 3369-3375.
33. Groen, K.; Maltby, V. E.; Sanders, K. A.; Scott, R. J.; Tajouri, L.; Lechner-Scott, J., Erythrocytes in multiple sclerosis - forgotten contributors to the pathophysiology? *Mult Scler J Exp Transl Clin* **2016**, 2..
34. Sprague, R. S.; Ellsworth, M. L.; Stephenson, A. H.; Kleinhenz, M. E.; Lonigro, A. J., Deformation-induced ATP release from red blood cells requires CFTR activity. *Am J Physiol-Heart C* **1998**, 275 (5), H1726-H1732.
35. Sprague, R. S.; Ellsworth, M. L.; Stephenson, A. H.; Lonigro, A. J., ATP: The red blood cell link to NO and local control of the pulmonary circulation. *Am J Physiol-Heart C* **1996**, 271 (6), H2717-H2722.
36. Ellsworth, M. L.; Sprague, R. S., Regulation of blood flow distribution in skeletal muscle: role of erythrocyte-released ATP. *J Physiol-London* **2012**, 590 (20), 4985-4991.
37. Kuchan, M. J.; Frangos, J. A., Role of Calcium and Calmodulin in Flow-Induced Nitric-Oxide Production in Endothelial-Cells. *Am J Physiol* **1994**, 266 (3), C628-C636.
38. Sprague, R. S.; Stephenson, A. H.; Dimmitt, R. A.; Weintraub, N. A.; Branch, C. A.; McMurdo, L.; Lonigro, A. J., Effect of L-NAME on pressure-flow relationships in

isolated rabbit lungs: Role of red blood cells. *Am J Physiol-Heart C* **1995**, 269 (6), H1941-H1948.

39. Smith, K. J.; Lassmann, H., The role of nitric oxide in multiple sclerosis. *Lancet Neurology* **2002**, 1 (4), 232-241.

40. Minagar, A.; Alexander, J. S., Blood-brain barrier disruption in multiple sclerosis. *Mult Scler* **2003**, 9 (6), 540-549.

41. Giovannoni, G., Cerebrospinal fluid and serum nitric oxide metabolites in patients with multiple sclerosis. *Mult Scler* **1998**, 4 (1), 27-30.

42. Giovannoni, G.; Heales, S. J. R.; Land, J. M.; Thompson, E. J., The potential role of nitric oxide in multiple sclerosis. *Mult Scler J* **1998**, 4 (3), 212-216.

43. Giovannoni, G.; Silver, N. C.; O'Riordan, J.; Miller, R. F.; Heales, S. J. R.; Land, J. M.; Elliot, M.; Feldmann, M.; Miller, D. H.; Thompson, E. J., Increased urinary nitric oxide metabolites in patients with multiple sclerosis correlates with early and relapsing disease. *Mult Scler* **1999**, 5 (5), 335-341.

44. Boje, K. M. K.; Lakhman, S. S., Nitric oxide redox species exert differential permeability effects on the blood-brain barrier. *J Pharmacol Exp Ther* **2000**, 293 (2), 545-550.

45. Smith, K. J.; Kapoor, R.; Hall, S. M.; Davies, M., Electrically active axons degenerate when exposed to nitric oxide. *Annals of Neurology* **2001**, 49 (4), 470-476.

46. Bolanos, J. P.; Almeida, A.; Stewart, V.; Peuchen, S.; Land, J. M.; Clark, J. B.; Heales, S. J. R., Nitric oxide-mediated mitochondrial damage in the brain: Mechanisms and implications for neurodegenerative diseases. *J Neurochem* **1997**, 68 (6), 2227-2240.

47. Stein, E. C.; Schiffer, R. B.; Hall, W. J.; Young, N., Multiple sclerosis and the workplace: report of an industry-based cluster. *Neurology* **1987**, 37 (10), 1672-1677.

48. Schiffer, R. B.; McDermott, M. P.; Copley, C., A multiple sclerosis cluster associated with a small, north-central Illinois community. *Arch Environ Health* **2001**, 56 (5), 389-395.

49. Ho, S. Y.; Catalanotto, F. A.; Lisak, R. P.; Dore-Duffy, P., Zinc in multiple sclerosis. II: Correlation with disease activity and elevated plasma membrane-bound zinc in erythrocytes from patients with multiple sclerosis. *Annals of neurology* **1986**, 20 (6), 712-715.

50. Letourneau, S. Delivery of Zinc to Red Blood Cells and the Downstream Effects in Multiple Sclerosis. Dissertation, Michigan State University, 2013.

51. Bredholt, M.; Frederiksen, J. L., Zinc in Multiple Sclerosis: A Systematic Review and Meta-Analysis. *ASN Neuro* **2016**, 8 (3).

52. Stuve, O.; Oksenberg, J., Multiple Sclerosis Overview. In *GeneReviews(R)*, Pagon, R. A.; Adam, M. P.; Ardinger, H. H.; Wallace, S. E.; Amemiya, A.; Bean, L. J. H.; Bird, T. D.; Fong, C. T.; Mefford, H. C.; Smith, R. J. H.; Stephens, K., Eds. Seattle (WA), 1993.
53. Voskuhl, R. R.; Gold, S. M., Sex-related factors in multiple sclerosis susceptibility and progression. *Nat Rev Neurol* **2012**, *8* (5), 255-263.
54. Airas, L.; Kaaja, R., Pregnancy and multiple sclerosis. *Obstet Med* **2012**, *5* (3), 94-97.
55. Lee, M.; O'Brien, P., Pregnancy and multiple sclerosis. *J Neurol Neurosurg Psychiatry* **2008**, *79* (12), 1308-1311.
56. Houtchens, M. K., Pregnancy and multiple sclerosis. *Semin Neurol* **2007**, *27* (5), 434-441.
57. Confavreux, C.; Hutchinson, M.; Hours, M. M.; Cortinvis-Tourniaire, P.; Moreau, T., Rate of pregnancy-related relapse in multiple sclerosis. Pregnancy in Multiple Sclerosis Group. *N Engl J Med* **1998**, *339* (5), 285-291.
58. Vukusic, S.; Confavreux, C., Pregnancy and multiple sclerosis: the children of PRIMS. *Clin Neurol Neurosurg* **2006**, *108* (3), 266-270.
59. Vukusic, S.; Ionescu, I.; El-Etr, M.; Schumacher, M.; Baulieu, E. E.; Cornu, C.; Confavreux, C.; Prevention of Post-Partum Relapses with, P.; Estradiol in Multiple Sclerosis Study, G., The Prevention of Post-Partum Relapses with Progestin and Estradiol in Multiple Sclerosis (POPART'MUS) trial: rationale, objectives and state of advancement. *J Neurol Sci* **2009**, *286* (1-2), 114-118.
60. Sicotte, N. L.; Liva, S. M.; Klutch, R.; Pfeiffer, P.; Bouvier, S.; Odesa, S.; Wu, T. C.; Voskuhl, R. R., Treatment of multiple sclerosis with the pregnancy hormone estriol. *Ann Neurol* **2002**, *52* (4), 421-428.
61. Palaszynski, K. M.; Liu, H.; Loo, K. K.; Voskuhl, R. R., Estriol treatment ameliorates disease in males with experimental autoimmune encephalomyelitis: implications for multiple sclerosis. *J Neuroimmunol* **2004**, *149* (1-2), 84-89.
62. Avila-Ornelas, J.; Avila, M.; Stosic, M.; Robles, L.; Prieto, P. G.; Hutton, G. J.; Rivera, V. M., The role of postpartum intravenous corticosteroids in the prevention of relapses in multiple sclerosis. *Int J MS Care* **2011**, *13* (2), 91-93.
63. Mantero, F.; Armanini, D.; Boscaro, M.; Carpene, G.; Fallo, F.; Opocher, G.; Rocco, S.; Scaroni, C.; Sonino, N., Steroids and hypertension. *J Steroid Biochem Mol Biol* **1991**, *40* (1-3), 35-44.

64. Gross, B. C.; Erkal, J. L.; Lockwood, S. Y.; Chen, C.; Spence, D. M., Evaluation of 3D printing and its potential impact on biotechnology and the chemical sciences. *Anal Chem* **2014**, *86* (7), 3240-3253.
65. Morrow, S. A.; McEwan, L.; Alikhani, K.; Hyson, C.; Kremenchutzky, M., MS patients report excellent compliance with oral prednisone for acute relapses. *Can J Neurol Sci* **2012**, *39* (3), 352-354.
66. Chen, C. 3D-Printed In Vitro Analytical Devices for Diabetes Therapeutics and Blood Banking Studies. Michigan State University, 2015.
67. Forsyth, A. M.; Wan, J.; Ristenpart, W. D.; Stone, H. A., The dynamic behavior of chemically "stiffened" red blood cells in microchannel flows. *Microvasc Res* **2010**, *80* (1), 37-43.
68. Sprague, R. S.; Ellsworth, M. L.; Stephenson, A. H.; Lonigro, A. J., ATP: the red blood cell link to NO and local control of the pulmonary circulation. *Am J Physiol* **1996**, *271* (6 Pt 2), H2717-H2722.
69. Price, A. K.; Fischer, D. J.; Martin, R. S.; Spence, D. M., Deformation-Induced Release of ATP from Erythrocytes in a Poly(dimethylsiloxane)-Based Microchip with Channels That Mimic Resistance Vessels. *Analytical Chemistry* **2004**, *76* (16), 4849-4855.
70. Sprague, R. S.; Olearczyk, J. J.; Spence, D. M.; Stephenson, A. H.; Sprung, R. W.; Lonigro, A. J., Extracellular ATP signaling in the rabbit lung: Erythrocytes as determinants of vascular resistance. *American Journal of Physiology* **2003**, *285* (2, Pt. 2), H693-H700.
71. Prineas, J., Red blood cell size in multiple sclerosis. *Acta Neurol Scand* **1968**, *44* (1), 81-90.
72. Liu, Y.; Chen, C.; Summers, S.; Medawala, W.; Spence, D. M., C-peptide and zinc delivery to erythrocytes requires the presence of albumin: implications in diabetes explored with a 3D-printed fluidic device. *Integr Biol (Camb)* **2015**, *7* (5), 534-543.
73. Lockwood, S. Y.; Summers, S.; Eggenberger, E.; Spence, D. M., An In Vitro Diagnostic for Multiple Sclerosis Based on C-peptide Binding to Erythrocytes. *EBioMedicine* **2016**, *11*, 249-252.
74. Smith, K. J.; Lassmann, H., The role of nitric oxide in multiple sclerosis. *Lancet Neurol* **2002**, *1* (4), 232-241.
75. Minagar, A.; Alexander, J. S., Blood-brain barrier disruption in multiple sclerosis. *Mult Scler* **2003**, *9* (6), 540-549.
76. Giovannoni, G.; Silver, N. C.; O'Riordan, J.; Miller, R. F.; Heales, S. J.; Land, J. M.; Elliot, M.; Feldmann, M.; Miller, D. H.; Thompson, E. J., Increased urinary nitric oxide

metabolites in patients with multiple sclerosis correlates with early and relapsing disease. *Mult Scler* **1999**, 5 (5), 335-341.

77. Giovannoni, G.; Heales, S. J.; Land, J. M.; Thompson, E. J., The potential role of nitric oxide in multiple sclerosis. *Mult Scler* **1998**, 4 (3), 212-216.

78. Giovannoni, G., Cerebrospinal fluid and serum nitric oxide metabolites in patients with multiple sclerosis. *Mult Scler* **1998**, 4 (1), 27-30.

79. Boje, K. M.; Lakhman, S. S., Nitric oxide redox species exert differential permeability effects on the blood-brain barrier. *The Journal of pharmacology and experimental therapeutics* **2000**, 293 (2), 545-550.

80. Perez, A.; Jansen-Chaparro, S.; Saigi, I.; Bernal-Lopez, M. R.; Minambres, I.; Gomez-Huelgas, R., Glucocorticoid-induced hyperglycemia. *J Diabetes* **2014**, 6 (1), 9-20.

81. Peng, Y. F.; Cao, W. Y.; Zhang, Q.; Chen, D.; Zhang, Z. X., Assessment of the Relationship Between Red Cell Distribution Width and Multiple Sclerosis. *Medicine (Baltimore)* **2015**, 94 (29), e1182.

82. Letourneau, S.; Hernandez, L.; Faris, A. N.; Spence, D. M., Evaluating the effects of estradiol on endothelial nitric oxide stimulated by erythrocyte-derived ATP using a microfluidic approach. *Anal Bioanal Chem* **2010**, 397 (8), 3369-3375.

83. Lacko, L.; Wittke, B.; Geck, P., Interaction of steroids with the transport system of glucose in human erythrocytes. *J Cell Physiol* **1975**, 86 Suppl 2 (3 Pt 2), 673-680.

84. Rocci, M. L., Jr.; D'Ambrosio, R.; Johnson, N. F.; Jusko, W. J., Prednisolone binding to albumin and transcortin in the presence of cortisol. *Biochem Pharmacol* **1982**, 31 (3), 289-292.

Chapter 4 – The Role of Albumin in Delivering C-peptide and Zinc to the RBC

4.1 Insulin and C-peptide

4.1.1 Diabetes and Insulin

As one of the first described diseases, diabetes was originally classified as “madhumeha”, or “honey urine” around 1500 BC, as the urine had a sweet taste and would attract ants and flies.¹ Described in section 2.1.1, diabetes is now often characterized by elevated blood glucose levels (hyperglycemia) in the body resulting from either low insulin production from damaged pancreatic β -cells, as seen in Type 1 Diabetes (T1D); or an improper response to insulin produced in the body, as seen in Type 2 Diabetes (T2D). Hyperglycemia leads to poor blood flow, a major complication experienced by diabetic patients, and Table 2.2 summarizes the specifics of the experienced complications.

Insulin is a hormone in the body that stimulates glucose clearance from the bloodstream into skeletal muscle, liver, and fat cells through the translocation and activation of glucose transporter 4 (GLUT4) to the membrane of cells.²⁻⁴ Insulin is produced in the islets of Langerhans in pancreatic β -cells, and Fredrick Banting and Charles Best discovered it as a vital hormone for T1D patients in 1921.¹ In 1922, the first administration of insulin occurred in a 14-year old boy who was suffering at the end stages of diabetes. After two insulin injections his blood glucose levels decreased, and with continued administration of insulin, the boy lived an additional 13 years before dying of pneumonia.¹

Since its discovery, improved insulin purification methods along with new insulin formulations have been developed. Insulin is most commonly administered by subcutaneous injections; however, inhaled insulin is also available.⁵ Fast acting, along with long action insulin products are available, and the specific prescription depends on each patient. Although insulin stimulates the translocation of GLUT4 to decrease blood glucose levels, most bloodstream cells do not contain GLUT4, but instead contain GLUT1. An accompaniment therapy to stimulate GLUT1 translocation in bloodstream cells may help decrease blood glucose levels, along with diabetic blood flow complications.

When patients present with diabetic symptoms, physicians must distinguish between T1D and T2D before determining the most effective treatment process. β -cell activity is tested to determine the correct diagnosis, as the main difference between T1D patients and T2D patients is the functionality of the pancreatic β -cells. Insulin has a half-life of about 10 minutes in the bloodstream, making it difficult to measure.¹ However, C-peptide, a peptide secreted in equimolar amounts with insulin, has a half-life of about 30 minutes in the bloodstream, and is thus a more ideal candidate to measure, and ultimately use as a biomarker to diagnose T1D or T2D.⁶ T1D patients will have very low (or nonexistent) concentrations of C-peptide due to their damaged β -cells, while T2D patients will have a significantly higher C-peptide concentration in their bloodstream.

4.1.2 Biological Effects of C-peptide

C-peptide is a 31-amino acid peptide and contains five acidic amino acids, giving it a charge of -5 at physiological pH. During production, C-peptide is connected to insulin in the pancreas as the proinsulin hormone, and the two are cleaved prior to secretion into the bloodstream. The proinsulin hormone, along with the amino acid sequence of C-peptide is shown in Figure 4.1.

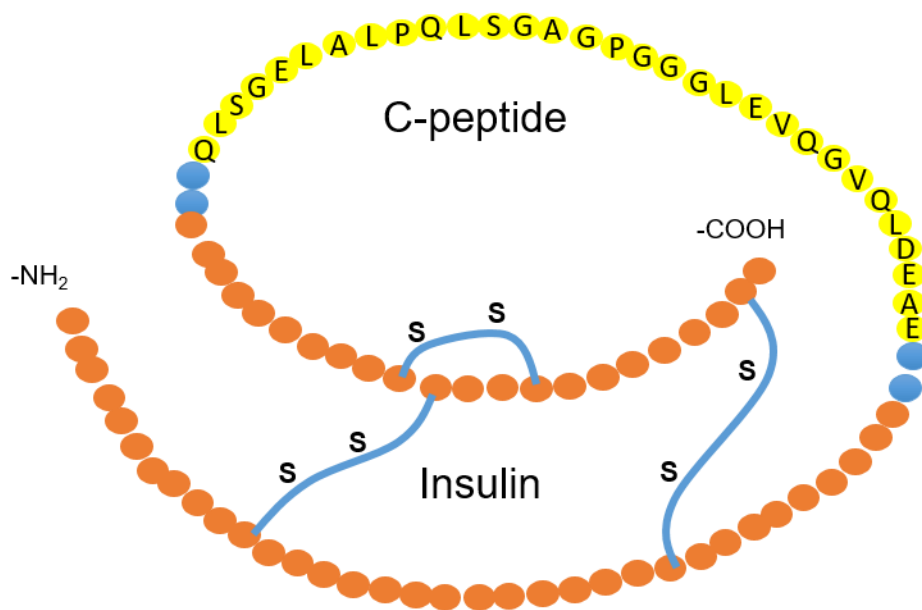


Figure 4.1 - Proinsulin. The full structure of proinsulin with the C-peptide amino acid sequence shown in yellow, and the A and B chains of insulin in orange. Before C-peptide and insulin are secreted into the bloodstream they are cleaved apart by enzymes at the locations depicted in blue. Once in the bloodstream, C-peptide has a half-life of about 30 minutes, while insulin has a half-life of about 4-6 minutes.

Originally, C-peptide was thought to have no biological activity after secretion, but recent work suggests otherwise.⁷⁻⁹ An increase in blood flow in the kidney and nervous system has been measured after administration of exogenous C-peptide, and C-peptide combined with insulin has been proposed as a T1D therapy to alleviate diabetic complications.¹⁰⁻¹¹ Reporting success in early phase trials, Cebix, a start-up company in LaJolla, CA, developed a long-acting C-peptide for use in T1D patients, supplementing insulin injections.¹² Although successful in animal studies, no improvement in nerve function was measured in T1D humans treated with C-peptide during the phase IIb clinical trial.¹²

Previous work in the Spence group has investigated the effect of C-peptide on RBCs. While C-peptide alone does not elicit any downstream effects on the RBC, when it is combined with Zn^{2+} and the bloodstream protein albumin, an increase in RBC ATP release is measured, as shown in Figure 4.2.¹³ An increase in downstream endothelial NO production is also only measured when C-peptide is combined with both Zn^{2+} and albumin.¹³ This is significant due to the vasodilation effects that NO has on smooth muscle cells, resulting in increased blood flow.

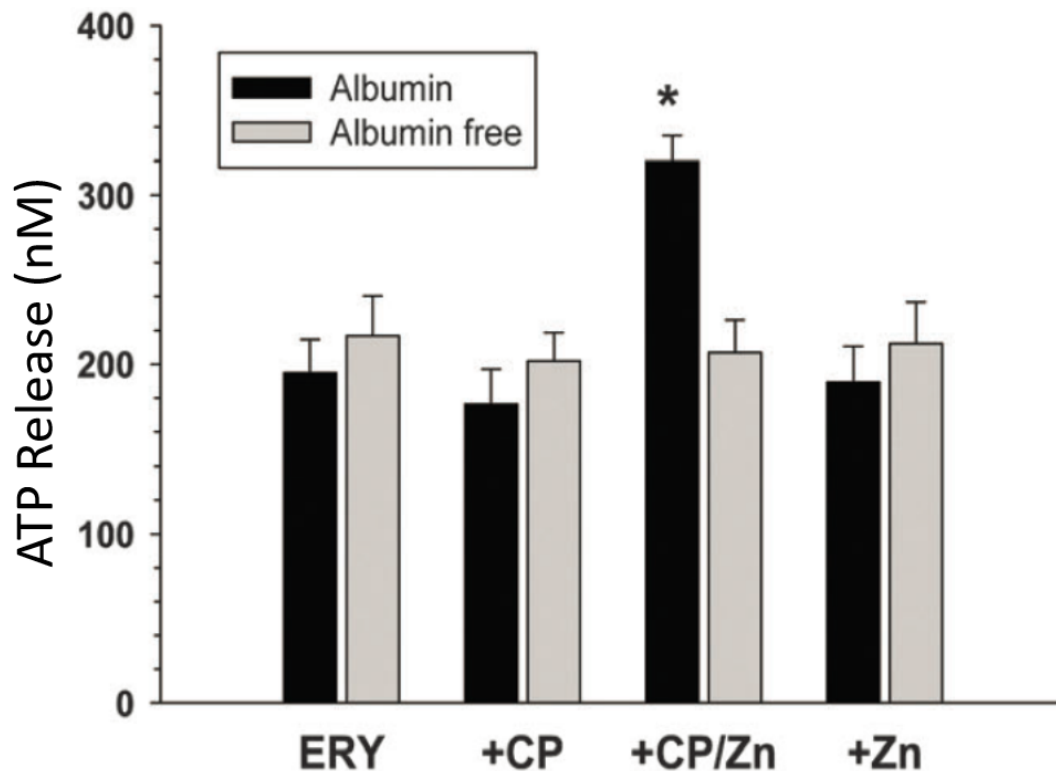


Figure 4.2 – RBC ATP Release With and Without Albumin. RBC ATP release with and without C-peptide, Zn^{2+} , and albumin. Albumin containing samples are depicted in the black bars and albumin free samples are depicted in the gray bars. An increase in ATP release is only measured in the presence of the complex of C-peptide, Zn^{2+} , and albumin. * $p < 0.005$ to RBCs with albumin, $n = 5$.¹³

RBCs produce ATP by glycolysis, and because GLUT1 is the main glucose transporter on RBCs, its content on RBCs may be an indicator of cell metabolism. RBC ATP release has been reported to have beneficial effects on blood flow, which is severely hindered in diabetic patients,¹⁴⁻¹⁸ and although insulin stimulates glucose uptake into cells, it has no effects on GLUT1 containing cells such as RBCs and lymphocytes. An accompaniment therapy to stimulate GLUT1 translocation in bloodstream cells may help decrease both the blood glucose levels and microvasculature complications of diabetic patients, and the

work presented in this chapter investigates C-peptide, Zn^{2+} , and albumin as a potential T1D accompaniment therapy to insulin.

4.2 Albumin

Human serum albumin (shown in Figure 4.3) is the most abundant protein found in human blood plasma, and constitutes about half of the overall serum protein.¹⁹ The concentration of albumin in the bloodstream of a healthy adult is around 600 μM , which has a half-life of approximately 19 days.²⁰ The main functions of human serum albumin are to maintain oncotic pressure in the blood vessels and transport drugs, hormones, metal ions, and fatty acids.²¹ Hypoalbuminemia occurs when the levels of albumin in the blood are low, which can be caused by liver disease and diabetes, among other conditions.²² As stated in section 2.1.1.2, glycated albumin is present in the diabetic bloodstream, and the glycosylation may hinder the ability of albumin to transport molecules properly.

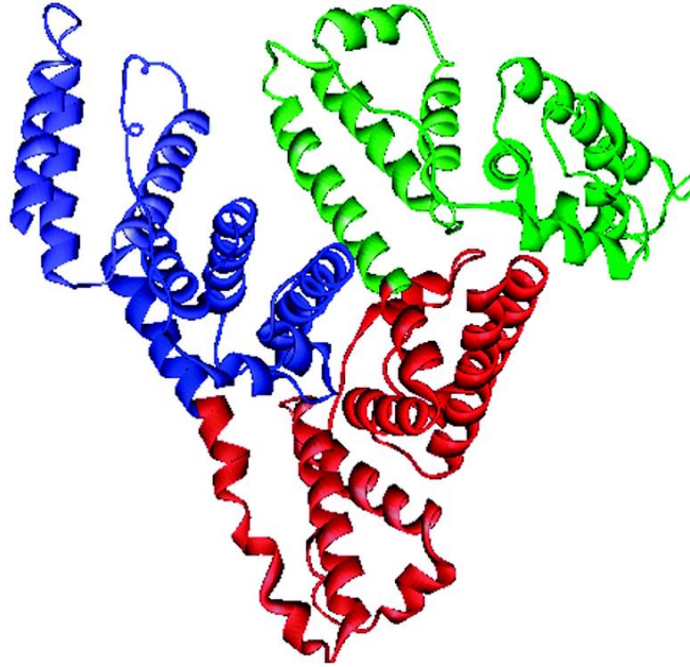


Figure 4.3 - Human Serum Albumin. The tertiary structure of human serum albumin, the most abundant blood protein. The three domains of the protein are depicted in blue, green, and red. In the bloodstream, human serum albumin is responsible for maintaining pressure and transporting drugs, hormones, metal ions, and fatty acids throughout the body.¹⁹

All experiments presented in this dissertation were performed with buffer containing bovine serum albumin due to its decreased cost and similar function to human serum albumin. Bovine and human serum albumin differ slightly in structure, one difference being that bovine serum albumin contains two tryptophan residues while human serum albumin only has one, which may affect substrate binding to the protein.¹⁹ While we predict the function of human serum albumin to be similar to what we measure using the bovine source, it is important to note that there is potential for slight differences.

Studies using isothermal titration calorimetry (ITC) have shown that bovine serum albumin will specifically bind two C-peptide molecules and three Zn^{2+} ions; however, C-peptide and Zn^{2+} are unable to bind each other in the absence of bovine serum albumin.¹³ ²³ Studies involving treatment with albumin, C-peptide, and Zn^{2+} elicit an increase in RBC ATP release, however no change in RBC ATP release is measured when albumin is absent from the samples (Figure 4.2).¹³ The same trend is observed with respect to endothelial NO production stimulated by RBC ATP release,¹³ suggesting that albumin is a necessary component in order for C-peptide and Zn^{2+} to elicit their desired effect on RBCs.

4.3 Experimental

4.3.1 Isolation and Purification of Red Blood Cells

Whole blood was obtained through venipuncture from consenting donors and collected into heparinized tubes (Fisher Scientific, Waltham, MA). Whole blood was then centrifuged at 500g for 10 minutes, and the plasma and buffy coat were removed and saved. The RBCs were resuspended in either physiological salt solution (PSS) or albumin-free PSS, containing 4.7 mM KCl, 2.0 mM $CaCl_2$, 140.5 mM NaCl, 12 mM $MgSO_4$, 21.0 mM tris(hydroxymethyl) aminomethane, 5.5 mM dextrose and 0.5% bovine serum albumin (omitted for albumin-free PSS) at pH 7.4. All RBCs were prepared the day of each experiment and used within 8 hours of collection.

4.3.2 Preparation of Reagents

Distilled deionized water (18 M Ω , DDW) was used for all experiments. Zn²⁺ stock solutions were prepared by dissolving 0.02 g Zinc (II) chloride (Jade Scientific, Canton, MI) in 100 mL DDW and diluting to 800 nM with DDW, and the initial ⁶⁵Zn²⁺ stock was prepared by diluting 500 μ Ci of ⁶⁵ZnCl₂ (Perkin Elmer, Boston, MA) in 30 mL DDW (80 μ M), followed by sequential dilutions in to 800 nM in 1 mL total volume. All solutions were prepared in DDW.

Crude C-peptide (80% pure, Peptide 2.0, Chantally, VA) was purified using reverse-phase high performance liquid chromatography (HPLC) with settings shown previously in Table 3.1. The purified C-peptide was subsequently lyophilized overnight prior to dissolution of 5 mg in 5 mL DDW. C-peptide purity was verified using HPLC- mass spectrometry, and a final 800 nM stock solution was prepared in DDW and the concentration was verified using C-peptide enzyme linked immunosorbent assay (ELISA) kit standards.

For ATP detection, a stock luciferin/luciferase solution was prepared by dissolving 20 mg of Luciferin (Golden Bio, Olivette, MO) and 100 mg firefly lantern extract (Sigma Aldrich, St. Louis, MO) in 10 mL DDW. Samples (1 mL total volume) were prepared at 7% hematocrit with and without C-peptide and Zn²⁺ by first adding 25 μ L of 800 nM C-peptide or 800 nM Zn²⁺, followed by PSS, and then RBCs (about 7.8×10^8 total cells). In certain experiments, PSS was substituted for control or T1D plasma to determine if albumin found in the plasma could serve as the C-peptide and Zn²⁺ carrier to the RBCs. The

plasma (2-3 mL) was removed from the whole blood following the initial centrifugation, and added to the specified samples in place of PSS.

The following reagents were all used for Western Blot analyses: Tris buffered saline (TBS) was prepared by dissolving 2.4 g of UltraPure Tris-hydrochloride and 29.2 g of sodium chloride in 1 L of water at a pH of 7.5, and TBS with Tween (TBST) was prepared by mixing 500 mL of TBS with 250 μ L of Tween-20 (Sigma Aldrich). Bicarbonate buffer was prepared by dissolving 4.1 g of sodium bicarbonate and 0.2 g of magnesium chloride in 500 mL of water. 10x running buffer was prepared by dissolving 144.0 g glycine, 30.2 g Tris, and 10.0 g SDS in 1 L of water, and 10x transfer buffer was prepared by dissolving 3.0 g Tris and 14.4 g glycine in 200 mL of methanol and 800 mL water at a pH of 8.3. Running buffer and transfer buffer were reused six times before disposal, and 500 mL of lysis buffer was prepared with 10.0 mM UltraPure Tris-hydrochloride and 0.2 mM EDTA at a pH of 7.2 in DDW.

4.3.3 Radioactive $^{65}\text{Zn}^{2+}$ Binding Determination

To measure $^{65}\text{Zn}^{2+}$ binding to RBCs, 7% RBC samples (1 mL total volume) were prepared with varying concentrations of $^{65}\text{Zn}^{2+}$ (Perkin Elmer, Downers Grove, IL), or a combination of C-peptide and $^{65}\text{Zn}^{2+}$ (0, 2.5, 5, 10, 20, 50 nM). The samples were prepared in either albumin-containing PSS, or albumin-free PSS, and all samples were incubated for 2 hours at 37°C followed by centrifugation at 500g for 5 minutes. The supernatant of each

sample was analyzed, and the amount of $^{65}\text{Zn}^{2+}$ binding was determined by subtraction of the remaining amount of $^{65}\text{Zn}^{2+}$ from the amount initially added. For detection, 200 μL of the sample supernatant was mixed with 100 μL of Ultima Gold Scintillation Cocktail (Perkin Elmer, Boston, MA) in a 96-well plate and analyzed using a Micro Beta scintillation counter (Perkin Elmer).

4.3.4 C-peptide Binding to Red Blood Cells

To measure C-peptide binding to RBCs in various matrices, 7% RBC samples were prepared with 20 nM C-peptide in PSS with and without albumin (1 mL total volume). Two other sets of samples were prepared in plasma obtained from either control donors or donors with T1D to evaluate the effect of physiological albumin on C-peptide binding. These samples were prepared in the same manner; however, the albumin source came from the plasma rather than the PSS. RBCs used for the albumin-free samples and all plasma samples were washed in albumin-free buffer before sample preparation, while RBCs for all other samples were washed in buffer containing bovine serum albumin. Samples were prepared in their respective buffers with 20 nM C-peptide and allowed to incubate at 37°C for 2 hours. After the incubation, the samples were centrifuged and the supernatant was removed and diluted 1:50 in DDW to assure final values within the dynamic range of the assay prior to analysis with commercially available C-peptide ELISA kits (ALPCO, Salem, NH). Similar to the $^{65}\text{Zn}^{2+}$ measurements, the amount of C-peptide binding to RBCs was calculated by subtracting the amount measured in the supernatant

from the amount added. The ELISA kit assay consists of wells coated with primary C-peptide antibodies to capture the C-peptide molecules in the sample. After the initial capture, secondary antibodies conjugated with an enzyme were added to each well. Before detection, a substrate was added that produced a colorimetric reaction when combined with the enzyme. A final addition of the stop solution halted the ongoing reaction and an absorbance measurement was taken at 450 nm by a plate reader.

4.3.5 Detection of Red Blood Cell Released ATP

A luciferin/luciferase chemiluminescence assay was used to quantify the amount of ATP released by RBCs. 7% RBC samples were prepared in albumin-containing PSS with 20 nM C-peptide only, 20 nM Zn^{2+} only, and a 20 nM Zn^{2+} and C-peptide mixture (1 mL total volume). A final set of samples contained 7% RBCs with 20 nM Zn^{2+} and C-peptide in albumin-free PSS. All samples were incubated at 37°C for 2 hours, and ATP standards (0, 20, 40, 60, and 80 nM) in PSS were prepared for use in calibration for quantitative analysis. After the incubation period, the standard addition method was used to quantify the amount of ATP released by the RBCs. For detection, 120 μ L of the RBC sample were mixed with 20 μ L of each ATP standard (one at a time) and 10 μ L of the luciferin/luciferase mixture in a 96-well plate prior to luminescence detection by a Spectra Max M4 plate reader (Molecular Devices, San Jose, CA) exactly 20 seconds later.

4.3.6 Preparing Red Blood Cell Ghost Samples

RBC sample preparation was similar to preparation described in section 4.3.5, resulting in 1 mL samples of 7% RBCs with and without C-peptide, Zn^{2+} , and albumin. Two other sets of samples evaluated the effect of control and T1D plasma on the GLUT1 content in control and T1D RBCs, in place of PSS. These two sets of samples were prepared in exactly the same manner, however the albumin source came from the respective plasma instead of PSS. After incubation and centrifugation, the supernatant of each sample was removed, and the remaining pelleted RBCs were lysed with 1 mL of lysis buffer. The samples were then stored at 4°C for 30 minutes and then centrifuged at 22,000g for 15 minutes at 4°C. The resulting supernatant was removed, and the pellet was resuspended in 1 mL of lysis buffer. Once again, the samples were centrifuged at 22,000g and 4°C for 5 minutes, the supernatant was removed, and the RBCs resuspended in 1 mL of lysis buffer. This process was repeated three times total or until no more hemoglobin (red color) was visible. Once all hemoglobin was removed, the remaining lysis buffer was removed, and the pellets were stored at -20°C until use. This was done to remove all cytosolic contents from the RBC to allow for analysis of the membrane protein content.

4.3.7 GLUT1 SDS-PAGE and Western Blot Analysis

Sodium dodecyl sulfate polyacrylamide gel electrophoresis (SDS-PAGE) and subsequent Western Blot analysis was used to probe GLUT1 content of each sample. Experimental procedures are as stated in section 3.4.12.

4.4 Results

The amount of $^{65}\text{Zn}^{2+}$ binding to RBCs in the presence and absence of C-peptide and albumin was evaluated and shown in Figure 4.4A. $^{65}\text{Zn}^{2+}$ does not bind to RBCs when C-peptide is absent (dark circles), and while binding does occur when albumin is absent (open circles); the binding is nonspecific. Only when the complex of $^{65}\text{Zn}^{2+}$, C-peptide, and albumin are present together does a specific binding curve of $^{65}\text{Zn}^{2+}$ to RBCs result (dark triangles and Figure 4.4B). The specific binding curve saturates around 10 nM of C-peptide and $^{65}\text{Zn}^{2+}$ added (correlating to about 2 pmoles of $^{65}\text{Zn}^{2+}$ bound to RBCs), before going onto nonspecific binding past 20 nM of C-peptide and $^{65}\text{Zn}^{2+}$ added.

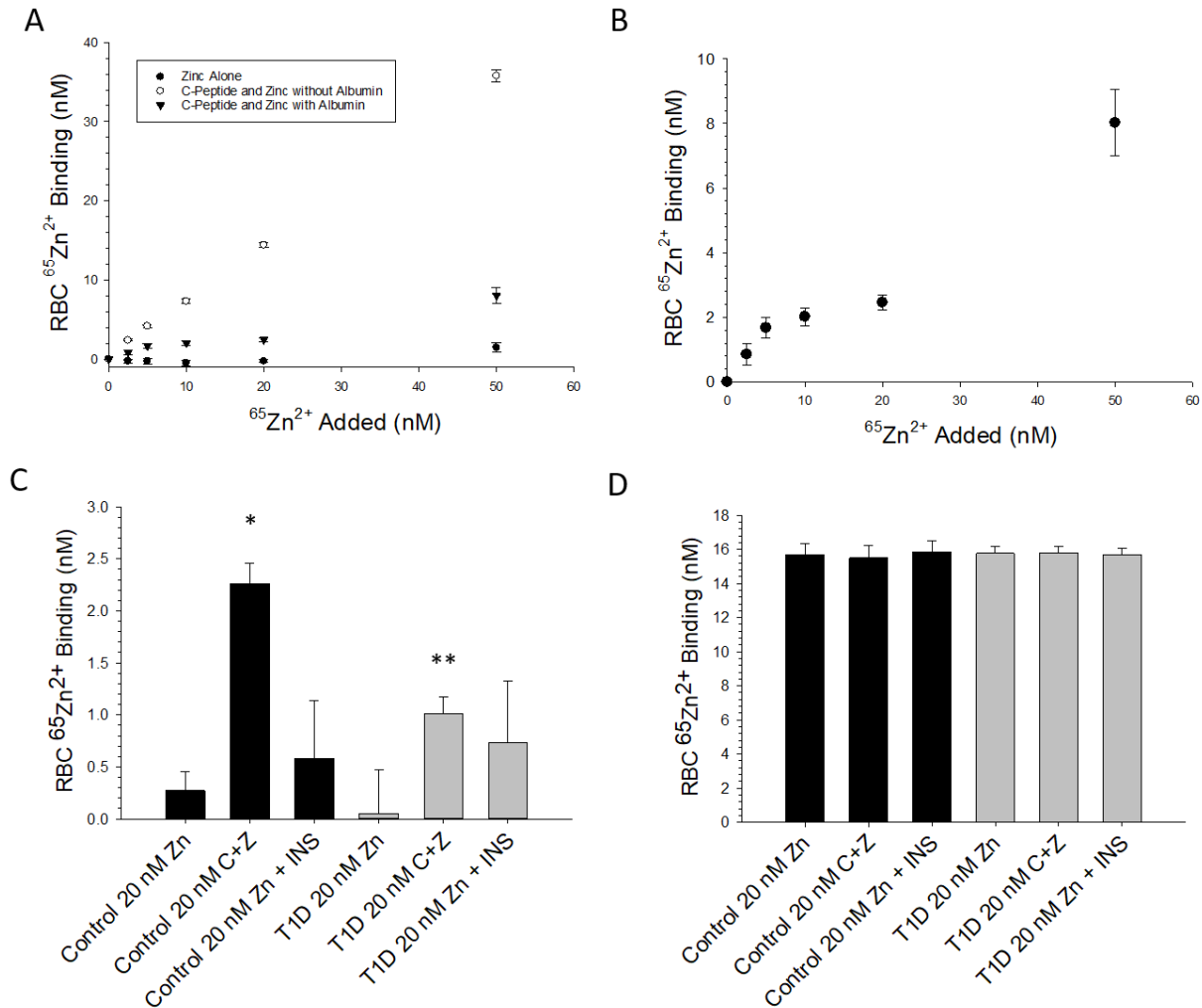


Figure 4.4 – Control and T1D RBC $^{65}\text{Zn}^{2+}$ Binding. **A.** RBC $^{65}\text{Zn}^{2+}$ binding in the presence and absence of C-peptide and albumin as increasing concentrations of $^{65}\text{Zn}^{2+}$ and C-peptide are added to the RBCs (along the x-axis). **B.** RBC $^{65}\text{Zn}^{2+}$ binding with C-peptide in the presence of albumin shown on a smaller scale to more clearly highlight the specific binding curve measured. $n \geq 8$ donors, error bars = SEM. **C.** Control and T1D RBC $^{65}\text{Zn}^{2+}$ binding with and without C-peptide and insulin, in the presence of albumin. Control RBC = black bars, T1D RBC = gray bars. * $p < 0.05$ to Control 20 nM Zn, ** $p < 0.05$ to T1D 20 nM Zn, $n \geq 5$ donors, error bars = SEM. **D.** Control and T1D RBC $^{65}\text{Zn}^{2+}$ binding with and without C-peptide and insulin, all without albumin. Control RBC = black bars, T1D RBC = gray bars. $n \geq 6$ donors, error bars = SEM.

The amount $^{65}\text{Zn}^{2+}$ binding to control and T1D RBCs when saturated with 20 nM $^{65}\text{Zn}^{2+}$ is shown in Figures 4.4C and 4.4D. Albumin was present in the samples shown in Figure 4.4C, while Figure 4.4D represents samples prepared without albumin. Without albumin, nonspecific binding of $^{65}\text{Zn}^{2+}$ to both control and T1D RBCs occurs, and there is no significant difference between any of the samples. When albumin is present, a significant difference in control and T1D RBC $^{65}\text{Zn}^{2+}$ binding is measured (Control: 2.26 ± 0.20 nM $^{65}\text{Zn}^{2+}$ T1D: 1.01 ± 0.15 nM $^{65}\text{Zn}^{2+}$, $p < 0.05$), but only when C-peptide is present. Notably, insulin did not have any significant effect on $^{65}\text{Zn}^{2+}$ binding to control or T1D RBCs.

Previous work demonstrated that C-peptide and Zn^{2+} stimulate *in vivo* ATP release; however, albumin is requisite for this result.¹³ Similar results are described here under static conditions. Figure 4.5A shows an average ATP release of 31.2 ± 0.80 nM from RBCs without albumin (black triangles), and a release of 41.6 ± 1.3 nM when albumin is present. C-peptide and Zn^{2+} are titrated into RBCs (along the x-axis), and the ATP release does not statistically change unless albumin is present in the samples (open circles). When albumin is present, the RBC ATP release increased from 42.1 ± 1.3 nM to 76.1 ± 1.5 nM in the shape of a specific binding curve.

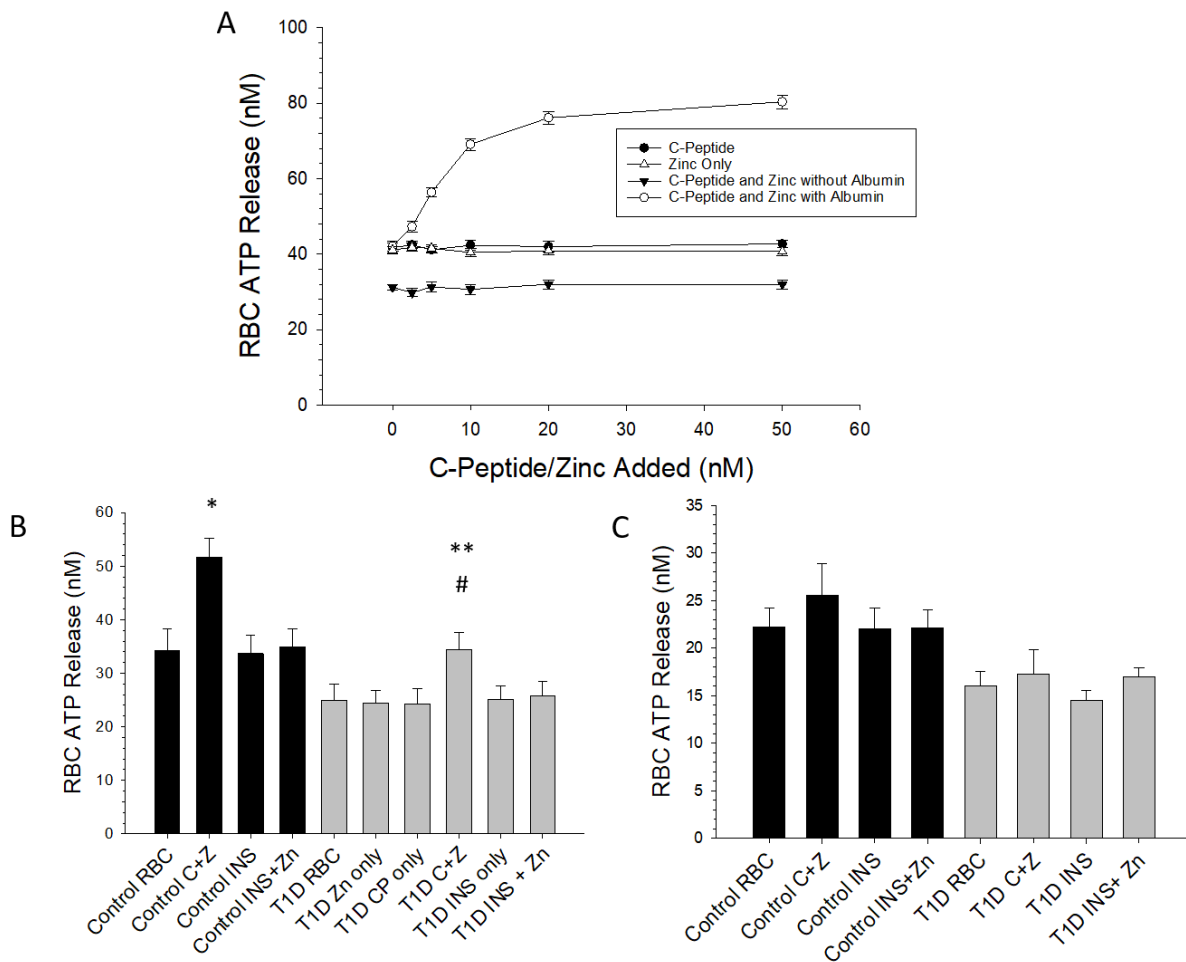


Figure 4.5 – Control and T1D RBC ATP Release. **A.** RBC ATP release in the presence and absence of C-peptide, Zn^{2+} , and albumin, with increasing concentrations of Zn^{2+} and C-peptide are added to the RBCs (along the x-axis). $n \geq 6$ donors, error bars = SEM. **B.** Control and T1D RBC ATP release with and without C-peptide, Zn^{2+} , and insulin, in the presence of albumin. Control RBC = black bars, T1D RBC = gray bars. * $p < 0.05$ to Control RBC, ** $p < 0.05$ to T1D RBC, # $p > 0.4$ to Control RBC, $n \geq 7$ donors, error bars = SEM. **C.** Control and T1D RBC ATP release with and without C-peptide, Zn^{2+} , and insulin, all without albumin. Control RBC = black bars, T1D RBC = gray bars. $n \geq 7$ donors, error bars = SEM.

When 20 nM C-peptide and Zn^{2+} are added to the RBCs in the presence of albumin, a significant increase in ATP release is measured from both control and T1D RBCs

(Control: 17.5 ± 3.3 nM increase, T1D: 9.6 ± 2.9 nM increase, Figure 4.5B). Without albumin, no significant change in ATP release is measured due to the addition of C-peptide and Zn^{2+} (Figure 4.5C). Noteworthy, T1D RBCs release significantly less ATP at basal levels in the presence of albumin compared to control RBCs (Control: 34.2 nM \pm 3.7 nM, T1D: 24.9 nM \pm 2.8 nM); however, when treated with 20 nM of C-peptide and Zn^{2+} , T1D RBCs released statistically the same amount of ATP as control RBCs. Similar to the $^{65}Zn^{2+}$ experiments, insulin did not have any significant effect on the RBC ATP release from control or T1D RBCs.

Glucose is necessary for RBC ATP production, and GLUT1 is the main glucose transporter on RBCs. As the previous results show, when albumin, C-peptide, and Zn^{2+} are combined with RBCs, the measured ATP release increases. It is thought that GLUT1 content is related to glucose flux and cell metabolism, and to verify that relation, RBC ghosts (RBCs with their hemoglobin removed) were prepared, and the GLUT1 and Beta Spectrin (housekeeping protein) content was measured by SDS-PAGE and Western Blot analysis. Figure 4.6A shows that C-peptide and Zn^{2+} do not statistically affect the RBC GLUT1 content unless albumin is present (black triangles). When C-peptide and Zn^{2+} are titrated into control RBCs in the presence of albumin, the GLUT1 content increases resembling a specific binding curve that levels off at a $25.5 \pm 1.3\%$ increase compared to the untreated control sample.

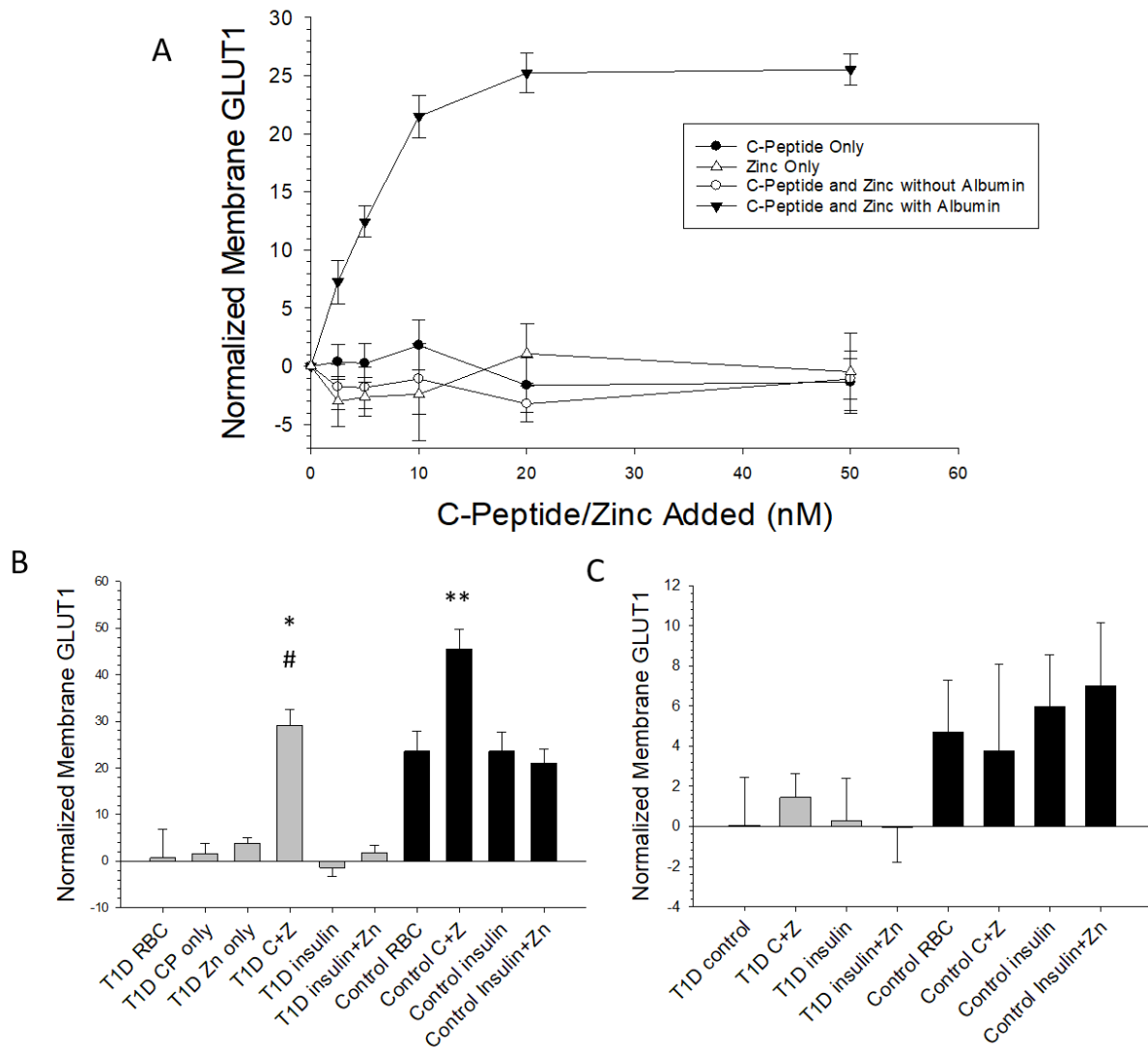


Figure 4.6 – Control and T1D RBC GLUT1 Content. **A.** RBC membrane GLUT1 content in the presence and absence of C-peptide, Zn^{2+} , and albumin as increasing concentrations of Zn^{2+} and C-peptide are added to the RBCs (along the x-axis). $n \geq 5$ donors, error bars = SEM. **B.** Control and T1D RBC GLUT1 content with and without C-peptide, Zn^{2+} , and insulin, in the presence of albumin. Control RBC = black bars, T1D RBC = gray bars. * $p < 0.05$ to T1D RBC, ** $p < 0.05$ to Control RBC, # $p > 0.1$ to Control RBC, $n \geq 7$ donors, error bars = SEM. **C.** Control and T1D RBC GLUT1 content with and without C-peptide, Zn^{2+} , and insulin, all without albumin. Control RBC = black bars, T1D RBC = gray bars. $n \geq 6$ donors, error bars = SEM.

Figure 4.6B shows the GLUT1 content of control and T1D RBCs treated with and without 20 nM C-peptide and Zn²⁺ in the presence of albumin; and Figure 4.6C shows the same samples without albumin. At basal levels, T1D RBCs contain 23.6 ± 4.2% less GLUT1 than control RBCs; however, when T1D RBCs are combined with C-peptide and Zn²⁺ in the presence of albumin, the GLUT1 content increases to statistically the same value as untreated control RBCs. This increase in GLUT1 content is not measured when any component of the complex is absent, and similar to the previous experiments, insulin had no effect on the RBC GLUT1 content.

When control or T1D plasma was substituted for PSS as the albumin source, the RBC GLUT1 levels were similar to those measured in normal PSS. Figures 4.7A and 4.7B show the T1D and control RBC GLUT1 levels in control and T1D plasma, respectively. In control plasma, control RBCs contained 14.7 ± 2.8% more GLUT1 than T1D RBCs at basal levels, and the addition of C-peptide and Zn²⁺ increased the GLUT1 content of control and T1D RBCs 19.9 ± 1.5% and 26.5 ± 3.9%, respectively. No significant increase in GLUT1 content was measured in control or T1D RBCs in the presence of insulin alone or insulin and Zn²⁺. In T1D plasma at basal levels, control RBCs contained 13.2 ± 2.3% more GLUT1 than T1D RBCs, and in the presence of C-peptide and Zn²⁺, the GLUT1 content of control and T1D RBCs increased by 17.9 ± 3.4% and 29.8 ± 3.6%, respectively. As with the control plasma, the presence of insulin alone or insulin and Zn²⁺ did not significantly affect the GLUT1 content of control or T1D RBCs.

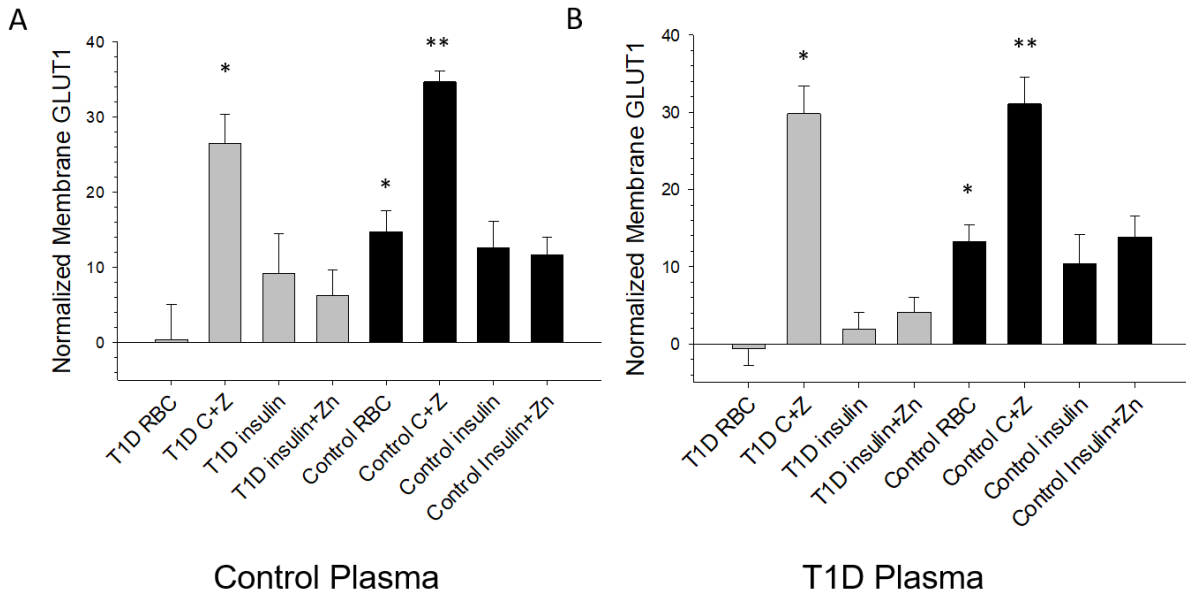


Figure 4.7 – RBC GLUT1 Content in Control and T1D Plasma. **A.** Normalized membrane GLUT1 content of control and T1D RBCs in control plasma with and without C-peptide, Zn²⁺, and insulin added to the RBCs. Control RBC = black bars, T1D RBC = gray bars. * p ≤ 0.05 to T1D RBC, ** p ≤ 0.05 to Control RBC, n ≥ 7 donors, error bars = SEM. **B.** Normalized membrane GLUT1 content of control and T1D RBCs in T1D plasma with and without C-peptide, Zn²⁺, and insulin. Control RBC = black bars, T1D RBC = gray bars. * p ≤ 0.05 to T1D RBC, ** p ≤ 0.05 to Control RBC, n ≥ 7 donors, error bars = SEM.

As shown in Chapter 1, previous work investigated the binding of increasing amounts of C-peptide in the presence of albumin to 7% RBCs.¹³ The aforementioned figure is shown again in Figure 4.8A, and depicts that RBCs become saturated when 10 nM C-peptide is added, which correlates to about 1500 molecules of C-peptide binding per RBC when saturated, and the addition of Zn²⁺ does not affect the amount of C-peptide binding.¹³ Figure 4.8B shows C-peptide binding to control and T1D RBCs with and without albumin when 20 nM C-peptide is added. Control RBCs bind significantly more C-peptide than T1D RBCs (Control: 1.95 ± 0.14 nM, T1D: 0.86 ± 0.11 nM), and no significant C-peptide binding is measured when albumin is absent from the samples.

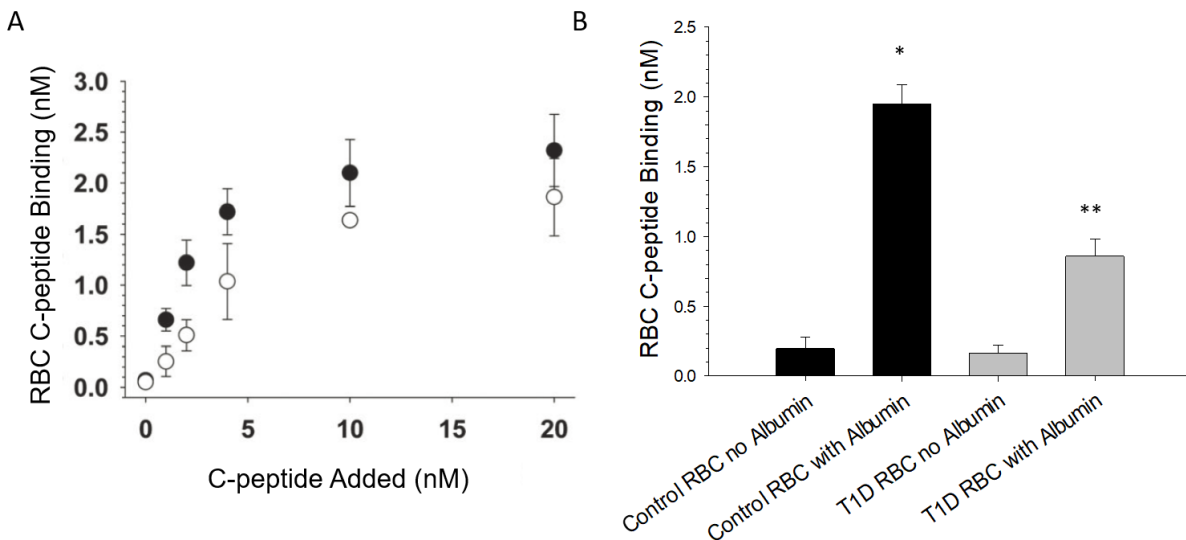


Figure 4.8 – Control and T1D C-peptide Binding. A. C-peptide binding to RBCs with (open circles) and without (filled circles) Zn²⁺, as increasing amounts of C-peptide and Zn²⁺ are added to RBCs (along x-axis). The C-peptide binding is not significantly different without Zn²⁺, and saturates around 2.0 pmoles C-peptide on RBCs. n = 4, error bars = SEM.¹³ B. Control and T1D RBC C-peptide binding when 20 nM C-peptide was added to RBCs with and without albumin. C-peptide binding was measured using a commercial ELISA kit and quantified using standards. Control RBC = black bars, T1D RBC = gray bars. * p < 0.05 to Control RBC no Albumin ** p < 0.05 to T1D RBC no Albumin, n ≥ 7 donors, error bars = SEM.

Control and T1D plasma was substituted for PSS as the albumin source, and the RBC C-peptide binding results are shown in Figure 4.9. The results show a significant increase in the RBC C-peptide binding in control plasma compared to T1D plasma, and Zn²⁺ has no significant effect on the amount of C-peptide binding. While T1D plasma does not support any significant C-peptide binding to T1D RBCs, 1.06 ± 0.14 nM C-peptide binds to control RBCs in T1D plasma. Control plasma supports significantly more C-peptide

binding than T1D plasma, with 2.00 ± 0.12 nM C-peptide binding to control RBCs, and 0.50 ± 0.09 nM C-peptide binding to T1D RBCs.

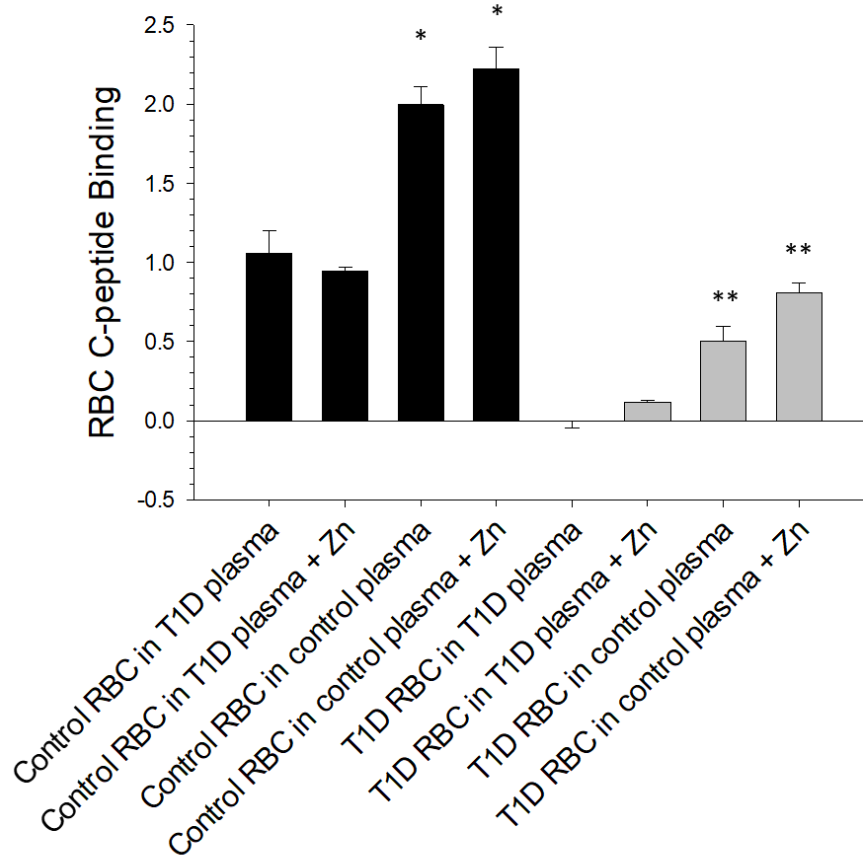


Figure 4.9 – RBC C-peptide Binding in Control and T1D Plasma. Control and T1D RBC C-peptide binding in control and T1D plasma. The addition of Zn^{2+} did not change the amount of C-peptide binding under any of the tested conditions. Control RBCs are depicted in the black bars, T1D RBCs are depicted in the gray bars. * $p \leq 0.05$ to Control RBC in T1D plasma, ** $p \leq 0.05$ to T1D RBC in T1D plasma, $n \geq 7$ donors, error bars = SEM.

4.5 Discussion

A therapy to improve microvasculature complications is needed for T1D patients, as many complications of diabetes, such as retinopathy,¹⁴ neuropathy,¹⁷ and nephropathy, are associated with insufficient blood flow.²⁴ Insulin is effective at maintaining healthy blood glucose levels; however, an accompaniment therapy is also necessary to help improve microvasculature blood flow. While insulin stimulates blood stream glucose clearance through GLUT4-containing muscle and adipose cells, most blood stream cells contain GLUT1.²⁵ C-peptide has previously been investigated as a means to improve diabetic complications with success improving renal blood flow, nerve conduction, and promoting nerve fiber regeneration,²⁶⁻³¹ and this work supports and furthers those findings. Results from this work propose that the complex of C-peptide, Zn^{2+} , and albumin may be a potential candidate to improve diabetic microvasculature complications, and results suggest that the complex may work in a similar manner as insulin does on cells containing GLUT1.

To summarize the finding of this work, a possible mechanism of increased RBC ATP release may involve C-peptide and Zn^{2+} increasing the GLUT1 translocation to the cell membrane. As more GLUT1 is translocated to the membrane, it is thought that glucose flux into the RBC will increase, leading to an increase in ATP production within the cell and subsequent ATP release. ATP release *in vivo* stimulates endothelial NO production and vasodilation,³²⁻³⁴ which improves blood flow and is proposed to alleviate diabetic microvasculature complications. However, C-peptide and Zn^{2+} are unable to bind each

other without albumin, and no significant change in RBC GLUT1 content or ATP release is measured without the full complex of C-peptide, Zn^{2+} , and albumin. Interestingly, insulin has no significant effect on $^{65}Zn^{2+}$ or C-peptide binding to RBCs, or RBC GLUT1 content or ATP release, which indicates that administration of insulin alone does not enhance this proposed mechanism, further supporting the use of this complex to supplement insulin and alleviate diabetic microvasculature complications.

Overall, the results from experiments involving T1D and control plasma as the albumin source suggest that T1D plasma and T1D RBCs are glycosylated or otherwise damaged, causing them to not bind as much C-peptide or translocate as much GLUT1 to the RBC membrane compared to control experiments. Additional findings from the experiments involving plasma were contradictory to each other. C-peptide binding studies indicated that no binding of C-peptide to T1D RBCs occurs when T1D plasma was used as the albumin source, however an increase in the GLUT1 content of T1D RBCs was measured under the same conditions. The cause of this discrepancy is not fully understood, but hypotheses may include a more complex mechanism than what is currently thought, or the potential for C-peptide to elicit an effect on RBCs without remaining specifically bound to the cells.

Previously, C-peptide purity has come into question, with some published work using C-peptide that is only 95% to 98% pure.³⁵ Our lab has previously investigated the contaminants in an impure C-peptide sample, and found impurities to mainly be Fe^{2+} .³⁶

Although this comprises a small percent of contamination by mass, when looked at on a mole basis, a 98% pure C-peptide sample by mass is actually close to a 1:1 molar ratio of C-peptide and Fe^{2+} .³⁵ This amount of Fe^{2+} contamination may affect C-peptide interactions throughout certain experiments, and is the reason that all C-peptide was purified by HPLC prior to use in experiments presented in this dissertation.

The company Cebix previously attempted to use C-peptide as a T1D replacement therapy to accompany insulin, however their phase IIb clinical trial did not improve nerve function of the T1D patients tested.¹² Important to note, the company was only treating patients with a long-acting C-peptide (unspecified purity), rather than the C-peptide, Zn^{2+} , albumin complex reported here. Although speculative, work presented in this chapter suggests that the trial may have ended with different results had the company administered the complex of (purified) C-peptide, Zn^{2+} , and albumin to the T1D patients, opposed to C-peptide only.

Results presented in this chapter suggest that T1D RBCs contain significantly less GLUT1, release significantly less ATP, and bind significantly less C-peptide and $^{65}\text{Zn}^{2+}$ compared to healthy control RBCs. However, an increase in control and T1D RBC GLUT1 content and ATP release was measured when RBCs were treated with the complex of C-peptide, Zn^{2+} , and albumin. Interestingly, as T1D RBCs are treated with C-peptide and Zn^{2+} in the presence of albumin, both the GLUT1 content and the RBC ATP release increased to statistically the same level as the control RBCs. These results support the

hypothesis that the complex of C-peptide, Zn^{2+} , and albumin may be working as insulin does on GLUT1 containing cells, and lead to increased blood flow to ultimately alleviate diabetic microvasculature complications such as retinopathy, neuropathy, and nephropathy; and ultimately help T1D patients live longer and healthier lives.¹⁴⁻¹⁸

REFERENCES

REFERENCES

1. Poretsky, L., *Principles of diabetes mellitus*. 2nd ed.; Springer: New York, 2010; p xviii, 887.
2. Kono, T.; Suzuki, K.; Dansey, L. E.; Robinson, F. W.; Blevins, T. L., Energy-dependent and protein synthesis-independent recycling of the insulin-sensitive glucose transport mechanism in fat cells. *J Biol Chem* **1981**, *256* (12), 6400-6407.
3. Brewer, P. D.; Habtemichael, E. N.; Romenskaia, I.; Mastick, C. C.; Coster, A. C., Insulin-regulated Glut4 translocation: membrane protein trafficking with six distinctive steps. *J Biol Chem* **2014**, *289* (25), 17280-17298.
4. Karnieli, E.; Zarnowski, M. J.; Hissin, P. J.; Simpson, I. A.; Salans, L. B.; Cushman, S. W., Insulin-stimulated translocation of glucose transport systems in the isolated rat adipose cell. Time course, reversal, insulin concentration dependency, and relationship to glucose transport activity. *J Biol Chem* **1981**, *256* (10), 4772-4777.
5. Hollander, P. A.; Blonde, L.; Rowe, R.; Mehta, A. E.; Milburn, J. L.; Hershon, K. S.; Chiasson, J. L.; Levin, S. R., Efficacy and safety of inhaled insulin (exubera) compared with subcutaneous insulin therapy in patients with type 2 diabetes: results of a 6-month, randomized, comparative trial. *Diabetes Care* **2004**, *27* (10), 2356-2362.
6. Polonsky, K. S.; Rubenstein, A. H., C-peptide as a measure of the secretion and hepatic extraction of insulin. Pitfalls and limitations. *Diabetes* **1984**, *33* (5), 486-494.
7. Lockwood, S. Y.; Summers, S.; Eggenberger, E.; Spence, D. M., An In Vitro Diagnostic for Multiple Sclerosis Based on C-peptide Binding to Erythrocytes. *EBioMedicine* **2016**, *11*, 249-252.
8. Hach, T.; Forst, T.; Kunt, T.; Ekberg, K.; Pflutzner, A.; Wahren, J., C-peptide and its C-terminal fragments improve erythrocyte deformability in type 1 diabetes patients. *Exp Diabetes Res* **2008**, *2008*, 730594.
9. Clark, J. L.; Cho, S.; Rubenstein, A. H.; Steiner, D. F., Isolation of a proinsulin connecting peptide fragment (C-peptide) from bovine and human pancreas. *Biochem Biophys Res Commun* **1969**, *35* (4), 456-461.
10. Navarro, X.; Sutherland, D. E.; Kennedy, W. R., Long-term effects of pancreatic transplantation on diabetic neuropathy. *Ann Neurol* **1997**, *42* (5), 727-736.
11. Fiorina, P.; Folli, F.; Zerbini, G.; Maffi, P.; Gremizzi, C.; Di Carlo, V.; Socci, C.; Bertuzzi, F.; Kashgarian, M.; Secchi, A., Islet transplantation is associated with improvement of renal function among uremic patients with type I diabetes mellitus and kidney transplants. *J Am Soc Nephrol* **2003**, *14* (8), 2150-2158.

12. Wahren, J.; Foyt, H.; Daniels, M.; Arezzo, J. C., Long-Acting C-Peptide and Neuropathy in Type 1 Diabetes: A 12-Month Clinical Trial. *Diabetes Care* **2016**, 39 (4), 596-602.
13. Liu, Y.; Chen, C.; Summers, S.; Medawala, W.; Spence, D. M., C-peptide and zinc delivery to erythrocytes requires the presence of albumin: implications in diabetes explored with a 3D-printed fluidic device. *Integr Biol (Camb)* **2015**, 7 (5), 534-543.
14. Icks, A.; Trautner, C.; Haastert, B.; Berger, M.; Giani, G., Blindness due to diabetes: Population-based age- and sex-specific incidence rates. *Diabetic Medicine* **1997**, 14 (7), 571-575.
15. Keenan, H. A.; Costacou, T.; Sun, J. K.; Doria, A.; Cavallerano, J.; Coney, J.; Orchard, T. J.; Aiello, L. P.; King, G. L., Clinical factors associated with resistance to microvascular complications in diabetic patients of extreme disease duration - The 50-year medalist study. *Diabetes Care* **2007**, 30 (8), 1995-1997.
16. Sheetz, M. J.; King, G. L., Molecular understanding of hyperglycemia's adverse effects for diabetic complications. *Jama-J Am Med Assoc* **2002**, 288 (20), 2579-2588.
17. Sugimoto, K.; Murakawa, Y.; Sima, A. A. F., Diabetic neuropathy - a continuing enigma. *Diabetes-Metab Res* **2000**, 16 (6), 408-433.
18. Boulton, A. J. M.; Gries, F. A.; Jervell, J. A., Guidelines for the diagnosis and outpatient management of diabetic peripheral neuropathy. *Diabetic Medicine* **1998**, 15 (6), 508-514.
19. Ramezani, F.; Rafii-Tabar, H., An in-depth view of human serum albumin corona on gold nanoparticles. *Mol Biosyst* **2015**, 11 (2), 454-462.
20. Sleep, D.; Cameron, J.; Evans, L. R., Albumin as a versatile platform for drug half-life extension. *Biochim Biophys Acta* **2013**, 1830 (12), 5526-5534.
21. Peters, T., *All about albumin : biochemistry, genetics, and medical applications*. Academic Press: San Diego, 1996; p xx, 432.
22. Swartz, R. D.; Rubin, J. E.; Leeming, B. W.; Silva, P., Renal failure following major angiography. *Am J Med* **1978**, 65 (1), 31-37.
23. Liu, Y. Delivery of a Pancreatic Beta Cell-Derived Hormone to Erythrocytes by Albumin and Downstream Cellular Effects. Michigan State University, 2015.
24. Aoun, S.; Blacher, J.; Safar, M. E.; Mourad, J. J., Diabetes mellitus and renal failure: effects on large artery stiffness. *J Hum Hypertens* **2001**, 15 (10), 693-700.
25. Vrhovac, I.; Brejčak, D.; Sabolic, I., Glucose transporters in the mammalian blood cells. *Period Biol* **2014**, 116 (2), 131-138.

26. Cotter, M. A.; Ekberg, K.; Wahren, J.; Cameron, N. E., Effects of proinsulin C-peptide in experimental diabetic neuropathy: Vascular actions and modulation by nitric oxide synthase inhibition. *Diabetes* **2003**, *52* (7), 1812-1817.
27. Ekberg, K.; Johansson, B.-L., Effect of C-peptide on diabetic neuropathy in patients with type 1 diabetes. *Experimental Diabetes Research* **2008**.
28. Johansson, B. L.; Borg, K.; Fernqvist-Forbes, E.; Kernell, A.; Odergren, T.; Wahren, J., Beneficial effects of C-peptide on incipient nephropathy and neuropathy in patients with type 1 diabetes mellitus. *Diabetic Medicine* **2000**, *17* (3), 181-189.
29. Kamiya, H.; Zhang, W.; Sima, A. A. F., C-peptide prevents nociceptive sensory neuropathy in type 1 diabetes. *Annals of Neurology* **2004**, *56* (6), 827-835.
30. Sima, A. A. F.; Zhang, W.; Grunberger, G., Type 1 diabetic neuropathy and C-peptide. *Experimental Diabetes Research* **2004**, *5* (1), 65-77.
31. Wahren, J.; Ekberg, K.; Joernvall, H., C-peptide and neuropathy in type 1 diabetes. *Immunology, Endocrine & Metabolic Agents in Medicinal Chemistry* **2007**, *7* (1), 69-77.
32. Ellsworth, M. L.; Sprague, R. S., Regulation of blood flow distribution in skeletal muscle: role of erythrocyte-released ATP. *J Physiol-London* **2012**, *590* (20), 4985-4991.
33. Sprague, R. S.; Ellsworth, M. L.; Stephenson, A. H.; Lonigro, A. J., ATP: The red blood cell link to NO and local control of the pulmonary circulation. *Am J Physiol-Heart C* **1996**, *271* (6), H2717-H2722.
34. Sprague, R. S.; Stephenson, A. H.; Dimmitt, R. A.; Weintraub, N. A.; Branch, C. A.; McMurdo, L.; Lonigro, A. J., Effect of L-NAME on pressure-flow relationships in isolated rabbit lungs: Role of red blood cells. *Am J Physiol-Heart C* **1995**, *269* (6), H1941-H1948.
35. Pinger, C. W.; Entwistle, K. E.; Bell, T. M.; Liu, Y.; Spence, D. M., C-Peptide replacement therapy in type 1 diabetes: are we in the trough of disillusionment? *Mol Biosyst* **2017**, *13* (8), 1432-1437.
36. Meyer, J. Successful and Reproducible Bioactivity with C-peptide via Activation with Zinc. Michigan State University, 2009.

Chapter 5 – Overall Conclusions and Future Directions

5.1 Overall Conclusions

The overall goal of the thesis presented in this dissertation is to improve the understanding and define new roles for red blood cells (RBCs) in autoimmune diseases. The metabolism of RBCs obtained from patients with type 1 diabetes (T1D) and multiple sclerosis (MS) was investigated and the results provide new insight to a potential T1D therapy and an alternate mechanism of action for MS therapies. This work evaluated RBC metabolism through measurements of both the RBC glucose transporter 1 (GLUT1) content, and the amount of RBC-derived adenosine triphosphate (ATP) released in response to flow-induced shear stress as well as molecular stimuli. In addition, cell-to-cell communication between RBCs and endothelial cells was enabled through the use of a 3D printed device that greatly improved precision over previous devices used by our group and others. Overall, the results presented in this work further the knowledge of both T1D and MS and aim to better treat each disease.

Initial studies aimed to evaluate the metabolism of both T1D and MS RBCs through measurements of the RBC GLUT1 content. RBCs do not contain a nucleus, and the only pathway for energy production is through anaerobic glycolysis, beginning with glucose entering the cell. The primary glucose transporter on RBCs is GLUT1,¹ and results presented in chapter 2 suggest that T1D RBCs contain 24% less GLUT1 than control RBCs, while MS RBCs contain 23% more GLUT1. Although not a direct measurement of

cell metabolism, when the RBC GLUT1 content is combined with results presented in chapters 3 and 4, the metabolism of T1D and MS RBCs is more fully represented, and may provide further insight into disease onset.

Within the RBC, as glucose is metabolized through glycolysis, two ATP molecules are produced, and as RBCs become deformed due to flow induced shear stress, that ATP is released as a signaling molecule into the bloodstream.²⁻³ P2Y purinergic receptors on endothelial cells bind ATP molecules and ignite a signaling pathway that produces nitric oxide (NO),⁴⁻⁶ which is significant in the bloodstream due to its ability to relax smooth muscle cells and dilate blood vessels.⁴ To more fully understand the cell metabolism of MS RBCs, along with downstream applications, the pathway of RBC ATP release and sequential endothelial cell NO production was evaluated.

5.1.1 Steroids and Multiple Sclerosis

Collaboration with the Neurology and Ophthalmology Clinic at Michigan State University enabled us to obtain blood samples from MS patients to evaluate in our lab. Using a 3D printed device to mimic the flow induced shear stress experienced by RBCs *in vivo* (experimental set-up shown in Figure 3.3), the ATP release of control and MS RBCs was measured after treatment with either the steroid hormone estriol or the steroid prednisolone. Estriol was studied due to the reports that high estrogen levels during pregnancy have protective effects on MS,⁷ and prednisolone (the active form of

prednisone) was studied because it is often prescribed to MS patients to help end MS exacerbations.⁸

Results suggest that MS RBCs release elevated amounts of ATP compared to control RBCs at basal levels, which was expected due to previously reported results.⁹ RBC ATP release after treatment with each steroid was also similar to ATP release results from estradiol treated RBCs reported by Letourneau, *et al.*⁹ As RBCs were treated with increasing amounts of estriol, the RBC ATP release decreased in both control and MS RBCs. Significantly, when treated with 7 nM estriol, the MS RBC ATP release decreased to statistically the same level as control RBC ATP release at basal level. The estriol concentrations used reflect levels of estriol per RBC seen during pregnancy. Scaled to the 7% RBC samples used throughout these studies, estriol is present at 7 nM in a healthy female, 30 nM is present during early pregnancy, and up to 0.5 μ M is present in late pregnancy.¹⁰ Samples prepared throughout these studies reflected these estriol concentrations along with additional concentrations to fully understand the effects of estriol on RBCs.

In a similar manner, RBC treatment with prednisolone decreased the RBC ATP release from both control and MS RBCs, and treatment of MS RBCs with 5 or 50 μ M prednisolone led to an ATP release statistically the same as the untreated control RBCs. A common dosage of prednisolone prescribed to patients is between 500 and 1000 mg once daily for three to five days total.⁸ Scaling to proper steroid concentration per RBC, the appropriate physiologically relevant prednisolone concentrations fall within a range of

50 - 100 μM for a 7% RBC sample. Lower prednisolone concentrations were also examined in this work to fully understand its effects on RBCs. Both estriol and prednisolone have the ability to decrease the MS RBC ATP release to that of the basal level of healthy RBCs, which may be an indicator of the mechanism of action that steroids have on RBCs, and a way that MS exacerbations are controlled by their presence in the bloodstream.

ATP is a stimulus of NO production *in vivo*, and NO has been previously implicated in MS.¹¹⁻¹² Elevated levels of NO have been found to break down the blood brain barrier (BBB),¹³⁻¹⁴ and NO metabolites have been found in the cerebral spinal fluid and urine of MS patients.¹⁵⁻¹⁷ Breakdown of the BBB is a hallmark feature of MS, and therapies to decrease the amount of BBB permeability would significantly help to alleviate complications experienced by MS patients.

To investigate the NO production of bovine pulmonary arterial endothelial cells (bPAECs, used as a human endothelial cell mimic) in contact with flowing RBCs, we used the 3D printed device described previously. As RBCs were circulated, they released ATP due to shear stress that bound to the P2Y purinergic receptors on the bPAECs and produced NO. The amount of NO production from bPAECs in contact with control RBCs treated with varying amounts of either estriol or prednisolone was evaluated, and for all physiologically relevant concentrations, a significant decrease in the NO production was measured. Although MS RBCs were not used in this study, due to the correlation between RBC ATP release and bPAEC NO production, a similar trend is expected from bPAECs

in contact with MS RBCs. As estriol and prednisolone decrease the amount of ATP released from RBCs of MS patients, a consequence is a decrease in the endothelial NO production, proposed to relieve MS complications. This finding is both a mechanism of action of steroids in the bloodstream along with a discovery to further the research involving novel MS therapies.

Further investigations as to how steroids directly affect RBCs focused on the deformability of RBCs. Previous work has reported that RBC deformability is associated with RBC ATP release, and the more deformable the RBC is, the more ATP is released from the cell.¹⁸⁻
¹⁹ When this theory was tested on RBCs treated with either estriol or prednisolone, a decrease in RBC deformability was measured with treatment of physiologically relevant concentrations. The decrease in deformability was not as predominant as the decrease in ATP release measured however, possibly suggesting that the deformability measurements were not sensitive enough to detect small differences. Regardless, the ability of steroids to decrease the deformability of RBCs is another piece of evidence, combined with the decrease in RBC ATP release, implicating that their mechanism of action may begin in the bloodstream with RBCs.

While shear stress and mechanical deformation is a main mechanism of RBC ATP release, chemical stimuli also leads to RBC ATP release.³ Previous work has proven that when the pancreatic peptide, C-peptide, is combined with Zn^{2+} and the blood protein albumin, an increase in RBC ATP release is measured.²⁰ If this complex increases the RBC ATP release, it follows that inhibiting the binding of C-peptide and Zn^{2+} to RBCs

would attenuate RBC ATP release, which may be significant in MS because MS RBCs have been shown to bind an elevated amount of C-peptide and Zn^{2+} at basal levels.²¹⁻²² However, this work suggests that RBCs treated with prednisolone bind less C-peptide and Zn^{2+} , and as a consequence, any downstream effects should also be attenuated, such as RBC ATP release.

To further investigate how steroids affect RBC metabolism, the GLUT1 content of RBCs treated with prednisolone was evaluated. While glucose uptake measurements were not directly performed, GLUT1 content is proposed to be associated with glucose flux, leading to ATP production within the cell. Findings revealed that the RBC GLUT1 content increased when RBCs were treated with prednisolone. Although contrary to the RBC ATP release results, a possible explanation may involve prednisolone acting as an antagonist to GLUT1, hindering the amount of glucose flux through the protein. Steroids are known to inhibit glucose transport,²³ and as the cell experiences hypoglycemic conditions due to prednisolone, additional GLUT1 proteins may be translocated to the cell membrane to allow additional glucose flux, thereby causing the increased GLUT1 content measured by this work.

Overall, a proposed mechanism of action involving steroids and RBCs has been suggested to result in a decrease of RBC glucose flux, deformability, and binding of C-peptide and Zn^{2+} . These effects are all associated with decreased RBC ATP release, and may occur through a proposed mechanism involving steroids intercalating into the RBC

membrane, antagonizing GLUT1 glucose transport, and altering the location of the C-peptide and Zn^{2+} binding site. As the RBC ATP release is decreased, less NO is produced by endothelial cells, causing less damage to the BBB and amelioration of MS symptoms.

5.1.2 Type 1 Diabetes Therapy to Improve Blood Flow

C-peptide and Zn^{2+} have been shown to increase the RBC ATP release and subsequent NO production from endothelial cells.²⁰ While this mechanism was previously studied with regard to MS, it may also be applicable to T1D. Poor blood flow is proposed to be the root cause of many diabetic complications such as diabetic retinopathy, neuropathy, and nephropathy, and a therapy to alleviate these complications is needed for diabetic patients.²⁴⁻²⁷ ATP is produced through glucose metabolism *in vivo*, and if glucose metabolism is enhanced within the diabetic bloodstream, blood flow may also be enhanced as the produced ATP is released into the blood stream.

T1D patients administer insulin to maintain proper blood glucose levels *in vivo*, which binds to receptors on cell membranes and activates the translocation of glucose transporter 4 (GLUT4) proteins to the cell membrane and facilitates the diffusion of glucose into GLUT4 containing cells. Insulin is very effective at this process; however, most bloodstream cells do not contain GLUT4, but instead contain GLUT1. Importantly, GLUT1 is not affected by insulin. If an accompaniment therapy to insulin would increase

the GLUT1 content of bloodstream cells, the elevated glucose clearance from the bloodstream would lead to elevated ATP production within bloodstream cells and potentially elevated ATP release.

Due to the finding in chapter 2 that T1D RBCs contain less GLUT1 than control RBCs at basal level, a therapy to increase RBC GLUT1 content along with RBC ATP release was hypothesized to have the most success as a blood flow enhancing therapy in T1D. Previously published work has implicated C-peptide as being beneficial for diabetic patients by increasing nerve function and renal blood flow,²⁸⁻³⁰ and a clinical trial by the company, Cebix, investigated C-peptide as an auxiliary therapy for T1D patients.³¹ While initial studies were positive, the phase IIb clinical trial resulted in no measureable benefit in T1D neuropathy from the addition of C-peptide.³¹ Interestingly, a study from the Spence group found that in order for C-peptide to elicit an effect on RBCs, it must be combined with Zn^{2+} and the blood protein albumin,²⁰ which Cebix did not use. Work presented in chapter 4 evaluated the necessity and effects of the C-peptide, Zn^{2+} , albumin complex on RBCs, and results may prove to be significant with regard to an auxiliary therapy to accompany insulin for T1D patients.

Results found that in order for both C-peptide and Zn^{2+} to bind to RBCs and potentially elicit an effect, albumin must be present at the time of complex formation. Measurements of RBC ATP release evaluated the effect that each component of the C-peptide, Zn^{2+} , albumin complex had on the RBC ATP release, and results found that only when the full

complex was combined with RBCs did the RBC ATP release increase. This result is significant with regard to the failed clinical trial by Cebix, and suggests that Cebix may not have obtained positive results from their phase IIb clinical trial because the complex, proven necessary by this work, was not administered.

Further investigation of the proposed complex evaluated the change in RBC GLUT1 content due to each component of the complex. This was performed because of the previously suggested relationship between GLUT1 and RBC metabolism. Similar to the RBC ATP release results, only when the full complex was present did the RBC GLUT1 content increase. As C-peptide, Zn^{2+} , and albumin elicit an effect on RBCs, a potential mechanism of action involves the complex stimulating GLUT1 translocation leading to increased ATP production within the cell and subsequent release that is able to bind to P2Y purinergic receptors on endothelial cells and stimulate NO production and vasodilation. Resulting vasodilation will enhance blood flow and potentially alleviate the complications of retinopathy, neuropathy, and nephropathy experienced by diabetic patients.

Overall, this research advances the knowledge of autoimmune diseases in the bloodstream. Although through different mechanisms, it is clear that RBC metabolism is altered in both T1D and MS patients. With this knowledge, new mechanisms of action are suggested for current MS therapies, and an auxiliary therapy to supplement T1D insulin injections is also proposed. Further work is necessary to more directly measure RBC metabolism, such as RBC glucose transport; however, results from this work are

hypothesized to strongly correlate to RBC metabolism. Research must continue to better understand the etiology of these diseases in order to offer more effective treatment options to patients.

5.2 Future Directions

5.2.1 Red Blood Cell Interferon Beta Treatment

While steroid treatments are administered at high doses for a short amount of time to alleviate MS exacerbations, other medications are administered over a much longer duration. Interferon beta (IFN- β) medications are commonly prescribed to MS patients as a disease modifying therapy, and overall, IFN- β medications reduce the relapse rate of MS patients by about a third.³²⁻³⁴ As cytokines, IFN- β medications are thought to inhibit the proliferation of T-cells and decrease the production of pro-inflammatory cytokines in the body, thereby protecting against MS complications.³⁵ Interestingly, IFN- β has three associated ligands: beta-D-glucose, 6-deoxy- α -d-glucose, and Zn²⁺. Although a proposed mechanism of action of IFN- β involves a reduction in pro-inflammatory cytokines, due to the ability of IFN- β to bind Zn²⁺, this work suggests that it may have an alternate mechanism of action effecting the metabolism of RBCs.

Since IFN- β is a Zn²⁺ binding protein, a hypothesized mechanism involves IFN- β binding Zn²⁺ in the bloodstream, attenuating the effect that C-peptide and Zn²⁺ binding has on

RBCs. To evaluate if IFN- β affects RBC metabolism, initial studies measured the GLUT1 content of RBCs treated with IFN- β and 20 nM C-peptide and Zn²⁺. Figure 5.1 shows an initial 25% increase in RBC GLUT1 content when treated with C-peptide and Zn²⁺, and as shown in Figures 5.2 and 5.3, IFN- β neutralizes the initial GLUT1 increase due to C-peptide and Zn²⁺ in both control and MS RBCs, respectively. These results support an additional role of IFN- β in the bloodstream involving Zn²⁺ binding. Hindering the binding and effect of the C-peptide and Zn²⁺ complex on RBCs will lead to a decrease in RBC metabolism. This data is preliminary work, and further studies must evaluate the reproducibility of this data as well as more directly correlate the results to RBC metabolism in the form of RBC ATP release or glucose transport.

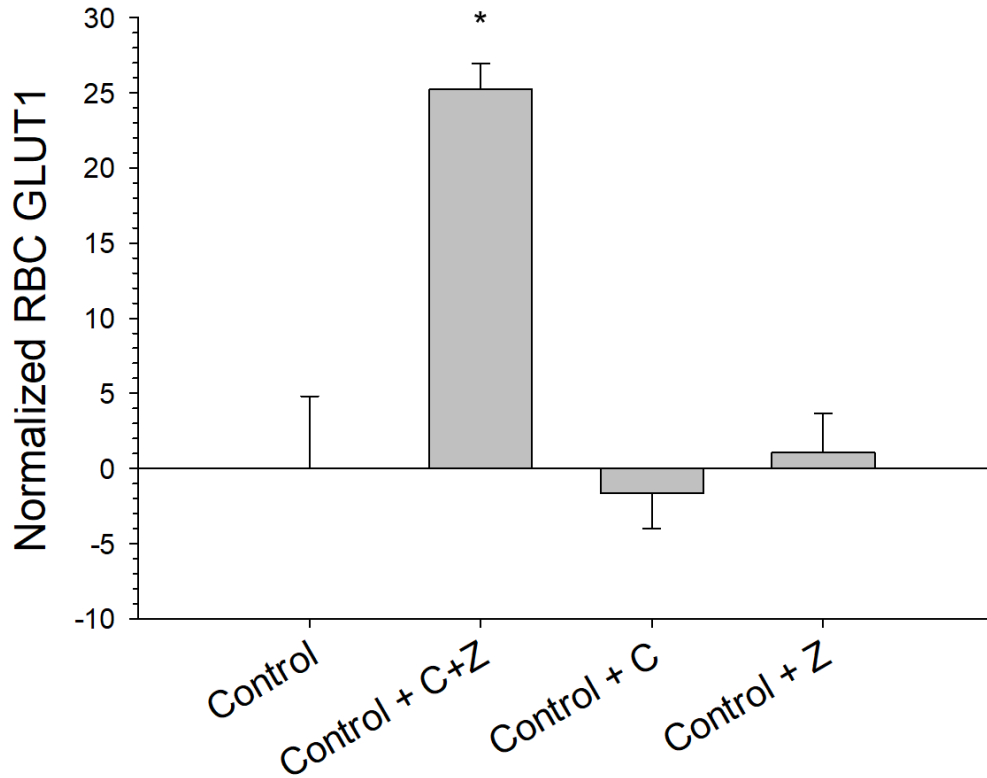


Figure 5.1 – RBC GLUT1 Content with C-peptide and Zn²⁺. As a 7% RBC sample is treated with 20 nM C-peptide and Zn²⁺, a 25 ± 2% increase in the GLUT1 content is measured. Interestingly, no significant increase was measured due to C-peptide only or Zn²⁺ only. n = 5 donors, *p < 0.05 to control, error bars = SEM.

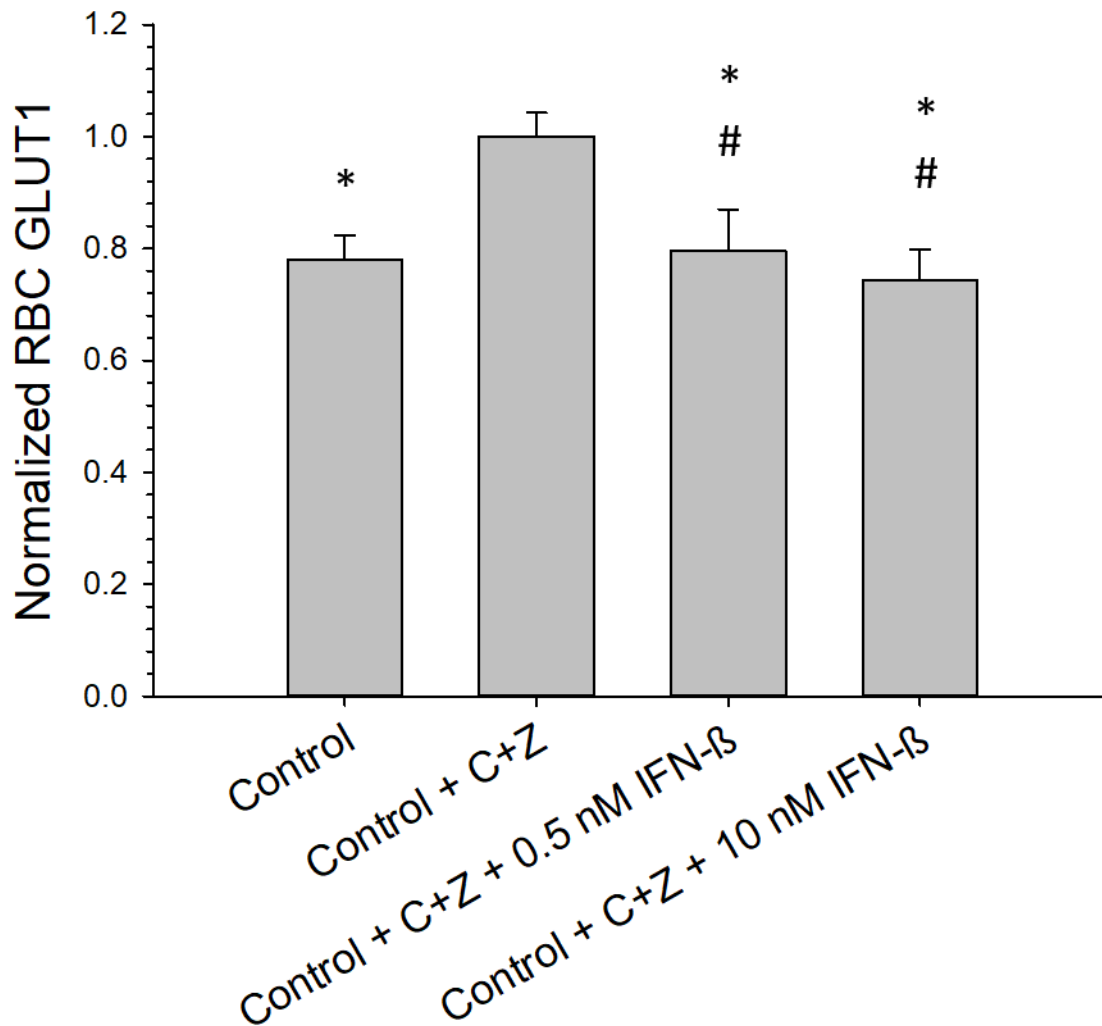


Figure 5.2 – Control RBC GLUT1 Content with IFN- β . As samples of 7% RBCs are treated with 20 nM C-peptide and Zn²⁺ along with IFN- β , the initial increase in GLUT1 content measured due to C-peptide and Zn²⁺, decreases 26-28%. This decrease leads to a GLUT1 content statistically the same as the basal level of control RBCs and is thought to be caused by IFN- β binding the Zn²⁺ in solution, hindering any effect on the RBCs caused by Zn²⁺ binding, shown here as RBC GLUT1 content. n = 3 donors, *p < 0.05 to Control + C+Z, #p > 0.2 to Control, error bars = SEM.

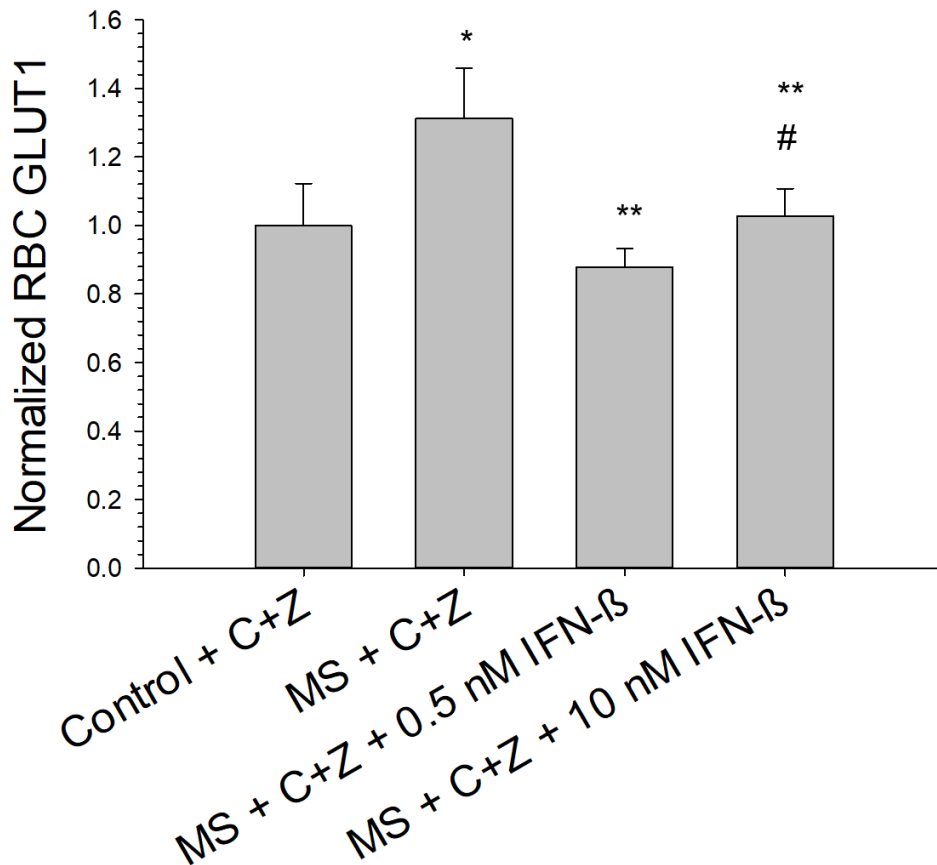


Figure 5.3 – RBC GLUT1 Content with IFN- β . When control and MS RBCs are treated with C-peptide and Zn²⁺, MS RBCs contain more GLUT1 than control RBCs. Interestingly, as MS RBCs are treated with IFN- β after treatment with C-peptide and Zn²⁺, the GLUT1 content decreased to significantly the same levels as control RBCs treated with C-peptide and Zn²⁺. n = 3 donors, *p < 0.05 to control + C+Z, **p < 0.05 to MS + C+Z, #p > 0.05 to control + C+Z, error bars = SEM.

5.2.2 Red Blood Cell Glucose Internalization Measurements

To date, all work has focused on indirect measurements of RBC metabolism. Although it is proposed here that GLUT1 content correlates to glucose flux into the cell, measurements of glucose transport have not been performed to directly correlate the two.

Studies involving radioisotope-labeled glucose may advance research by measuring the amount of glucose internalized into cells. Fludeoxyglucose (FDG) is a glucose analog with an ^{18}F substituted for the hydroxyl group at the C-2 position of glucose. This molecule is a positron-emitting radionuclide used in positron emission tomography (PET) imaging, and glucose internalization is monitored by the amount of FDG in various tissue, which is correlated to metabolism within the tissue. Once internalized, phosphorylation of FDG by hexokinase prevents its release from the cell. This allows imaging without constant transport of the molecule in and out of the tissue. Although commonly used to image tumors, it is proposed that this system is applicable to RBC glucose internalization, as reports suggest that GLUT1 will transport FDG; however, whether or not its affinity for GLUT1 is the same as glucose is debated.³⁶⁻³⁸

FDG is a gamma-emitting molecule, and working with large quantities of it can be dangerous, as gamma-emitting particles are able to penetrate the skin and damage DNA molecules within the body. However, working with proper shielding and low levels of radiation greatly decreases any health risk to the scientists involved in its use. In addition, the half-life of FDG is short, only 110 minutes, which allows its radiation to be penetrating for only a short amount of time before the ^{18}F decays into stable ^{18}O . For all preliminary experiments, the scientists involved took all necessary precautions.

Attempts to optimize an assay to measure FDG internalization has focused on varying the glucose concentration in the physiological salt solution (PSS) used to prepare

samples. This was done due to the small number of FDG molecules present in our buffer, which was required to ensure safety during experimentation. To afford FDG a greater opportunity for RBC internalization, PSS was prepared with 0, 0.1, or 0.25 mM glucose. As the glucose amount in the PSS was decreased, an elevated amount of FDG was able to be measured within the RBCs. All measurements were performed using a 2480 WIZARD2 Automatic Gamma Counter (Perkin Elmer, Waltham, MA), and the final samples consisted of pelleted RBCs. Washing steps proved necessary to remove nonspecifically bound FDG before analysis; however, continual glucose transport during the washing steps has come into question, and a method to replace the aforementioned washings is advantageous.

Preliminary studies involving RBC internalization of FDG when RBCs were initially treated with C-peptide and Zn^{2+} have not proven successful to date. Although the results presented in this dissertation suggest that RBC metabolism is increased due to addition of C-peptide and Zn^{2+} , when the FDG internalization was measured after 5 and 45 minutes of incubation, a decrease in the FDG internalization was measured after treatment with C-peptide and Zn^{2+} , suggesting a decrease in cell metabolism. It is noteworthy that glucose transport happens very quickly through GLUT1, and it has been suggested that in order to properly study sugar transport across GLUT1, transport measurements must be limited to less than one second or temperatures must be lowered to 4°C.³⁹ All preliminary studies involved incubations at 37°C (physiological temperature) for 5 minutes or greater, which may be a factor in the obtained results. Future work optimizing a protocol to measure RBC internalization of FDG would more directly

measure glucose utilization of the RBC compared to previous work presented in this dissertation, and may require incubations at 4°C instead of 37°C to slow down the transport of glucose. Overall, a more direct method to measure glucose transport through GLUT1 is necessary to correlate the results obtained in this dissertation directly with RBC metabolism, and while not the only method available, FDG internalization measurements may prove to be a viable method.

REFERENCES

REFERENCES

1. Vrhovac, I.; Breljak, D.; Sabolic, I., Glucose transporters in the mammalian blood cells. *Period Biol* **2014**, *116* (2), 131-138.
2. Suzuki, Y.; Tateishi, N.; Soutani, M.; Maeda, N., Deformation of erythrocytes in microvessels and glass capillaries: effects of erythrocyte deformability. *Microcirculation* **1996**, *3*, 49-57.
3. Ellsworth, M. L.; Sprague, R. S., Regulation of blood flow distribution in skeletal muscle: role of erythrocyte-released ATP. *The Journal of physiology* **2012**, *590* (Pt 20), 4985-4991.
4. Sprague, R. S.; Olearczyk, J. J.; Spence, D. M.; Stephenson, A. H.; Sprung, R. W.; Lonigro, A. J., Extracellular ATP signaling in the rabbit lung: Erythrocytes as determinants of vascular resistance. *American Journal of Physiology* **2003**, *286*(2, Pt. 2), H693-H700.
5. Sprague, R. S.; Stephenson, A. H.; Ellsworth, M. L.; Keller, C.; Lonigro, A. J., Impaired release of ATP from red blood cells of humans with primary pulmonary hypertension. *Exp. Biol. Med. (Maywood, NJ, U. S.)* **2001**, *226* (5), 434-439.
6. Sprung, R.; Sprague, R.; Spence, D., Determination of ATP release from erythrocytes using microbore tubing as a model of resistance vessels in vivo. *Analytical Chemistry* **2002**, *74* (10), 2274-2278.
7. Vukusic, S.; Confavreux, C., Pregnancy and multiple sclerosis: the children of PRIMS. *Clin Neurol Neurosurg* **2006**, *108* (3), 266-270.
8. Morrow, S. A.; McEwan, L.; Alikhani, K.; Hyson, C.; Kremenchutzky, M., MS patients report excellent compliance with oral prednisone for acute relapses. *Can J Neurol Sci* **2012**, *39* (3), 352-354.
9. Letourneau, S.; Hernandez, L.; Faris, A. N.; Spence, D. M., Evaluating the effects of estradiol on endothelial nitric oxide stimulated by erythrocyte-derived ATP using a microfluidic approach. *Anal Bioanal Chem* **2010**, *397* (8), 3369-3375.
10. Sicotte, N. L.; Liva, S. M.; Klutch, R.; Pfeiffer, P.; Bouvier, S.; Odesa, S.; Wu, T. C.; Voskuhl, R. R., Treatment of multiple sclerosis with the pregnancy hormone estriol. *Ann Neurol* **2002**, *52* (4), 421-428.
11. Encinas, J. M.; Manganas, L.; Enikolopov, G., Nitric oxide and multiple sclerosis. *Curr Neurol Neurosci Rep* **2005**, *5* (3), 232-238.
12. Sprague, R. S.; Ellsworth, M. L.; Stephenson, A. H.; Lonigro, A. J., ATP: the red blood cell link to NO and local control of the pulmonary circulation. *The American journal of physiology* **1996**, *271* (6 Pt 2), H2717-H2722.

13. Boje, K. M.; Lakhman, S. S., Nitric oxide redox species exert differential permeability effects on the blood-brain barrier. *The Journal of pharmacology and experimental therapeutics* **2000**, 293 (2), 545-550.
14. Giovannoni, G.; Heales, S. J.; Land, J. M.; Thompson, E. J., The potential role of nitric oxide in multiple sclerosis. *Mult Scler* **1998**, 4 (3), 212-216.
15. Giovannoni, G., Cerebrospinal fluid and serum nitric oxide metabolites in patients with multiple sclerosis. *Mult Scler* **1998**, 4 (1), 27-30.
16. Giovannoni, G.; Silver, N. C.; O'Riordan, J.; Miller, R. F.; Heales, S. J.; Land, J. M.; Elliot, M.; Feldmann, M.; Miller, D. H.; Thompson, E. J., Increased urinary nitric oxide metabolites in patients with multiple sclerosis correlates with early and relapsing disease. *Mult Scler* **1999**, 5 (5), 335-341.
17. Rejdak, K.; Eikelenboom, M. J.; Petzold, A.; Thompson, E. J.; Stelmasiak, Z.; Lazeron, R. H.; Barkhof, F.; Polman, C. H.; Uitdehaag, B. M.; Giovannoni, G., CSF nitric oxide metabolites are associated with activity and progression of multiple sclerosis. *Neurology* **2004**, 63 (8), 1439-1445.
18. Price, A. K.; Fischer, D. J.; Martin, R. S.; Spence, D. M., Deformation-Induced Release of ATP from Erythrocytes in a Poly(dimethylsiloxane)-Based Microchip with Channels That Mimic Resistance Vessels. *Analytical Chemistry* **2004**, 76 (16), 4849-4855.
19. Sprague, R. S.; Ellsworth, M. L.; Stephenson, A. H.; Kleinhenz, M. E.; Lonigro, A. J., Deformation-induced ATP release from red blood cells requires CFTR activity. *American Journal of Physiology* **1998**, 275 (5, Pt. 2), H1726-H1732.
20. Liu, Y.; Chen, C.; Summers, S.; Medawala, W.; Spence, D. M., C-peptide and zinc delivery to erythrocytes requires the presence of albumin: implications in diabetes explored with a 3D-printed fluidic device. *Integr Biol (Camb)* **2015**, 7 (5), 534-543.
21. Lockwood, S. Y.; Summers, S.; Eggenberger, E.; Spence, D. M., An In Vitro Diagnostic for Multiple Sclerosis Based on C-peptide Binding to Erythrocytes. *EBioMedicine* **2016**, 11, 249-252.
22. Letourneau, S. Delivery of Zinc to Red Blood Cells and the Downstream Effects in Multiple Sclerosis. Dissertation, Michigan State University, 2013.
23. Lacko, L.; Wittke, B.; Geck, P., Interaction of steroids with the transport system of glucose in human erythrocytes. *J Cell Physiol* **1975**, 86 Suppl 2 (3 Pt 2), 673-680.
24. Keenan, H. A.; Costacou, T.; Sun, J. K.; Doria, A.; Cavallerano, J.; Coney, J.; Orchard, T. J.; Aiello, L. P.; King, G. L., Clinical factors associated with resistance to microvascular complications in diabetic patients of extreme disease duration - The 50-year medalist study. *Diabetes Care* **2007**, 30 (8), 1995-1997.

25. Sheetz, M. J.; King, G. L., Molecular understanding of hyperglycemia's adverse effects for diabetic complications. *Jama-J Am Med Assoc* **2002**, *288* (20), 2579-2588.
26. Sugimoto, K.; Murakawa, Y.; Sima, A. A., Diabetic neuropathy--a continuing enigma. *Diabetes Metab Res Rev* **2000**, *16* (6), 408-433.
27. Boulton, A. J. M.; Gries, F. A.; Jervell, J. A., Guidelines for the diagnosis and outpatient management of diabetic peripheral neuropathy. *Diabetic Medicine* **1998**, *15* (6), 508-514.
28. Cotter, M. A.; Ekberg, K.; Wahren, J.; Cameron, N. E., Effects of proinsulin C-peptide in experimental diabetic neuropathy: Vascular actions and modulation by nitric oxide synthase inhibition. *Diabetes* **2003**, *52* (7), 1812-1817.
29. Hach, T.; Forst, T.; Kunt, T.; Ekberg, K.; Pfutzner, A.; Wahren, J., C-peptide and its C-terminal fragments improve erythrocyte deformability in type 1 diabetes patients. *Exp Diabetes Res* **2008**, *2008*, 730594.
30. Fiorina, P.; Folli, F.; Zerbini, G.; Maffi, P.; Gremizzi, C.; Di Carlo, V.; Socci, C.; Bertuzzi, F.; Kashgarian, M.; Secchi, A., Islet transplantation is associated with improvement of renal function among uremic patients with type I diabetes mellitus and kidney transplants. *J Am Soc Nephrol* **2003**, *14* (8), 2150-2158.
31. Wahren, J.; Foyt, H.; Daniels, M.; Arezzo, J. C., Long-Acting C-Peptide and Neuropathy in Type 1 Diabetes: A 12-Month Clinical Trial. *Diabetes Care* **2016**, *39* (4), 596-602.
32. Kappos, L.; Polman, C. H.; Freedman, M. S.; Edan, G.; Hartung, H. P.; Miller, D. H.; Montalban, X.; Barkhof, F.; Bauer, L.; Jakobs, P.; Pohl, C.; Sandbrink, R., Treatment with interferon beta-1b delays conversion to clinically definite and McDonald MS in patients with clinically isolated syndromes. *Neurology* **2006**, *67* (7), 1242-1249.
33. Comi, G.; Filippi, M.; Barkhof, F.; Durelli, L.; Edan, G.; Fernandez, O.; Hartung, H.; Seeldrayers, P.; Sorensen, P. S.; Rovaris, M.; Martinelli, V.; Hommes, O. R.; Early Treatment of Multiple Sclerosis Study, G., Effect of early interferon treatment on conversion to definite multiple sclerosis: a randomised study. *Lancet* **2001**, *357* (9268), 1576-1582.
34. Reuss, R., PEGylated interferon beta-1a in the treatment of multiple sclerosis - an update. *Biologics* **2013**, *7*, 131-138.
35. Dhib-Jalbut, S.; Marks, S., Interferon-beta mechanisms of action in multiple sclerosis. *Neurology* **2010**, *74* Suppl 1, S17-S24.
36. Oehr, P., *PET and PET-CT in Oncology*. Springer: 2003.

37. Hasselbalch, S. G.; Knudsen, G. M.; Holm, S.; Hageman, L. P.; Capaldo, B.; Paulson, O. B., Transport of D-glucose and 2-fluorodeoxyglucose across the blood-brain barrier in humans. *J Cereb Blood Flow Metab* **1996**, *16* (4), 659-666.
38. Avril, N., GLUT1 expression in tissue and (18)F-FDG uptake. *J Nucl Med* **2004**, *45* (6), 930-932.
39. Carruthers, A.; DeZutter, J.; Ganguly, A.; Devaskar, S. U., Will the original glucose transporter isoform please stand up! *Am J Physiol Endocrinol Metab* **2009**, *297* (4), E836-E848.